Polarization Pattern Perception: implications for the assessment of macular function in health and disease

Jasmine Elizabeth Smith
Doctor of Optometry

Aston University
February 2021

Thesis Summary

Polarization Pattern Perception: implications for the assessment of macular function in health and disease

Aston University, Doctor of Optometry, Jasmine E Smith, 2021

The ability of humans to perceive polarized light was first documented by Haidinger in 1844, who discussed the entoptic phenomenon of what was later to be known as Haidinger's brushes. Until recently, Haidinger's brushes were believed to constitute the full extent of human polarization sensitivity. It is now known that the human visual system is capable of detecting visual stimuli modulated solely by light polarization (Misson et al., 2015, Temple et al., 2015). Misson and Anderson (2017) developed the technique of polarization pattern perception (PPP) and showed that human polarization sensitivity was significantly more acute and quantifiable than previously thought. Furthermore, like its related phenomenon of Haidinger's brush, they showed that PPP is confined to the macula, and matches the spectral characteristics and distribution of the macular pigments. The known protective functions of macular pigments, and the association of its deficiency with susceptibility to macular degeneration, make a measure of PPP potentially useful as a clinical screening tool for at-risk individuals and for the early detection of macular disease.

Normative polarization pattern perception values had not yet been established in humans, and the repeatability of the technique was yet to be explored. The effect of age and variations in corneal and macular characteristics on PPP are also currently unknown. The principal aim of this research project is to quantify normative monocular sensitivity values for PPP in healthy individuals and address these gaps in the field.

Grating stimuli were displayed in polarization-only contrast on a delaminated LCD screen. This technique was shown to give rapid, inexpensive, quantifiable data, which, with some development, could be used to assess and monitor macular function and screen at risk individuals. PPP values across a range of ages are presented and discussed, with reference to each participant's corneal and macular characteristics.

The monocular polarization pattern sensitivity for healthy participants aged 19-59 years was 5.17, which equates to an average ability to discriminate stimuli differing by 8 degrees. This provided evidence in support of the human ability to perceive polarized light to a much higher degree than previously expected, and was similar to data from previously published pilot studies developing the technique (Misson et al., 2019, Misson and Anderson, 2017). There was no significant change in human PPP across the age range 19-59 years. Test-retest measures showed a positive correlation, but the overall repeatability of the technique would need improvement if it were to become a useful clinical measurement. A significant positive correlation between MPOD and PPP was found, which together with the lack of influence from variations in other ocular characteristics (age, refraction, central foveal thickness, central corneal thickness, corneal retardance, corneal birefringence and ocular dominance) make a measure of PPP potentially highly beneficial for macular assessment.

Key words: human polarization perception, polarization pattern sensitivity, polarization contrast, PPP, macular pigment optical density.

Acknowledgements

I wish to extend my heartfelt thanks to Prof Stephen Anderson, my primary supervisor, who has guided me through this research project, provided invaluable support and shared his knowledge. I would also like to thank Prof Gary Misson, my associate supervisor, who provided calibration and technical support, helping me from the start to the end of this project. Both of your expertise and guidance were monumental to the success of this study.

I wish to show my appreciation for my employers, Mary Bramley and Wendy d'E. Vallancey, and all the staff at Aves Optometrists. They allowed me to complete the in-practice data collection, provided vital equipment used in the project, supported me throughout, and accommodated any time requirements needed.

The support and love from my family and friends kept me motivated throughout the doctorate modules and research project. Completing this would not have been possible without them, so I would like to extend my special thanks to my partner, Hannah; my mother, Angela; and my father, Martyn.

I would also like to show my appreciation for the lecturers at the School of Life and Health Sciences at Aston University for their teaching during the doctorate modules which prepared me for this final research project. I would like to give a final thanks to all my patients from Aves Optometrists who kindly participated in this project.

List of Contents

Page

List of Figures

Chapter 1

General Introduction

1.1. Basis of Polarized Light

Light is often described in terms of its wavelength and intensity, but the property of polarization can also provide useful information. Polarization is the property of the electric field vector (**e**-vector) of electromagnetic waves to oscillate in a defined way. When considering polarization, it is convention to think in terms of manipulating components of the **e**-vector to change the information contained within the light reaching a given point. When a light wave oscillates in all random orientations it is said to be unpolarized. This can be transformed into polarized light by altering the proportion of light oscillating in each **e**-vector plane.

Three characteristics of polarized light are: (i) its intensity; (ii) its degree of polarization; and (iii) its angle of polarization (Foster et al., 2018, Cronin et al., 2003). The sun produces fully depolarized light (random **e**-vector orientations), but this can become linearly polarized in the natural environment, primarily by scattering and reflection (Cronin et al., 2003, Wehner, 2001) or artificially by transmission through a polarizer (see figure 1) (Cronin and Marshall, 2011). Some materials are isotropic and do not affect the polarization of light passing through them (e.g. glass). Other anisotropic materials can exhibit dichroic or birefringent properties, thus altering the polarization of the light passing through (e.g. the cornea).

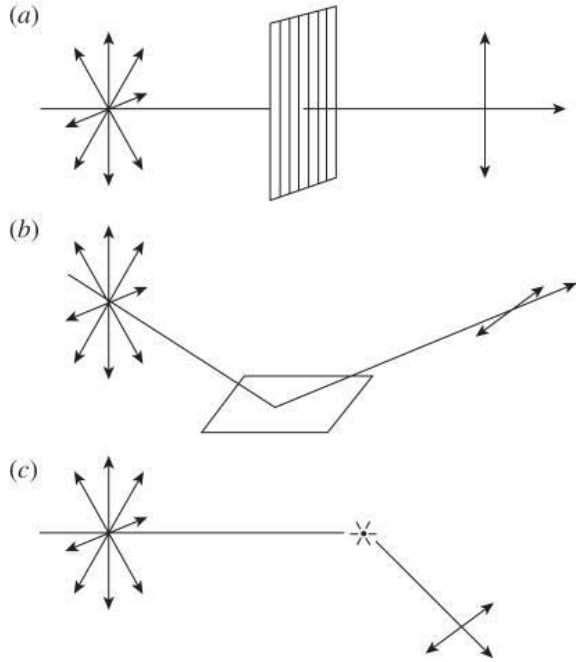

Figure 1. *Three common ways to polarize light. (a) Transmission—some dichroic materials can preferentially absorb or transmit certain planes of light (e.g. a polarizing filter). (b) Reflection from a smooth surface can produce plane-polarized light depending on the refractive indices of the materials (e.g. the surface of water). (c) Scattering from particles in the air (e.g. Rayleigh scattering) (taken from Cronin and Marshall, 2011).*

Polarized light may be linear, circular or elliptical (see figure 2). Linear polarization, most relevant to the present study, is where the resultant **e**-vector oscillates in a single plane at a given orientation. Elliptical polarization can occur when two light waves of different **e**-vector orientations propagate together. When these two linear components are of different amplitudes with components with a phase difference not equal to π/2, the resultant **e**-vector constantly changes orientation, describing an ellipse as it propagates. Circular polarization is a special case of elliptical polarization, occurring only with waves with equal perpendicular components with a phase difference of π/2. The resultant **e**-vector orientation rotates smoothly in a circular pattern (Foster et al., 2018, Johnsen, 2011, Cronin et al., 2003)**.**

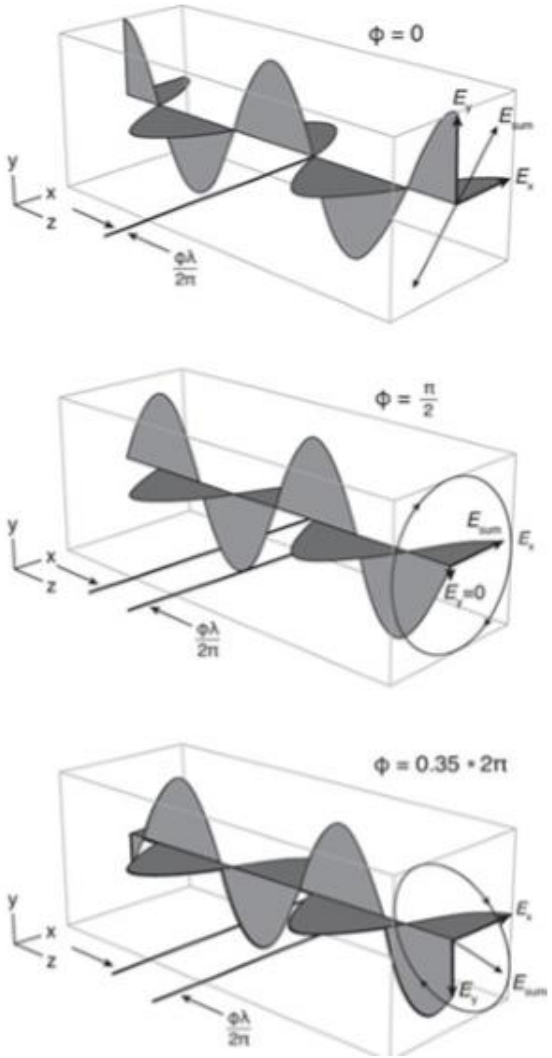

Figure 2. *Diagrams describing linear, circular, and elliptical polarization (taken from Johnsen, 2011).*

1.2. Polarized Vision in Animals

Many invertebrates have evolved dedicated polarization-sensitive visual systems and developed polarization-related behaviours (Marshall et al., 2019, Cronin et al., 2003).

Invertebrates have rhabdomeric photoreceptors that are inherently polarization-sensitive because of their structure (Roberts et al., 2011, Cronin et al., 2003, Wehner, 2001). Polarization-sensitive invertebrates achieve polarization sensitivity by utilising the dichroic properties of the visual pigments in their photoreceptors (Marshall et al., 2019, Cronin et al., 2003, Bone and Landrum, 1984). Some invertebrates have also developed specific polarization sensitive cortical mechanisms (McGregor et al., 2014).

It is well documented that many invertebrates use these polarization cues to aid survival (Marshall et al., 2019). Improved polarization perception has been proven to be beneficial for signalling (see figure 3 and 4), camouflage, object detection and navigation (Marshall et al., 2019, Roberts et al., 2011, Cronin et al., 2003, Wehner, 2001). Cuttlefish have shown to have the most acute perception to date, detecting **e**-vector orientation differences to just one degree (Temple et al., 2012). Many invertebrates can detect around 10-20° difference in **e**-vector orientation, but superior detection could give valuable additional information to a visual scene, as nearby areas and objects often only differ by a few degrees (Labhart, 2016, Temple et al., 2012).

Most vertebrates are not known to be polarization sensitive. Vertebrates have ciliary photoreceptors that are inherently polarization-insensitive due to their structure. A small number of vertebrate species (e.g. some fish species such as the anchovy and teleost) have evolved some degree of polarization sensitivity through structural changes in their ciliary photoreceptors arrangement (Kondrashev et al., 2012, Kamermans and Hawryshyn, 2011, Roberts et al., 2011, Cronin et al., 2003).

For the interested reader, comprehensive reviews of polarized vision in animals are Marshall, et al., (2019), Labhart (2016) and Cronin, et al., (2003).

Humans lack such dedicated receptors and higher-order neural processes for polarization vision (Marshall et al., 2019, Foster et al., 2018), but still maintain a degree of polarisation sensitivity. This is discussed in detail below.

1.3. Polarized Vision in Humans

1.3.1. Haidinger's Brush and Polarization Pattern Perception (PPP)

Haidinger's brush phenomenon, a transient orthogonal blue and yellow hourglass seen when looking at uniform fields of linearly polarized white light, was first described in 1844 (Haidinger, 1844). Until recently this was believed to constitute the full extent of human polarization perception (Misson and Anderson, 2017, Misson et al., 2015, Naylor and Stanworth, 1955), a visual attribute far inferior to that of many polarization-sensitive organisms (Labhart, 2016, Temple et al., 2012, Cronin et al., 2003).

The perception of Haidinger's brush can vary greatly among individuals (Rothmayer et al., 2007). The phenomenon can often be seen transiently when looking at the sky (Horvath et al., 2017, Muller et al., 2016), as depicted in figure 3. It is commonly believed to be visible due to the diattenuating structures in the eye (Misson and Anderson, 2017, Muller et al., 2016, Rothmayer et al., 2007, Bone, 1980). Haidinger's brush is only visible in the central 4-5° from fixation (McGregor et al., 2014, Le Floch et al., 2010, Snodderly et al., 1984a, Naylor and Stanworth, 1955, Forster, 1954) and lasts 2-3 seconds for an unchanging polarization field stimulus (Snodderly et al., 1984a, Naylor and Stanworth, 1955, Forster, 1954, De Vries et al., 1950). The phenomenon fades due to the Troxler effect, a manifestation of adaptation to a stabilized retinal image, which causes static unchanging stimuli to disappear when stable fixation is maintained (Clark, 1960).

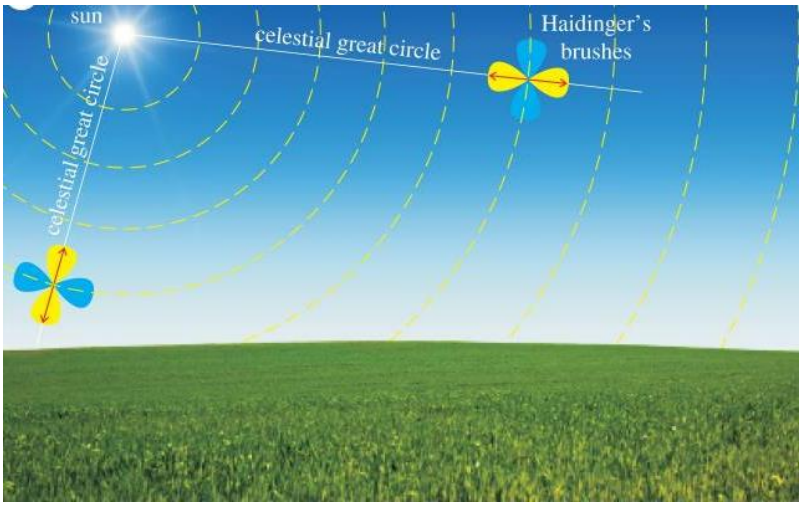

Figure 3. *Schematic diagram showing Haidinger's brush visible in the sky, demonstrating its orientation changes relative to the position of the observer, possibly aiding navigation (taken from Horvath et al., 2017). Areas with vertical* ***e****-vector orientation generate a horizontal yellow Haidinger's brush.*

A comprehensive analysis of the individual physiological parameters affecting Haidinger's brush perception and realistic simulations of its appearance and behaviour were provided by Misson, Temple and Anderson (2018). Their computational simulations of Haidinger's brush showed that individual variations in corneal birefringence, macular pigment density and macular pigment distribution may account for the reported varied human perceptions of Haidinger's brush.

Studies now show that human polarization sensitivity is not limited to Haidinger's brush (Temple et al., 2015, Misson et al., 2015), and the phrase 'polarization pattern perception' (PPP) has been adopted to describe human polarization sensitivity to polarization-modulated grating stimuli (Misson and Anderson, 2017). This novel technique has been developed utilising a modified LCD screen, displaying polarized gratings patterns, which are able to quantify sensitivity to polarized light (Misson and Anderson, 2017). Remarkably, it is now known that humans can discriminate between areas of linear polarization differing in **e**-vector orientation by as little as 4.4° (Misson and Anderson, 2017). As humans lack any known specialised photoreceptors or higher cortical processing mechanisms for detecting polarized light, this high level of sensitivity was an unexpected finding.

1.3.2. Mechanism of Human Polarized Light Perception

A common mechanism is believed to be involved in human perception of polarization patterned stimuli and Haidinger's brushes (Misson and Anderson, 2017), namely that humans can perceive both phenomena due to the radial arrangement of fibres in the Henle fibre layer at the macula combined with the presence of macular pigment (Misson and Anderson, 2017, Bone, 1980, Naylor and Stanworth, 1954a). This is depicted diagrammatically in figure 4. The Henle layer fibres comprise photoreceptor cell axons and other cells e.g. elongated Müller cells, that are radially arranged, and contain macular pigment molecules predominantly orientated perpendicular to the fibre direction (Bone and Landrum, 1984). The Henle fibres' lipid bilayer structure helps to maintain this regular macular pigment orientation (Bone and Landrum, 1984).

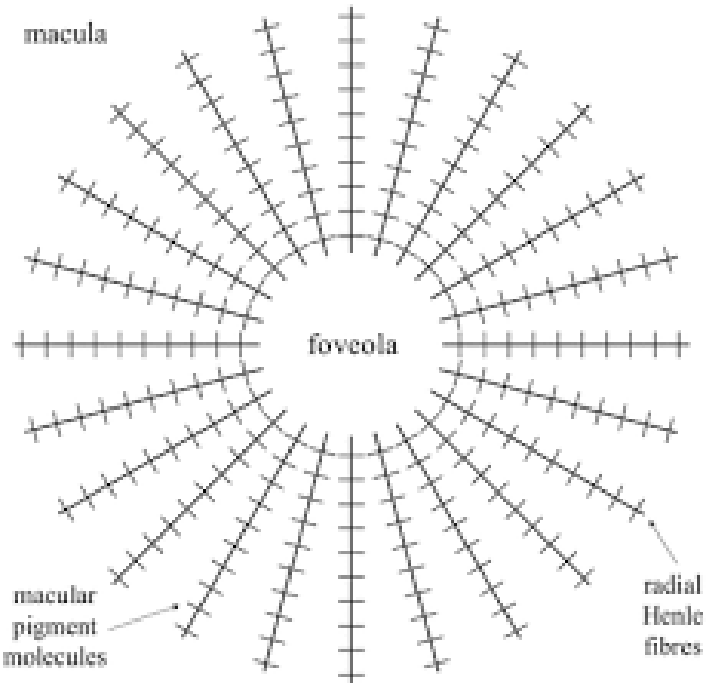

Figure 4. *Schematic radial diattenuator diagram showing radial Henle fibres with macular pigment molecules aligned perpendicular along their length, radiating out from the fovea (taken from McGregor et al., 2014).*

There are three macular pigments; lutein, zeaxanthin and mesozeaxanthin (Bernstein et al., 2016, Muller et al., 2016, Nolan et al., 2013). The macular pigments are inherently dichroic, and hence will differentially absorb light depending on its axis of polarization (Rothmayer et al., 2007, Bone and Landrum, 1984). If the incident polarized light stimulus is linear, the macular pigment molecules aligned with it, situated either side of the fovea, will absorb more strongly than adjacent molecules. This differential absorption, together with the radial symmetry of the Henle fibres, causes the macula to act as a radial diattenuating structure. In consequence, a plain field of polarized light, with no spatial structure within it, will nonetheless result in a spatially varied luminance contrast signal being generated. This can then be propagated to the cortex and processed in the usual way by the luminance- and contrast-sensitive mechanisms of the human visual system.

An incoming polarized light ray with a horizontal **e**-vector orientation will generate a vertically dark Haidinger's brush. This is so because the macular pigments above and below the fovea will absorb the strongest, as the dichroic macular pigments here will be

aligned with the incoming polarized light orientation. This is displayed diagrammatically in figure 5.

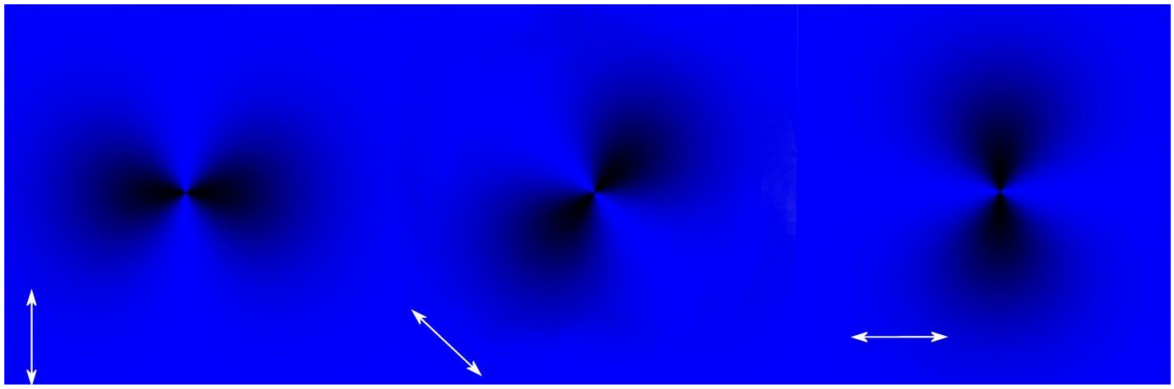

Figure 5. *Simulation of Haidinger's Brush with monochromatic illumination for three* ***e****-vector orientations. The white arrows depict the* ***e****-vector of the polarized light. In the right image, the white arrow depicts incoming horizontally linearly polarized light which generates a vertical dark brush. Images of simulated Haidinger's Brush courtesy of Prof G Misson.*

Other candidate structures for the perception of polarized light have been suggested, such as the form dichroism properties of photoreceptor cell axons (Hemenger, 1982) and short-wavelength sensitive blue cone geometry and dichroism (Le Floch et al., 2010). However, there is now a general consensus that the radial diattenuator model is the most likely physiological basis of polarization perception in humans (Misson and Anderson, 2017, Misson et al., 2015, Temple et al., 2015, Rothmayer et al., 2007, Bone and Landrum, 1984, Bone, 1980, Naylor and Stanworth, 1954a).

The radial diattenuator model has been accepted in large part because: (i) polarization perception shows a clear correspondence with the peak absorption spectrum of macular pigment molecules (figure 6), (Misson and Anderson, 2017, Muller et al., 2016, Stockman et al., 2000, Bone et al., 1992, Bone and Landrum, 1984, Naylor and Stanworth, 1954a); and (ii) polarization perception is confined to the central few degrees of vision, where macular pigments and the radial geometry of retinal structures are present (figure 10), (Misson and Anderson, 2017, Muller et al., 2016, Naylor and Stanworth, 1955).

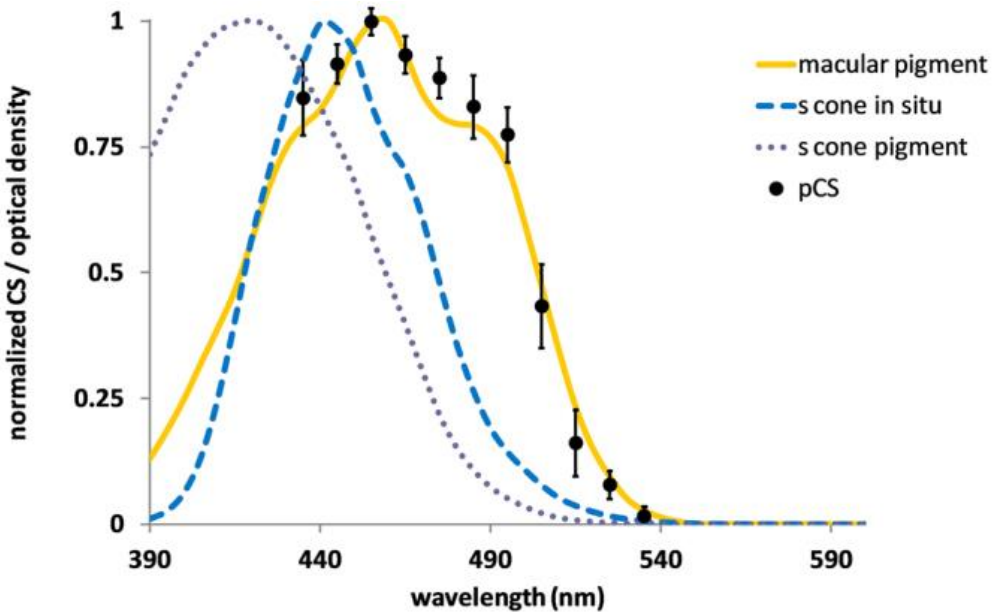

Figure 6. *Spectral characteristics of polarization perception are shown to closely follow the absorption spectrum of the macular pigments (taken from Misson and Anderson, 2017). Note that PPP does not follow the absorption spectrum of s cones in situ or s cones pigment absorption spectra, reducing the possibility of these as candidate structures for human polarization perception.*

1.3.3. Relevant literature for Human PPP studies

An influential study by Misson, Timmerman and Bryanston-Cross (2015) demonstrated, both theoretically and experimentally on a limited number of individuals, that humans could perceive patterned polarization stimuli. Their patterned and optotype stimuli differed in angle of polarization but with constant degree of polarization (see figure 7 and 8, respectively). Using the radial diattenuator model for Haidinger's brush perception, a simulation of the visual perception for different stimuli was made. Figure 7 shows how humans can perceive edge boundaries, which were then modified into grating and optotype stimuli. All participants could perceive the polarization-modulated spatial patterns, with some variability among individuals. The effect was limited to an area 6° wide, corresponding to the macular pigment area. Unlike Haidinger's brush, which fades quickly due to the Troxler effect (Clark, 1960), humans could perceive the static as well as kinetic stimuli. To control for potential luminance artefacts, they repeated the experiments with a quarter-wave retarder placed in front of the display screen. The retarder had the effect of converting the linearly polarized light into circularly polarized light, rendering the stimulus invisible for all participants. This was so

because circularly polarized light does not yield a luminance contrast signal. They proposed that, with further development, polarization stimuli may potentially be used to detect, quantify, and monitor macular changes.

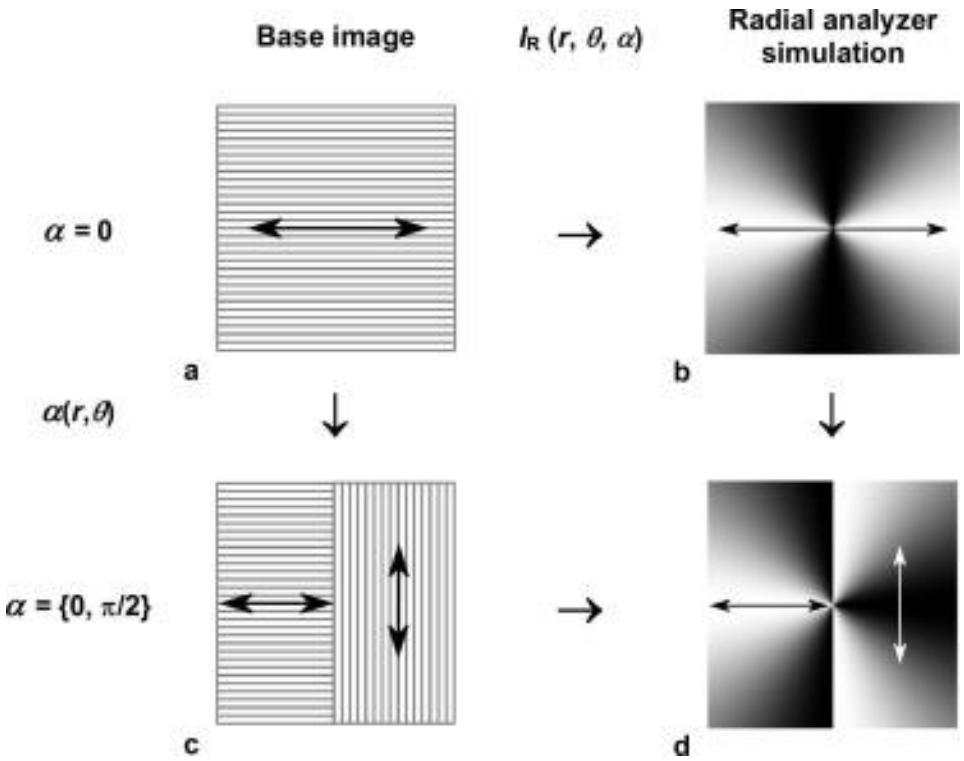

Figure 7. *Schematic diagram depicting horizontally polarized light generating a vertical dark Haidinger's brush, top row. The lower image shows how combining adjacent areas of differing e-vector orientation, show to the macula, would generate half a vertical Haidinger's brush and half a horizontal Haidinger's brush, thus maintaining the boundary perception (taken from Misson et al., 2015).*

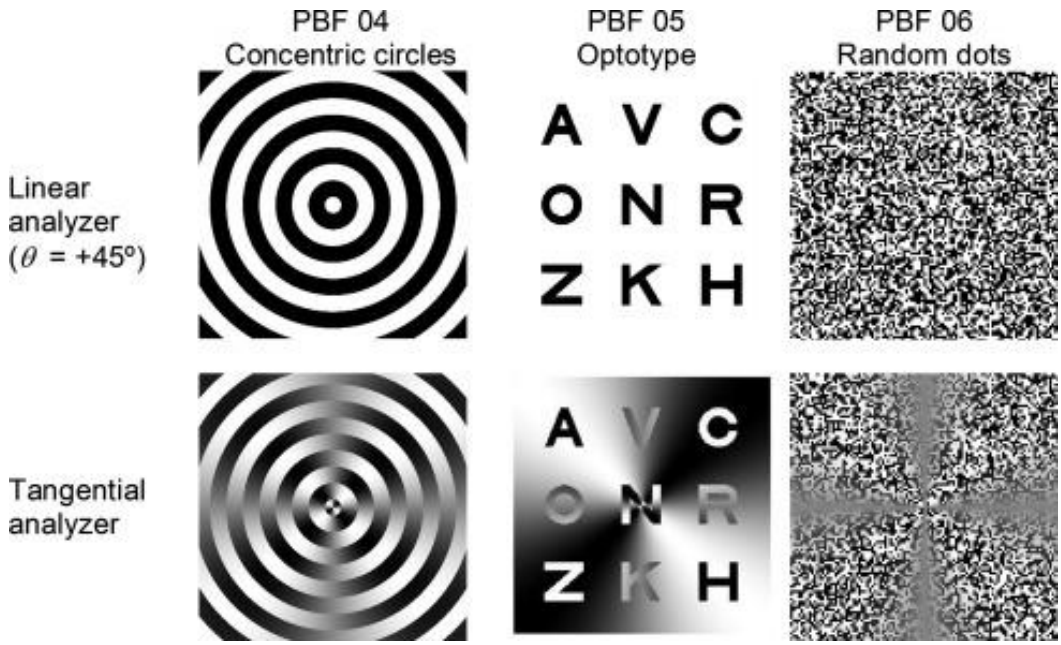

Figure 8. *Simulations depicting how complex polarization patterns, including concentric circles, optotypes and a brush, can be generated and perceived using polarized light. Black and white areas depict orthogonal states of linear polarized light (oriented at ±45°). The theory of the maintenance of the edge boundaries between the adjacent areas of differing* ***e****-vector orientation has been harnessed not only to produce gratings but also more complex shapes (taken from Misson et al., 2015).*

A similar LCD screen was used by Temple et al. (2015) to determine the lower limit of human polarization perception. They developed a two-orientation grating shown in polarization-only contrast, such that alternate bars of their grating differed in degree of polarization whilst maintaining a constant angle of polarization. By using various degrees of polarization, they could measure the lower threshold limits of human polarized light detection, achieving an average percent polarization threshold of approximately 56%, making humans the most sensitive vertebrate tested at that time. They suggested individual variations in corneal birefringence, macular pigment density and macular pigment organisation may explain the variability evident in the data (see figure 9). They proposed that polarization-only contrast gratings could allow for affordable, longitudinal monitoring of central visual field defects, congenital macular abnormalities, some forms of colour blindness, macular oedema, amblyopia, and low MPOD. The latter is a known risk factor for developing age-related macular degeneration (Evans and Lawrenson, 2017, Putnam, 2017, AREDS2, 2013, Dennison et al., 2013).

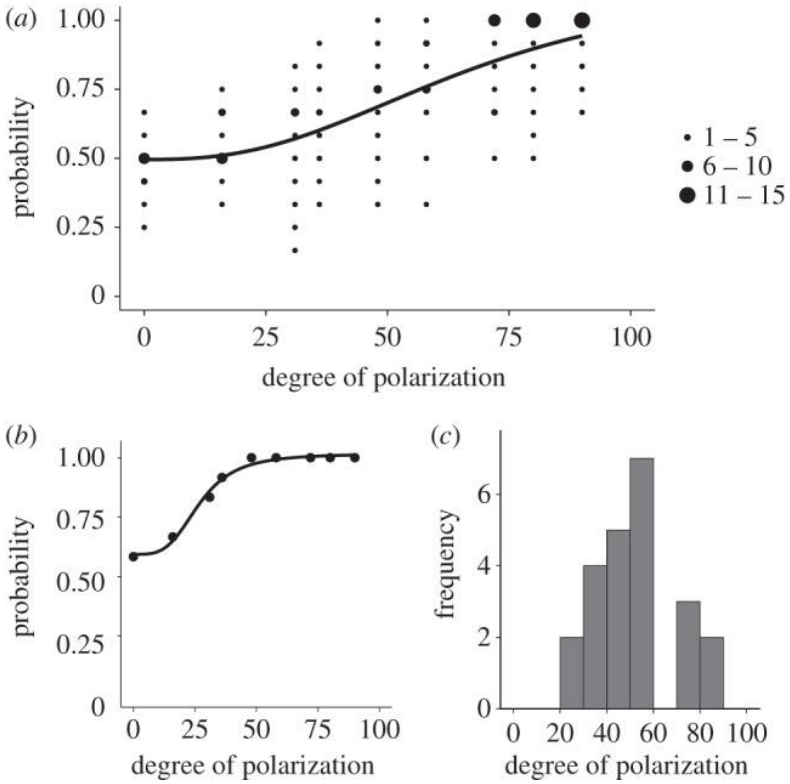

Figure 9. *Polarization thresholds for human participants with normal vision. (a) The mean (black curve) and variance (circles indicating number of participants) for the percentage polarization threshold curves. The mean percentage threshold of 56% corresponded to the stimulus setting where the 23 participants successful orientation discrimination fell below a probability of 0.75. (b) shows the results from one highly acute participant who was able to discriminate the grating to a polarization threshold of around 25% (c) shows that the variation in polarization threshold values followed the normal distribution. Individual percentage thresholds ranged from 23 to 87% (taken from Temple et al., 2015).*

A paper by Misson and Anderson (2017) introduced and quantified the spectral, spatial and contrast sensitivity of human polarization pattern perception (PPP) for both grating and optotype stimuli. They concluded that human PPP is of macular pigment origin as it closely followed the macular pigment distribution and density, peaking at the central fovea and declining sharply to negligible sensitivity levels at retinal eccentricities greater than 3° (see figure 10). This polarization sensitivity pattern matched the typical human macular pigment density pattern. Furthermore, polarization sensitivity showed a clear correspondence with the macular pigments' absorption spectrum, both peaking at 460nm (figure 6). The participants could discriminate polarization patterns in a range of sizes and contrasts. They demonstrated that the human eye could discriminate

differences in the angle of polarization between adjacent bars of the grating differing by as little as 4.4° (figure 11). They concluded that their findings supported the macular diattenuator model of polarization perception and support the development of human polarization pattern perception as a unique way of quantifying macular dysfunction in its earliest stages.

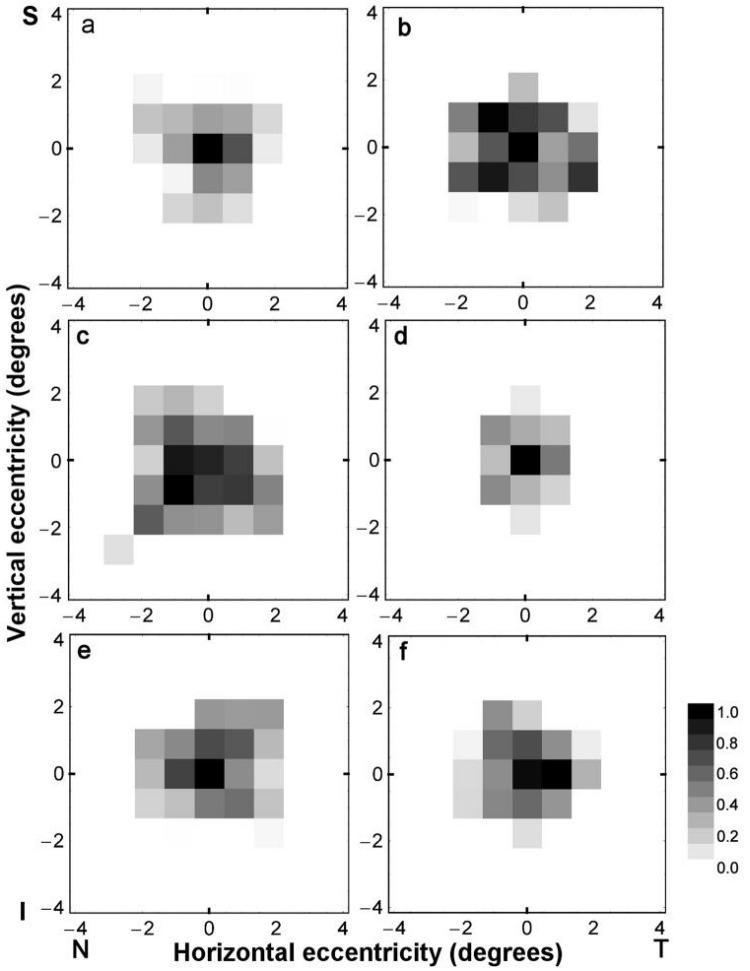

Figure 10. *Two-dimensional spatial map, for 6 individuals, detailing how PPP varies with eccentricity from the fovea. Darker greyscale represents higher PPP sensitivity. Note that PPP is confined to the macula, following the known distribution of the macular pigments (taken from Misson and Anderson, 2017).*

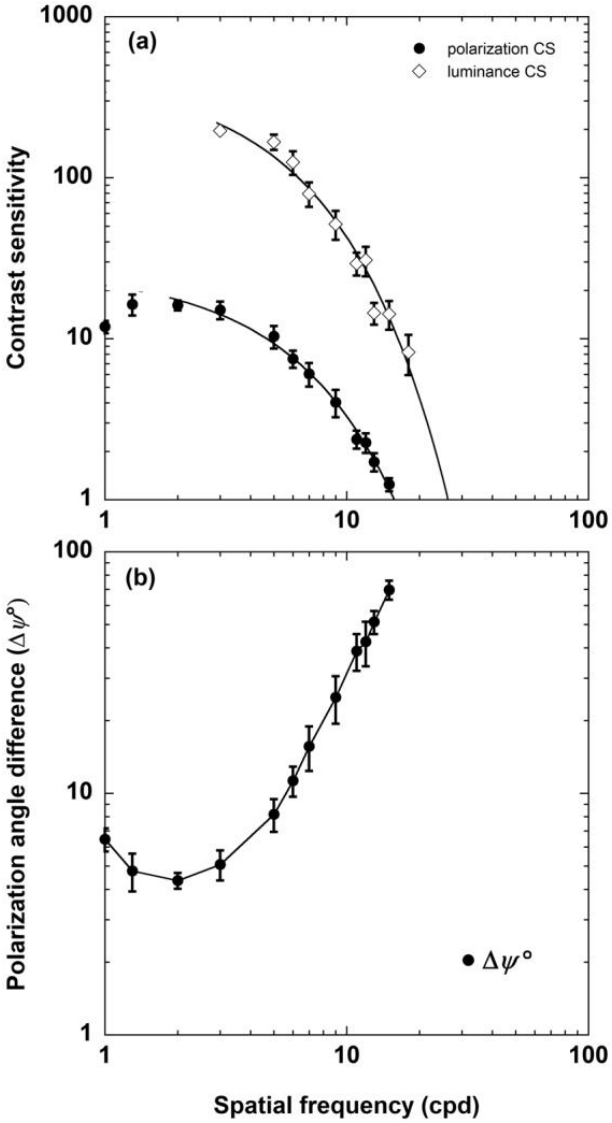

Figure 11. *Graph depicting binocular PPP measurement sensitivity from 6 observers (upper), replotted as minimum detectable polarization angle difference (lower). Peak sensitivity 2-3 cpd. Luminance contrast sensitivity is plotted showing the order of magnitude difference to polarization contrast sensitivity (taken from Misson and Anderson, 2017).*

Research on human polarization perception has used either the degree of polarization (Misson et al., 2019, Temple et al., 2015) or angle of polarization (Misson and Anderson, 2017, Misson et al., 2015) as a test variable. Here, for simplicity, 'degree contrast' is the term used when the stimulus and background have the same luminance and **e**-vector orientation but different degrees of polarization. Similarly, 'angle contrast' is used when the stimulus and background have the same degree of polarization and luminance but differ in **e**-vector orientation.

A simulation model of human polarization sensitivity was presented by Misson, Temple and Anderson (2019), comparing angle of polarization and degree of polarization stimuli. A twisted nematic LCD screen was used to generate changes in angle of polarization, and an in-plane switching LCD was used to generate degree of polarization changes—in all cases, equal display screen luminance and spectral outputs were maintained with changes in angle/degree of polarization. They showed that humans are approximately twice as sensitive to changes in angle contrast than degree contrast (see figure 12 for details). They concluded that changing the angle of polarization may prove to be a more robust measure of changes in macular function. In that study, participants detected changes in angle of polarization down to just 9° (Misson et al., 2019), similar to previous results (see figure 11). Note, however, that their modelling of the data did not include the effects of individual ocular retardation, which is a possible confounding effect requiring further investigation.

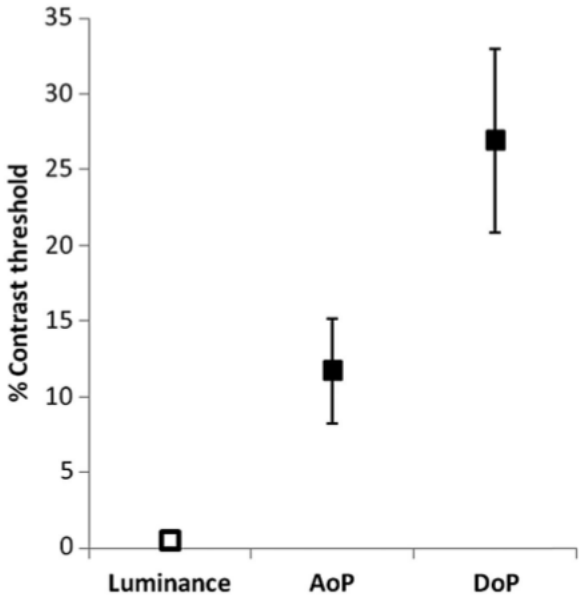

Figure 12. *Graph depicting the mean contrast threshold percentage for the detection of a 3cpd stimulus gratings displayed in luminance, degree, and angle polarization contrast for 5 experimental participants. It shows a mean contrast threshold of 11.7% ± 3.5 SEM, and mean 26.9% ± 6.1% SEM, for angle of polarization (AoP) and degree of polarization (DoP) respectively. Note from this graph that humans are approximately twice as sensitive to changes in angle contrast than degree contrast (taken from Misson et al., 2019).*

The study by Temple, Roberts and Misson (2019) theorized an exponential relationship between macular pigment optical density (MPOD) and polarization perception, providing experimental evidence in support of this on a limited number of individuals (see figure 13). They proposed a new method of macular pigment density screening using polarized light, asking participants to determine the direction of rotation of Haidinger's brush for various degrees of polarization. Individuals with more macular pigment were able to detect the stimuli at lower thresholds, believed to be due to their more effective macular radial diattenuator. Using their proposed single descent method gave a Coefficient of Repeatability (COR) of 0.119, which compares well with other MPOD techniques. Whilst this is acceptable for determining low, medium, or high levels, as is often required for giving advice in clinical settings, it may not be robust enough for monitoring slight changes in macular pigment density over time. Their data is displayed in figure 13. Note that there is considerable spread of data about the fitted exponential trendline, justifying the need for further research on the relationship between MPOD and polarized light sensitivity.

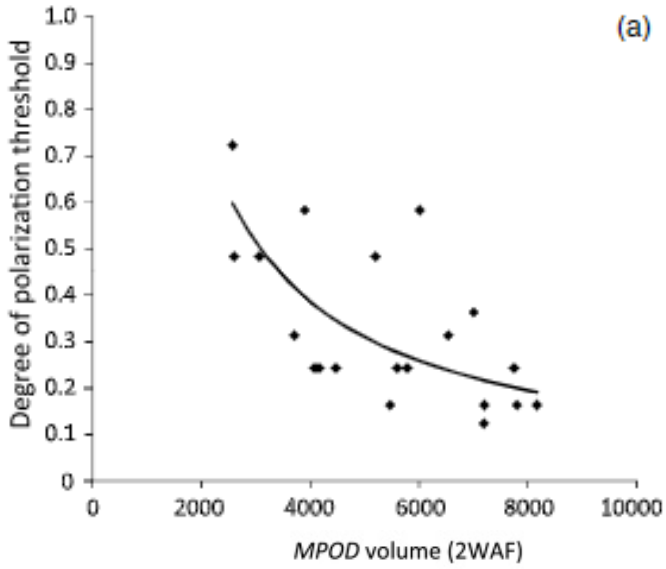

Figure 13. *Relationship between MPOD volume and degree of polarization threshold, as determined by measuring MPOP using the two-wavelength autofluorescence technique on the Heidelberg Spectralis (taken from Temple et al., 2019).*

Rotating Haidinger's brush direction was also utilised by Müller et al. (2016) at differing wavelengths. They studied healthy individuals and those with different types of macular

disease (see figure 14). Individuals with significant macular disease and low macular pigment density were mostly unable to perceive Haidinger's brush, even with preserved visual acuity, supporting the role of Haidinger's brush perception in macular pigment optical density and macular disease screening.

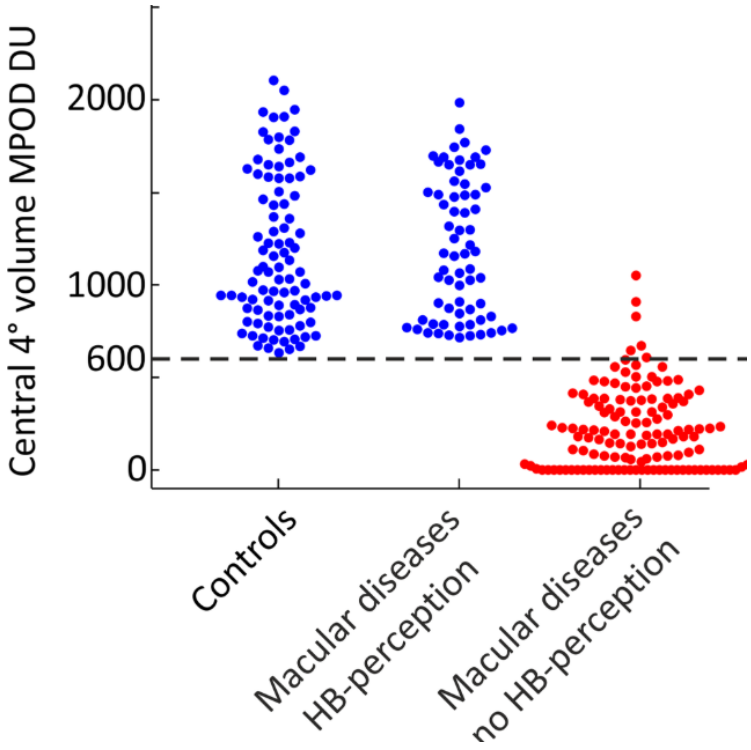

Figure 14. *Haidinger's brush (HB) perception and MPOD in macular disease. MPOD volume and ability to perceive Haidinger's brush are compared for control participants and those with macular disease, blue indicates that the participant was able to perceive Haidinger's brush and red indicates they were not. Note that Haidinger's brush was only perceived by those with MPOD volumes over the 600 DU limit, suggesting a dependency of Haidinger's brush perception on MPOD. Note also, that participants with macular disease were considerably less likely to perceive Haidinger's brush than the controls (taken from Müller et al., 2016).*

A recent paper was published by Misson, Temple and Anderson (2020) on the origin of, and relationship between, Maxwell's spot and Haidinger's brush (see section 4.4.2. for further details on Maxwell's spot). They found a novel phenomenon that as the polarization orientation or degree of polarization of the light was changed, the appearance of Maxwell's spot changed. Their work supported a common origin of Maxwell's spot and Haidinger's brush as their perceived sizes were correlated (Misson

et al., 2020b), which supports the radial diattenuator model as the origin of both (McGregor et al., 2014). This study supported the ongoing research into developing Maxwell's spot and Haidinger's brush for detecting and monitoring macula disease (Misson et al., 2020b).

1.4. Why PPP shows Considerable Variability Between Individuals

1.4.1. Individual Variation in Human Polarization Sensitivity

There is wide variation in the perception of both Haidinger's brush and PPP between different individuals. This variation is primarily thought to be due to inter-individual variations in macular structure, macular pigment optical density and corneal birefringence (Misson et al., 2018, Rothmayer et al., 2007).

Corneal birefringence is a property of the cornea to have a different refractive index depending on the polarization orientation of the incoming light. Corneal retardance is a measure of the corneal retardation from the phase shift between the two orthogonal components of light after they have passed through the cornea (Knighton and Huang, 2002). Variations in corneal retardation between individuals have been shown to affect the perception of Haidinger's Brush. The cornea is the main contributor to anterior segment retardance, while the lens and vitreous contribute a negligible amount (Bour, 1991, Bour and Lopes Cardozo, 1981). Muller fibres, the retinal nerve fibre layer and photoreceptor outer segments are also birefringent to a small degree within the retina, but are unlikely to significantly affect perception (Misson, 1993, Shute, 1978).

Given the low contrast nature of the Haidinger's brush entoptic phenomenon, its perception demands a considerable degree of visual attention. The latter is known to play a significant role in the ability to detect visual targets (Yamagishi et al., 2010) and, therefore, some of the individual variation reported for the perception of Haidinger's brush may be due to variation in visual attention. In this research project, to help minimise the effects of variations in visual attention, forced-choice procedures were used to measure PPP.

1.4.2. Individual Variability in Corneal Birefringence may affect PPP

The human cornea is intrinsically birefringent due to the ordered organisation of collagen layers within the stroma. Corneal birefringence is related to the double refraction created from the lamellar structure of the cornea and is known to vary widely among individuals (Knighton and Huang, 2002, Zhou and Weinreb, 2002). Often, the

cornea alters the polarization state of linearly polarized light, causing it to become partially elliptical when reaching the retina (Misson et al., 2018, Knighton and Huang, 2002, Misson, 1993). This effect is due to retardance of the incoming rays which depends on corneal thickness, birefringence and corneal fast/slow azimuth of retardation (Temple et al., 2015, Rothmayer et al., 2007, Knighton and Huang, 2002, Shute, 1974).

A study by Rothmayer et al. (2007) investigated the rotational dynamics of Haidinger's brush perception. They used simulations to determine the influence of birefringent structures in the eye on human polarization perception. They found that corneal birefringence has a significant influence on human polarization perception, and an individual with a significantly birefringent cornea will have a larger phase shift and show larger ellipticity in most orientations. This may reduce the contrast of the brush, unless it is aligned with the fast or slow corneal axis (see figure 15), making it more difficult to perceive Haidinger's brush (Misson, 1993). It is not known to what extent such factors affect an individual's PPP and will be explored by this research project.

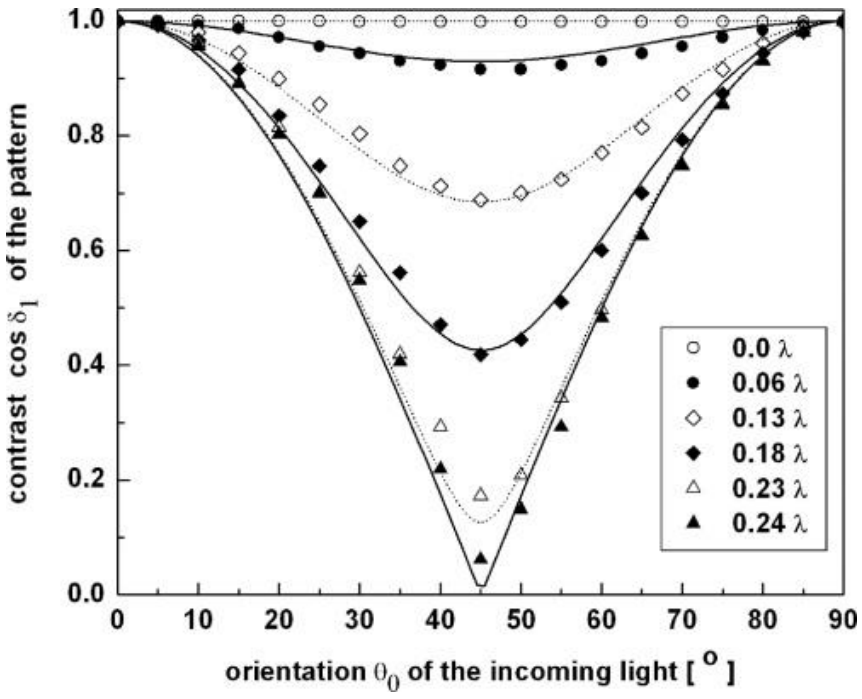

Figure 15. *The relationship between corneal retardation and contrast of the perceived Haidinger's brush pattern across a range of incoming light orientations. Note that as corneal retardation increases, the contrast of the brush becomes more variable, significantly diminishing in contrast at certain orientations. In some cases, for those with a highly birefringent cornea the contrast decreases to almost zero, rendering the Haidinger's brush stimuli indistinguishable when not aligned with their corneal fast and slow axes (taken from Rothmayer et al., 2007).*

1.4.3. Individual Variability in MPOD may affect PPP

Macular pigment optical density differs significantly among individuals and may contribute to differences in polarization perception. The macular pigments (lutein, zeaxanthin and mesozeaxanthin carotenoids) (Howells et al., 2011), can be obtained through diet (e.g. pigmented green vegetables such as spinach and kale, or by supplementation) (Neuringer et al., 2004). Macular pigments are thought to be located in the Henle fibre layer photoreceptor axons, predominantly lying between the outer plexiform and outer nuclear layer in the fovea and the inner plexiform layer in the parafovea (Muller et al., 2016, Bernstein et al., 2010, Bone and Landrum, 1984). Macular pigment optical density is determined by the amount of these carotenoids in the retina. The density of macular pigments is greatest near the fovea, decreasing rapidly into the periphery to negligible levels beyond 6-8° (Muller et al., 2016, Bernstein et al., 2010).

In healthy individuals, MPOD remains relatively stable throughout life (Meyer Zu Westrup et al., 2016, Beirne, 2014, Demirel et al., 2014), but macular pigments' spatial distribution pattern and density vary considerably among individuals (Ctori and Huntjens, 2017, Bernstein et al., 2010, Sharifzadeh et al., 2006, Davies and Morland, 2004, Hammond et al., 1997). These significant differences are likely to affect an individual's PPP to an unknown degree and require further study. It is thought that individuals with a higher volume of macular pigment may perceive polarization stimuli more acutely that those with low volumes, due to it acting as a superior radial diattenuator (see figure 4).

1.4.4. Heterochromatic Flicker Photometry and the MPS II

There are various methods to measure MPOD available to clinicians and researchers. MPOD can now be measured non-invasively in clinics using *in-vivo* psychophysical or objective methods. Unfortunately, there is not yet an absolute accepted gold standard (Putnam, 2017, Howells et al., 2011). The main psychophysical method used in practice is heterochromatic flicker photometry, but objective fundus autofluorescence and fundus reflectometry are also available (Putnam, 2017). MPOD varies widely between individuals from none, to over 1 log unit (Howells et al., 2011).

Average MPOD values are highly variable as the studies use various differing ways of measuring MPOD (e.g. heterochromatic flicker photometry, autofluorescence and fundus reflectometry), different equipment (e.g. Macuscope and MPSII), and have different study populations and ethnicities. Average MPOD values must be carefully compared as to the technique and machine being used, as they are not

interchangeable (Putnam, 2017, Creuzot-Garcher et al., 2014, Dennison et al., 2013, Canovas et al., 2010, van de Kraats et al., 2008, Wustemeyer et al., 2003). For example, van de Kraats et al. (2008) found a mean MPOD of 0.69 ±0.171 using a fundus reflectometry method, Wustemeyer et al. (2003) found 0.22 ±0.07 using an autofluorescence method, and van der Veen et al. (2009) found 0.33± 0.187 using heterochromatic flicker photometry.

Heterochromatic flicker photometry, as will be used in this research project, uses the spectral absorption properties of macular pigments to establish MPOD. The procedure uses two lights of different wavelength, one short-wavelength light that is maximally absorbed by macular pigments, and one long-wavelength light that is not absorbed by macular pigments (Putnam, 2017, Snodderly et al., 1984b). The two light sources are typically alternated such that they are seen to flicker. The radiance of the short-wavelength light is then adjusted until the perceived flicker is minimised. This is repeated at both foveal and parafoveal locations, where macular pigment is maximal and negligible, respectively (Putnam, 2017, Snodderly and Hammond, 1999). More short-wavelength light is required at the fovea than at a parafoveal location because a greater proportion of the light is absorbed by the macular pigments (Kirby et al., 2009, Loane et al., 2007). Comparing the log ratio of the intensity of blue light at the central and parafoveal locations gives the peak MPOD value (Putnam, 2017).

The MPS II is a desktop instrument that measures MPOD using heterochromatic flicker photometry. It is marketed as the MPS II/MPS 9000 in Europe by Elektron, and QuantifEYE by ZeaVision in the US. These supersede the first-generation instrument, formerly M:POD by Tinsley Instruments Ltd. It benefits from participants responding to the appearance, rather than disappearance, of the flicker, which is said to be easier for naïve participants (van der Veen et al., 2009). Standard mode estimates the parafoveal location from age norms, which is faster and has been shown to give acceptable values (see figure 16) (Makridaki et al., 2009).

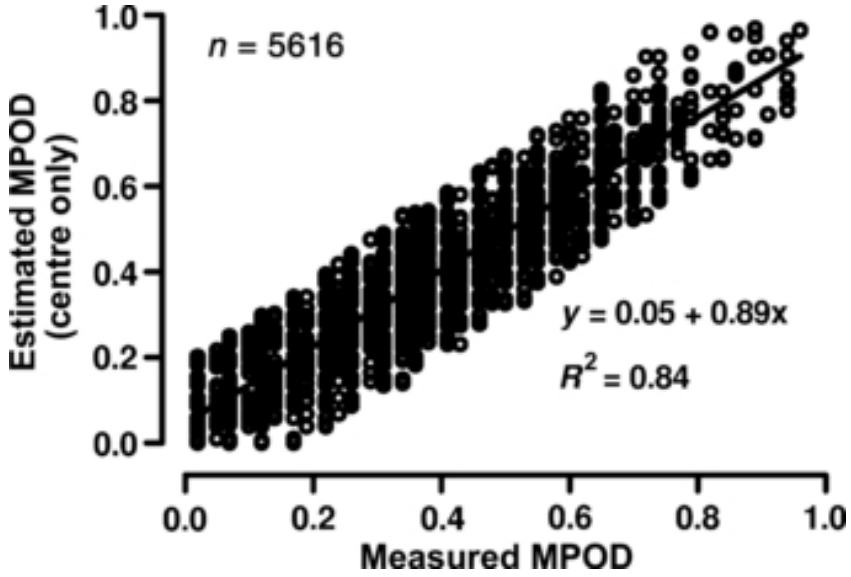

Figure 16. *This graph displays the relationship between MPOD measured using the standard centre only mode which estimated the parafoveal location using age norms, and the actual MPOD, calculated by measuring centrally and parafoveally. Note the close association between the two values, but at very low and high MPOD values the standard mode may overestimate or underestimate MPOD respectively (taken from Makridaki et al., 2009).*

1.4.5. Reliability and Repeatability of the MPS II

MPOD values from the MPS II have been shown to correlate well with in-vitro MPOD methods (Howells et al., 2011, Hammond et al., 2005). van der Veen et al. (2009) reported that the MPS II gave “fast, reliable and reproducible” estimates of MPOD which correlated well to an established objective reflectometry method. Howells et al. (2011)’s review of MPOD methods reported that heterochromatic flicker photometry has proven validity and provides repeatable measurements with good test-retest reliability for most participants.

Currently, subjective heterochromatic flicker photometry has gained general acceptance as the clinical standard and is an affordable and established option, but some models show poor repeatability and reliability results in some studies (Putnam, 2017). A common example is the MacuScope which showed poor reliability and high coefficient of variance (de Kinkelder et al., 2011, Hagen et al., 2010), and is not sensitive enough to monitor clinical changes (between sessions COR 0.58) (Bartlett et al., 2010a). Studies have been undertaken, using MPS II or equivalent, to determine its repeatability but data on a standardized technique and large-scale repeatability studies

are limited (Davey et al., 2016). Currently, the literature is variable. For the interested reader, see Howells et al. (2011), Bartlett et al. (2010b) and Putnam (2017) for reviews of *in-vivo* techniques.

The MPS II performs better in reliability studies than other commercially available subjective methods (de Kinkelder et al., 2011), (between sessions COR 0.33) (Bartlett et al., 2010b), or with technique modifications (COR 0.08) (Howells et al., 2013). This study on methods to improve the repeatability of the technique advocates removing suboptimal graphs and data, and repeating the result at least twice (Howells et al., 2013).

A few studies have concluded that the test-retest variability of the MPS II was unacceptable (Loughman et al., 2012, Bartlett et al., 2010b), but most show support for the technique (Davey et al., 2016, de Kinkelder et al., 2011, van der Veen et al., 2009). Studies supporting this device state that the MPS II provides good short-term repeatability and COR of 0.11 (Davey et al., 2016), and that it exhibits high test-retest agreement (-0.02 +/- 0.18) (de Kinkelder et al., 2011). The two main studies promoting the MPS II as unreliable used a limited number of individuals, aimed at detecting subtle changes in MPOD in a research setting only, and did not incorporate the technique modifications advised by Howells et al. (2013).

Heterochromatic flicker photometry using the MPS II has been selected to measure MPOD for this research project because it displays good reliability, in a compact and effective desktop unit. The technique modifications discussed to improve the repeatability will be incorporated by repeating the test three times and only using optimal graph shapes (see Appendix 3) to allow valid comparison to PPP results.

1.5. Justification for PPP measurement

Polarization pattern perception should, in principle, vary according to the organizational structure of the macula (Muller et al., 2016, Temple et al., 2015, Rothmayer et al., 2007, Bone and Landrum, 1984, Bone, 1980). Reduced PPP may indicate disruption of macula function, and as such it is hypothesized that monitoring PPP may aid early detection of macular disease. Given the ease with which a standard LCD monitor can be converted into a screen suitable for measuring polarization perception (details in Appendix 1), an inexpensive device to quantify PPP could be easily developed to allow a rapid and easily accessible test to routinely assess the macula. Such a device would allow health care professionals, in both developed and third-world countries, the

opportunity to manage many eye conditions before significant damage occurs. Current macular assessment methods (e.g. optical coherence tomography, Amsler grid or indirect ophthalmoscopy with a Volk lens) often have drawbacks such as expense or lack sensitivity. There is hope that measuring and quantifying PPP could help overcome this.

Macular disease encompasses a range of conditions affecting a patient's central vision. This can lead to a loss of vision, loss of independence, decreased quality of life and a social and economic burden, and hence the need to develop methods of detecting disease at earlier stages (Elshout et al., 2017, Cruess et al., 2008, Mitchell and Bradley, 2006). Age-related macular degeneration is currently the leading cause of sight impaired and severely sight impaired registrations in England and Wales (Quartilho et al., 2016).

Early detection is of primary importance in macular diseases that are currently controllable in their initial stages. These include diabetic maculopathy, macular oedema, and hydroxychloroquine retinopathy, diseases that can often be difficult to detect until irreversible damage has occurred. The importance of early detection has been the impetus for the current investment by the NHS in the nation-wide diabetic retinopathy screening service. Hydroxychloroquine retinopathy affects 7.5% of individuals taking this medication for over five years, and increases rapidly with increasing dose and duration of treatment (Yusuf et al., 2017). Initial signs of damage are hard to detect as they are asymptomatic and subclinical (Latasiewicz et al., 2017, Yusuf et al., 2017, Marmor et al., 2016, Melles and Marmor, 2014). Hopefully, advances in detection methods such as PPP may allow early detection of macular dysfunction, perhaps significantly earlier than is currently possible.

The clinical potential of using Haidinger's brush to gain information on macular function in disease has been considered previously (Muller et al., 2016, Forster, 1954, Goldschmidt, 1950), but has not been accepted into routine clinical practice. It has previously been suggested that being able to detect Haidinger's brush is good predictive marker prior to cataract surgery, as it is believed to help establish macular health behind the opacity (Muller et al., 2016, Sherman and Priestley, 1962, Naylor and Stanworth, 1955, Sloan and Naquin, 1955, Forster, 1954, Goldschmidt, 1950). Additionally, Haidinger's brush phenomenon has been employed to assess binocular vision anomalies and amblyopia (Wick, 1976, Sleight and Mashikian, 1971), and macular sparing in hemianopia (Perenin and Vadot, 1981). Le Floch et al. (2010) noted

that individuals perceive Haidinger's brush differently in their dominant and non-dominant eyes, suggesting that it could be used as a way of assessing eye dominance.

Although dry age-related macular degeneration is currently untreatable, it is clear that providing advice on modifiable lifestyle and nutrition factors can slow progression of the disease (Evans and Lawrenson, 2017, AREDS2, 2013). Low levels of macular pigments are a significant risk factor for the development of age-related macular degeneration (Trieschmann et al., 2003, Beatty et al., 2001, Bone et al., 2001), and detection helps tailor diet and supplementation advice (Weigert et al., 2011). Practitioners are aware that increasing levels of lutein and zeaxanthin in the diet increases MPOD (Weigert et al., 2011), helping to lower the risk of age-related macular degeneration (Evans and Lawrenson, 2017, Putnam, 2017, AREDS2, 2013, Dennison et al., 2013). Finally, potential novel treatments for dry macular degeneration such as stem cell therapy or novel drug treatments including neuroprotective brimonidine, anti-inflammatory corticosteroid fluocinolone and vasodilating drugs to improve choroidal blood flow, are in development (Sacconi et al., 2017). In brief, early detection of macular dysfunction is highly desirable, despite the fact that a limited number of treatments are currently available.

A study showed that, while all healthy participants were able to perceive Haidinger's brush under optimised viewing conditions, only 34% of those with macular disease could detect the phenomenon (Muller et al., 2016). Müller et al. (2016) argued that the structure and orientation of the macular pigment molecules need to remain relatively intact to perceive Haidinger's brush, and that the macular pigment density needs to remain above a certain level to perceive the phenomenon. This promoted its future role to determine an index of macular pigment density and macular health. Bone (1980) suggested an individual with higher MPOD should be able to detect polarized light more readily, as more macular pigments are present to act as a radial diattenuator (see also Temple, et al.,2019).

Haidinger's brushes fade quickly due to the Troxler effect and can be difficult for individuals to detect due to their subtle appearance (Misson et al., 2015, Rothmayer et al., 2007). The PPP grating methods employed by this research project aim to quantify polarization perception using hard-edged grating stimuli that do not fade quickly, and can be recognised by grating orientation (Misson and Anderson, 2017, Misson et al., 2015). It is believed that such stimuli may provide easily recognisable, quantifiable data to assess macular function in health and disease. This rapid, inexpensive, compact

PPP method may also allow for home monitoring or use in remote areas where alternative equipment is not available.

1.6. Justification of Aims

Early diagnosis of macular dysfunction is vital for providing early advice and treatment, which can ultimately prevent vision loss. Polarized stimuli have shown promise for development to fulfil this role of early detection and monitoring of macular dysfunction. Haidinger's brush stimuli have been used previously but were unacceptable due to their transient nature and subtlety. PPP appears superior as it is quantifiable, the image is sustained, and the task is easily understood by patients. Currently, normative PPP data, repeatability, how it correlates with MPOD and various ocular attributes are unknown.

This research project will establish normative human PPP sensitivity values across several decades of life, on a considerably larger group than previously examined. This, along with comparison to each participant's corneal and macular characteristics are expected to fill in the missing knowledge needed for a more complete understanding and future development of the technique. Importantly, the repeatability of the technique will also be explored. A correlation between PPP and each participant's ocular characteristics will primarily focus on the influence of corneal birefringence and MPOD variability as they are likely to have the greatest effect. Corneal retardation values are measured using the GDx VCC (Laser Diagnostic Technologies, Inc, San Diego, CA) scanning laser polarimeter with a variable corneal compensator. When combined with central corneal thickness (CCT) measurements from the optical coherence tomographer (Heidelberg Spectralis), a participant's maximum corneal birefringence can be calculated. The MPS II will be used to measure MPOD, allowing the relationship between MPOD and PPP to be determined.

1.7. Aims

The principal aim of this study was to collect normative data for sensitivity to patterned polarization stimuli across a range of ages on healthy adult participants aged 19-59. A secondary aim was to compare polarization sensitivity measures against existing metrics of macular thickness, central corneal thickness, corneal retardation and birefringence, refraction, and ocular dominance to determine the influence of each on PPP. These various metrics will be measured using a routine eye examination, optical coherence tomography and scanning laser polarimetry. To aid future development of clinical protocols for the assessment of macular function in health and disease, the repeatability of this technique will also be evaluated using a subgroup of participants. The final aim is to compare each participant's macular pigment optical density, as measured using heterochromatic flicker photometry, with their PPP sensitivity. The latter will help determine whether there is any significant correlation between these indirect measures of pigment density.

In summary:

(i) determine, as a function of age, a normative data set for sensitivity to patterned polarization stimuli (PPP).

(ii) compare and contrast these measures against variations between the participants' individual corneal and macula characteristics and baseline measurements.

(iii) assess the repeatability of the PPP technique.

(iv) evaluate the concordance between macular pigment optical density and PPP sensitivity measures.

Chapter 2

General Methods

2.1. Participants

A total of 84 participants (28 male, 56 female), aged between 19 and 59 years, took part in the study. Of these individuals, 35 continued their participation in the study by consenting to repeatability and corneal measurements, while 29 participants continued to MPOD measures. Participants included 29 staff from Aves Optometrists in Hertfordshire, and 55 individuals who had attended the said practice for a private eye examination. All were healthy individuals with no history of ocular pathology.

The inclusion criteria were: (i) Individuals aged 19 to 59 inclusive, with an up-to-date private eye examination conducted by the researcher; (ii) no significant ocular pathology in either eye; (iii) normal or corrected-to-normal monocular visual acuities of <0.1 Log MAR (6/7.5 or better Snellen); and (iv) participants must be able to provide fully informed consent and understand instructions given in English.

The exclusion criteria were: (i) Individuals aged under 19 or over 59 years old, or those with reduced understanding or reduced ability to provide informed consent; (ii) significant ocular pathology in either eye (e.g. cataracts, age-related macular disease, significant drusen within the macula area, acquired or genetic macular diseases, corneal diseases or visual field defects); and (iii) reduced visual acuity for any reason (e.g. amblyopia) in the eye being tested.

If a patient or member of staff met the inclusion criteria, they were invited to participate in the study. A participant information sheet was provided with time to make an informed decision, written consent was obtained before any additional examinations required for this study took place. Consent forms and participant information sheets can be found in Appendix 2. All participants were adults with sound ability to consent, removing higher-risk participants more prone to physical and psychological impact. Favourable opinion was given by Aston Ethics Committee (#1405), and all experimental procedures were in accordance with the tenets of the Declaration of Helsinki.

Power calculations were performed using GPower (version 3.1.9.2) (Faul et al., 2009). These indicated that 84 participants would be required for the main study to detect a significant result, using Pearson's correlation coefficient, for medium size effects (0.3) at the 5% significance level (α=0.05) with 80% power. Further GPower calculations for

the repeatability study showed that a subset of 34 of the participants were required to perform a t-test to detect statistically significant medium size effects (0.5) at the 5% significance level (α=0.05) with 80% power.

Further GPower calculations showed that 26 participants were required in experimental parts two and three, using a medium size effect (0.5) at the 5% significance level (α=0.05) with 80% power. These sample sizes provided a balance between the practical feasibilities of recruitment in a primary care setting and determining significant meaningful results.

2.2. Equipment and Procedures for Polarization Pattern Perception Measures

2.2.1. Delaminated LCD screen and Polarization stimuli generation

Liquid-crystal display screens (LCD) rely on altering the polarization of light. A conventional twisted nematic LCD screen, as outlined below, was manipulated for use in this study. Commercially available twisted nematic LCD screens consist of a laminate of five components as demonstrated in figure 17. To create a bright pixel, unpolarized light passes through the rear polarizer, then through liquid crystal molecules which twist the now polarized light through 90 °, allowing the light to pass through a front polarizer that is oriented perpendicular to the rear polarizer. To create a dark pixel, a voltage difference is applied across the transparent glass electrodes causing the liquid crystal molecules to align and change the orientation of the axis of (twist) polarization such that the light cannot pass through the front polarizer. Intermediate voltages can cause smaller twists of the angle of polarization, creating an intermediate greyscale value (Foster et al., 2018).

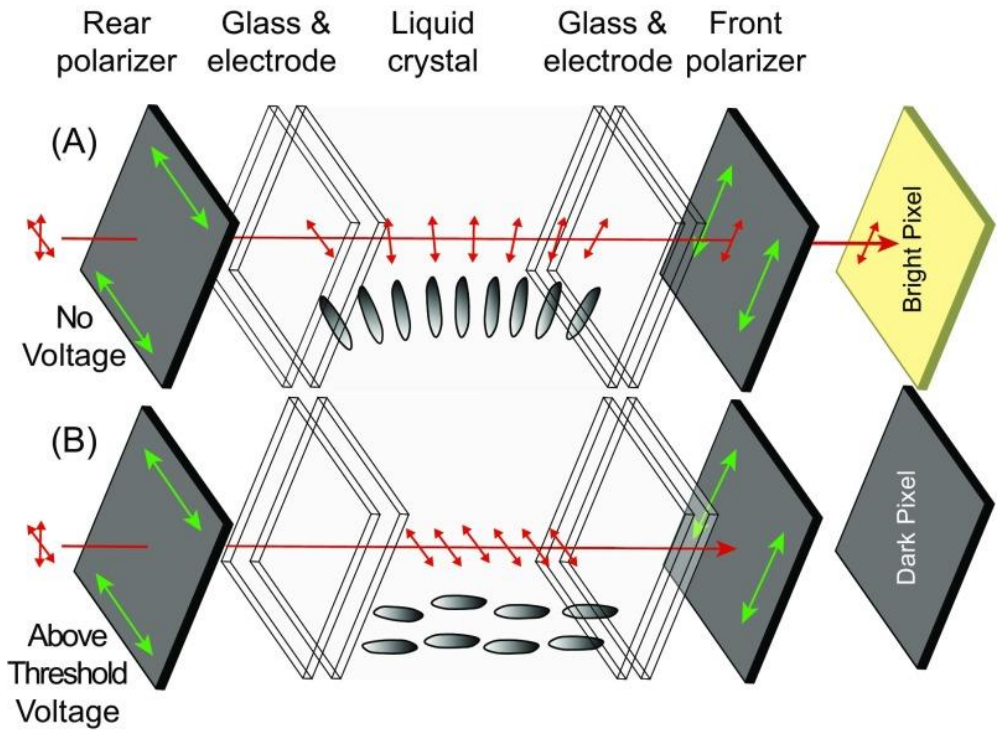

Figure 17. *A schematic diagram of twisted nematic LCD monitor layers (taken from Foster et al., 2018). See text for explanation.*

A conventional twisted nematic LED-backlit thin-film liquid crystal display was modified for this study, now called a delaminated LCD. The front polarizing filter was removed which allows an isoluminant, isochromatic stimulus, with a variable **e**-vector polarization angle to be produced. A blue filter (Lee filter #075, 'evening blue') was placed between the original LCD light source and the back polarizing filter, giving a stimulus light output peaking at 460nm, where the absorption spectrum of the macular pigments *in situ* is maximal. This protocol helps to generate a maximum polarization response (see figure 6) (Misson and Anderson, 2017). Full details of the screen, modification and calibration can be found in Appendix 1.

Stimuli were generated on a laptop computer and passed by HDMI cable to be displayed on the delaminated LCD screen. As depicted in figure 7, gratings displayed in this manner maintain their edge boundary between adjacent bars, allowing their orientation to be discriminated above threshold, even in polarization only contrast.

Each greyscale value sent from the laptop yields a specific polarization angle orientation on the delaminated LCD, rather than a specific shade of grey as would be

produced by a regular LCD screen. A luminance-modulated grating would usually be made up of adjacent bars with two differing luminance/greyscale values, but as each greyscale now produces a different angle of polarization, this can be manipulated into gratings showing a range of polarization angle differences. The luminance-modulated grating, when shown on the delaminated LCD, appears as a polarization-modulated grating, with adjacent bars having the same luminance but differing angles of polarization.

Just as in a normal luminance setting where the difference in luminance difference between adjacent bars would be gradually reduced until a participant could no longer detect the difference, the delaminated screen allows smaller differences in the angle of polarization between adjacent bars until they can no longer be distinguished apart. This allows a polarization pattern perception threshold value to be obtained in terms of angle of polarization, taking the reciprocal of this converts readings into polarization contrast sensitivity. Using filters or different LCD display technology (e.g. in-plane switching) it is also possible to do this for degree of polarization as reported by Temple et al. (2015) and Misson, Temple and Anderson (2019).

For the LCD used in this study, different greyscales represent different angles of polarized light; hence it is possible to assign a certain polarization angle generated on the delaminated LCD to a given greyscale value. This is a non-linear relationship, the exact greyscale values needed for each polarization angle orientation for this screen are shown in supplementary figure 5, Appendix 1 along with the method for converting to polarization angle difference.

The delaminated LCD screen was prepared and calibrated by Prof Gary Misson (Aston University). Full spectrometry, photometry and degree of polarization calibration, and screen details for this modified LCD screen are displayed in Appendix 1. The spectral output profile and luminance was the same for all greyscale values used, achieving a high degree of polarization, with minimal ellipticity.

2.2.2. PPP Measurement Procedure

For the main study, monocular readings were performed on each participant's dominant eye. Dominance was determined using a basic sighting test known as Miles technique (Mapp et al., 2003), with hands extended in a triangle.

Following their routine eye examination, all 84 participants for the main study had three monocular PPP measurements on their dominant eye using the modified LCD screen. They also underwent optical coherence tomography scans of their dominant eye. The

measurements were made in one sitting and took approximately 20 minutes to complete.

The participants viewed the polarized stimuli through optically isotropic glass trial lenses, with an appropriate reading addition for one meter incorporated for presbyopic participants. Non-birefringent glass lenses were used, rather than the patient's spectacles, as stress in plastic lenses or varifocals could influence the polarization state of light reaching the eye.

A square wave polarization grating was displayed on the modified LCD at a viewing distance of one meter in a semi-darkened room. The same room and lighting conditions were used for all PPP measurements, taken during a six-month period. The spatial frequency of the stimulus grating was 3 cycles/degree. This periodicity was chosen because it is near the optimum spatial periodicity for viewing polarization patterns (Misson and Anderson, 2017), and it allowed a sufficient number of cycles to be displayed on the LCD screen. The target filled the screen size, which was 12.1cm x 17.3cm. Using 3 cycles/degree at 1 meter allows a minimum of 21 cycles of square wave grating to be displayed on the screen.

Prior to any PPP measurements, participants were shown a demonstration of the stimuli as an equivalent luminance-modulated grating on a conventional liquid crystal display and were given the opportunity to practice pressing the four directional arrow choices on the keypad. They were then shown the stimuli on the delaminated LCD screen with the polarizing filter in front, so that they could become accustomed to the blue screen and the size of the grating bars expected. The polarizing filter was then removed. A chin and forehead rest at 1m was used to keep the participants viewing normal to the screen, eliminating intensity artefacts from oblique viewing (Foster et al., 2018). Participants were reassured that the stimuli are faint and that they were not expected to see a grating on all trials. They were allowed free eye movement across the screen to help them view the PPP stimuli. Results were selected by the participant pressing the equivalent direction button on the handheld keypad. When a grating orientation was chosen, a noise was generated to indicate if the response was correct or incorrect and the next grating was then displayed.

Participants discriminated the orientation of the grating using a four-alternate forced-choice paradigm, displayed with a modified version of the Freiburg Visual Acuity and Contrast test (FrACT Version 3.9.8). The paradigm used the best parameter estimation by sequential testing algorithm (best PEST) for adaptive threshold determination (Bach, 2007). This staircase method aims to improve the psychophysical threshold estimate

within a short time period by presenting the stimuli more often near the most likely threshold. Each run consisted of 24 trials. This was completed three times for each participant (3x 24 trials), and a mean of the three readings was obtained.

This polarization pattern perception sensitivity data is utilised in all experimental sections in this research project. Experimental part one used the main study group to assess monocular sensitivity to polarization pattern stimuli as a function of age, and the repeatability subgroup to measure the repeatability of the technique. Experimental part two utilised the MPOD study subgroup to compare monocular PPP sensitivity with macular pigment optical density measures. Experimental part three compared monocular PPP sensitivity with other ocular characteristics, including measures of macular and corneal thickness, spectacle refraction, eye dominance and corneal birefringence.

2.2.3. PPP Repeatability Procedure

A subgroup of 35 participants volunteered for the repeatability subgroup study, with 34 completing all measurements. Using the same polarization pattern perception measurement procedures described above, this group of participants performed the measurements monocularly on both eyes, and then repeated these measurements, on a separate, mutually convenient occasion.

The repeatability subgroup data was analysed to assess the techniques repeatability by using a Bland-Altman intra-class correlation coefficient plot to obtain the Coefficient of Repeatability.

2.3. Equipment and Procedures for Ocular Characteristics Measures

A brief description of the commercially available instruments used (Heidelberg Spectralis optical coherence tomographer, GDx VCC scanning laser polarimeter and MPS II macular pigment screener) is given below, together with details of how they were employed in this experiment.

2.3.1. Optical Coherence Tomography

The Heidelberg Spectralis optical coherence tomographer (Heidelberg Engineering, Heidelberg, Germany), was used to measure corneal and macular characteristics. It analyses the reflection of light from ocular structures via a split beam, using spectral-domain technology and advanced eye tracking, to produce high-resolution 3D scans. The Spectralis is widely accepted as a gold standard, non-invasive technique to image

the fundus (Barteselli et al., 2013), and can be adapted to image the cornea by the addition of an anterior lens to give a high-resolution cross-section of the central cornea.

Optical coherence tomography was used to measure central corneal thickness and central foveal thickness of the dominant eye of each participant in the main study group, and both eyes of the repeatability subgroup.

The device was focussed and positioned over the centre of the cornea. The inbuilt automatic real-time eye tracking (ART) was enabled and set at 60, thus combining 60 scans into one single high-resolution composite B scan of the cornea. The central corneal thickness, defined as the distance from the posterior surface of the corneal endothelium to the anterior surface of the epithelium, was measured manually. This was achieved by enlarging the composite corneal scan to 800%, selecting the measuring icon tool, then clicking on the appropriate corneal structures to be measured between (i.e. the central posterior corneal endothelium and anterior corneal epithelium).

The anterior module lens was then exchanged with a standard 30° objective lens to image the macula. The participant was instructed to look at a blue fixation cross in the Spectralis, and the operator adjusted the focus onto their retina. The Glaucoma Premium Module and ART were activated, and a horizontal three-dimensional volume dense scan consisting of 61 horizontal B-scans (with an ART of 9 to reduce noise) was taken. This scan took a 30° x 20° image, centred on the fovea, and aligned with the optic disc. The foveal pit and Bruch's membrane opening were determined automatically by the Spectralis and confirmed manually by the operator and adjusted as necessary. This scan type was used as it ensures the image is centred on the fovea, so that an accurate minimum foveal thickness could be recorded.

The confocal imaging system and infrared beam (870nm) do not significantly stimulate pupil constriction, so dilation was not necessary (Barteselli et al., 2013).

2.3.2. GDx VCC

A Zeiss GDx VCC (Glaucoma detection scanning laser polarimeter with variable corneal compensator, Laser Diagnostic Technologies, Inc, San Diego, CA) scanning laser polarimeter, is typically used for glaucoma detection. However, with a variable corneal compensator attached, it can be used to measure corneal retardation magnitude. A beam of polarized light (780nm) is split by a polarizer and then projected into the eye (Da Pozzo et al., 2009). Different wavelengths are used between the GDx and PPP screen, as they measure different properties. The GDx measures corneal

retardance, while the PPP technique measures polarization contrast sensitivity. The cornea acts as a linear retarder, with slow and fast axes orthogonal to each other. The polarized light travels faster when its **e**-vector is aligned with the fast axis of the cornea, which causes the projected linearly polarized laser beam to become partially elliptical when reaching the fundus. The variable corneal compensator measures an individual's anterior segment retardance prior to taking retinal measurements, so the effect of the cornea can be counteracted. The GDx VCC uses the non-uniform polarization pattern generated by the cornea, which generates a bow tie image on the uniformly birefringent Henle fibre layer image of the macula, enabling corneal retardance to be determined (Knighton et al., 2008, Knighton et al., 2002, Zhou and Weinreb, 2002).

Each member of the repeatability subgroup underwent a GDx VCC scan, to give an index of their corneal retardation magnitude. To perform this technique, the participants were seated comfortably and asked to fixate the red blinking light fixation target. The device was aligned and focussed until 'OK' was displayed by the device for alignment, fixation, and refraction. Each scan generated a quality score automatically. Only good quality scores, as defined by the manufacturer (namely, ≥8/10), were accepted (Da Pozzo et al., 2009).

The device is centred over the macula initially to assess the effects of the corneal retardation, then over the optic nerve head to measure the retinal nerve fibre layer thickness around the disc. Both macula and optic nerve head scans had to be completed to allow the device to save the data and produce the corneal retardation data needed for this study. After completion of these measurements, a macular retardation map was produced, with corneal retardation magnitude and axis values automatically generated. When combined with central corneal thickness, the corneal retardation magnitude data was used to calculate the maximum corneal birefringence using the formula:

Corneal Birefringence= Corneal Retardance (µm)/Central Corneal Thickness (µm).

2.3.3. MPOD measurement

The MPS II was used to measure macular pigment optical density (MPOD). This desktop instrument uses the heterochromatic flicker principle to establish macular pigment density. An inbuilt pre-test determines individual sensitivity to flicker to give an individualised test at an appropriate level. The radiance of a blue light (460nm) and green light (540nm) are altered for a series of blue-green luminance ratios until a flicker response curve is generated (Putnam, 2017, Snodderly et al., 1984b). The MPS II presents a range of different intensity ratios and the flicker frequency for each is slowly

changed. The flicker is harder to detect near an individual's isoluminance point, so the frequency of the flicker must be lower before it can be detected, creating a minima on the graph. This continues until the minima is passed. A shift of the minimum point towards the right along the x-axis means more blue light is required in the ratio to minimize flicker, thus giving a higher MPOD value (Davey et al., 2016, Loughman et al., 2012). The MPS II also takes into account age-related yellowing of the lens via a correction factor (Davey et al., 2016). More short-wavelength light is required at the fovea than at a parafoveal location, because a greater proportion of the light is absorbed by the macular pigments (Kirby et al., 2009, Loane et al., 2007).

Macular pigment optical density measures were competed on 29 participants, measured centrally on standard mode, using a 1° diameter foveal target (van der Veen et al., 2009). The procedure was carried out in accordance with the manufacturer's standard mode protocol. The procedure was carried out under mesopic conditions, with a near correction in place if required. The participant was asked to fixate the central target and press a response button when they first perceived the onset of flicker. The standard mode was chosen as all participants met the criteria for standard mode being applicable by the manufacturer, namely those with no significant ocular pathology and who conform to age-normal parameters. In this mode, the parafoveal measurement, where macular pigment is negligible, is estimated by the machine. The MPS II provides a reliability guide for each MPOD reading, and any poor-quality readings were repeated until three acceptable readings, with clearly defined output curves, were obtained. Curves with the expected downward S, U or V shape with definite low points were accepted. Refer to Appendix 3 for acceptable curve shapes. The mean of three good measurements was determined to give a mean MPOD value for each participant.

Chapter 3- Results and Discussion

3.1. Experimental Part 1

Normative PPP: The influence of age and the repeatability of Polarization Pattern Perception

3.1.1. Introduction and Aims

Until recently, Haidinger's brushes (Haidinger, 1844) were believed to constitute the full extent of human polarization sensitivity. Prior to studies by Misson et al. (2015) and Temple et al. (2015), human polarization sensitivity was thought to be rudimentary. They developed novel, static, polarization-modulated patterned stimuli, displayed on a modified LCD screen in polarization-only contrast and showed that humans are much more sensitive to polarized light stimuli than previously thought (Misson et al., 2015, Temple et al., 2015). This was developed into quantifiable polarization-modulated gratings stimuli in 2017, namely Polarization Pattern Perception (PPP) (Misson and Anderson, 2017). Misson and Anderson (2017) demonstrated that human polarization sensitivity was significantly more acute than previously thought and provided evidence in support of polarization perception being of macular origin, as it closely matched the spectral characteristics and distribution of the macular pigments.

It is widely accepted that human polarization sensitivity to Haidinger's brush and PPP arises due to the organizational arrangement of the Henle fibres and macular pigment molecules within the macula, which act as a radial diattenuating structure (Misson et al., 2019, Misson et al., 2018, Misson and Anderson, 2017, Muller et al., 2016, Bone, 1980, Naylor and Stanworth, 1954a). Macular pigment molecules are inherently dichroic, thus absorb more strongly when the **e**-vector of incoming polarized light is aligned with the molecule's orientation. This differential absorption, together with the radial symmetry of structures around the macula, results in a luminance contrast signal being generated. This then propagates to the cortex and is processed in the usual way by the human visual system. When considering this mechanism of detection, it is likely that PPP will be reduced if the structure of the macula is disrupted (e.g. in age related macular degeneration).

The main objectives of this section were to establish monocular sensitivity to polarization patterned stimuli as a function of age (19-59 years), and to assess the

repeatability of the PPP technique. Data on the normative trend with age and repeatability of the technique is currently unknown. Establishing repeatability data will aid in the future development of protocols, especially with the view to assessing macular function in health and disease.

3.1.2. Methods

A detailed account of the participants, polarization stimuli, equipment, and experimental procedures are provided by chapter 2. The specific methods related to this part are reported here. Detailed screen calibration data is reported in Appendix 1. A simplified diagram of the set-up is depicted in figure 18.

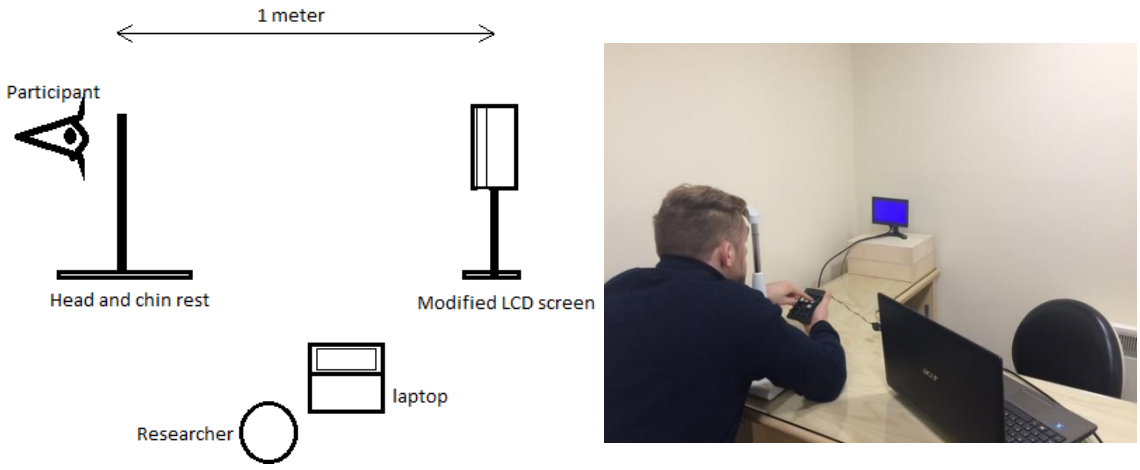

Figure 18. *Left: A diagrammatic representation of the set-up used for PPP measurement. Right: A photograph of the same set-up, shown with the room lights on for imaging purposes only. Permission from the model was obtained.*

A total of 84 participants (age range 19-59 years) had their polarization pattern perception assessed with dominant eye viewing. This was done immediately following their routine eye examination. A subgroup of 34 of these participants also completed polarization measures with non-dominant eye viewing. In addition, this subgroup returned on another mutually convenient occasion to repeat all the measurements. Ten of these participants also completed binocular polarization sensitivity measurements.

Square wave modulated polarization gratings were used to establish contrast threshold polarization perception values for each participant. Contrast threshold polarization measures were determined using FrACT psychophysical software, based on three separate runs of 24 trials to determine mean polarization sensitivity. Sensitivity of

contrast threshold was plotted i.e. the reciprocal of contrast threshold. Details of the conversion to polarization angle difference are given in Appendix 1.

A Shapiro Wilk test for normality was performed on the collected PPP data, which showed that polarization pattern sensitivity is not normally distributed (S-W statistic = 0.93, df = 84, p = <.001). A histogram of this data showed there is positive skewness (statistic = 1.10, standard error = .26) and significant kurtosis (statistic = 1.39, standard error = .520). As PPP is not normally distributed, non-parametric statistical tests have been used to analyse the PPP data.

3.1.3. Results and Discussion

3.1.3.1. Age

Mean polarization pattern contrast sensitivity is plotted as a function of age, for 84 participants, aged 19 to 59 years in figure 19. The mean, monocular, polarization contrast sensitivity for the population studied was 5.17 (SEM 0.26). The dotted trend line depicts the line of best fit through the scatter graph data points. Note that there was a minimal decrease in polarization sensitivity with age, but that this was not statistically significant (Spearman's rank correlation coefficient = -0.205, n = 84, p = .061, two-tailed).

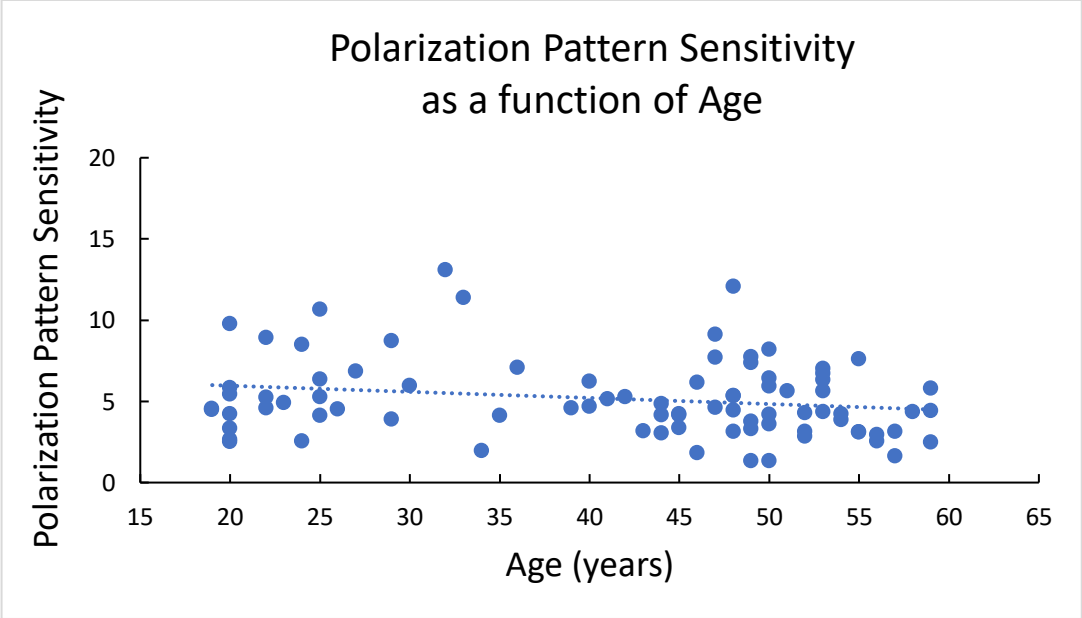

Figure 19. *The relationship between mean PPP sensitivity and age, for all participants' dominant eyes. There was no statistically significant relationship (p > .05) between age and PPP. The blue dotted line shows the regression line, plotted with the equation y = -0.0376x + 6.7145.*

In figure 20, the polarization data for the entire cohort was divided into two age range bins, namely, 19-39 years, and 40-59 years. This bar chart shows that there was no significant difference in PPP sensitivity between the younger group (μ = 5.88, SEM, 0.51) and the older group (μ = 4.77, SEM, 0.28). The error bars do not overlap, but this difference did not prove to be statistically significant (p >.05) using a Mann Whitney U test (U = 625, p = .084).

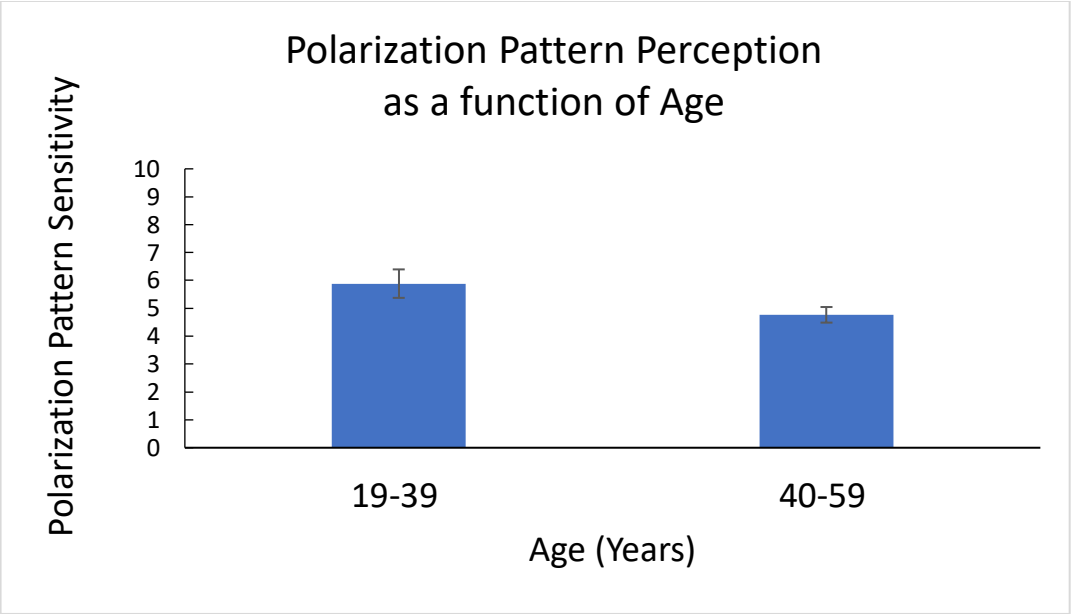

Figure 20. *Bar chart comparing mean PPP sensitivity with age. Error bars show SEM for each group. There was no significant difference in PPP sensitivity between the groups.*

These results are in general agreement with evidence that, in healthy individuals, macular pigment optical density remains relatively stable throughout life (Meyer Zu Westrup et al., 2016, Beirne, 2014, Demirel et al., 2014), and that despite some composition and thickness changes, the general macular structure remains relatively stable in the absence of any pathology (Nusinowitz et al., 2018, Ardeljan and Chan, 2013, Okubo et al., 1999). As the spatial arrangement and function of macular pigment forms the basis of polarization perception, this stability could account for the lack of any significant decline found in PPP with increasing age. The lack of any significant effect of age on PPP, between 19 and 59 years, is also consistent with the results of Müller et al. (2016), who reported that age did not have a statistically significant impact on the perception of Haidinger's brushes. These findings are for participants between 19 and 59 years old, however there may be an effect beyond the age range tested.

The stability of polarization sensitivity within this age range is consistent with other studies showing stability, or minimal declines, in other visual characteristics within these ages (Haegerstrom-Portnoy et al., 1999, Johnson and Choy, 1987). For example, Haegerstrom-Portnoy et al (1999) demonstrated a minimal and gradual decline in contrast sensitivity with age in adulthood up until 65 years, after which a more significant decline occurs (see figure 21).

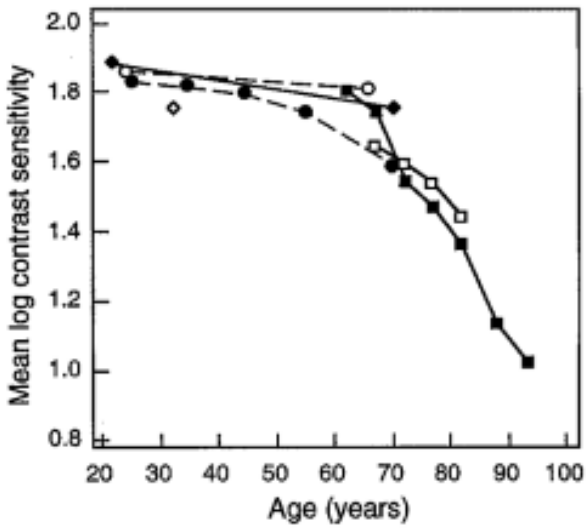

Figure 21. *The graph depicts the decline in contrast sensitivity, measured using a Pelli-Robson chart, with age using results from four studies. Note the common theme of a minimal change up to approximately age 65, then rapid decline following this (taken from Haegerstrom-Portnoy et al., 1999).*

The monocular polarization pattern sensitivity value for healthy individuals aged 19-59 was 5.17 (range 1.34 to 13.12), obtained from a sample of 84 naïve participants. Figure 22 depicts a comparison between this research project's results and the results from two previously published studies (Misson et al., 2019, Misson and Anderson, 2017), which were conducted using a comparable equipment/protocol to this experiment. The values obtained are comparable to the previously published, smaller scale experimental pilot studies (Misson et al., 2019, Misson and Anderson, 2017). Note, however, that Misson et al's. (2017, 2019) binocular PPP values are higher than the monocular value reported here. This is to be expected, as it is well known that various binocular measures of visual performance are approximately √2 to 2x larger than monocular measures (Baker et al., 2018).

To allow for a robust comparison, binocular polarization pattern sensitivity measures were completed on a limited number of individuals from the repeatability subgroup (n=10), using the same protocol as the monocular measures. The binocular polarization contrast sensitivity of the ten participants was 7.35 (SEM 0.71), which is consistent with published studies where a binocular protocol was employed. The study results were also consistent with Baker et al. (2018) as the binocular measures were 1.4x more sensitive than monocular measures (approximately √2). These binocular measures showed similar trends to the monocular data, with a significant positive correlation between repeated readings (Spearman's rank correlation 0.685, p = .029). The minimal decrease in binocular polarization contrast sensitivity with age (Spearman's rank correlation -0.354) was not statistically significant.

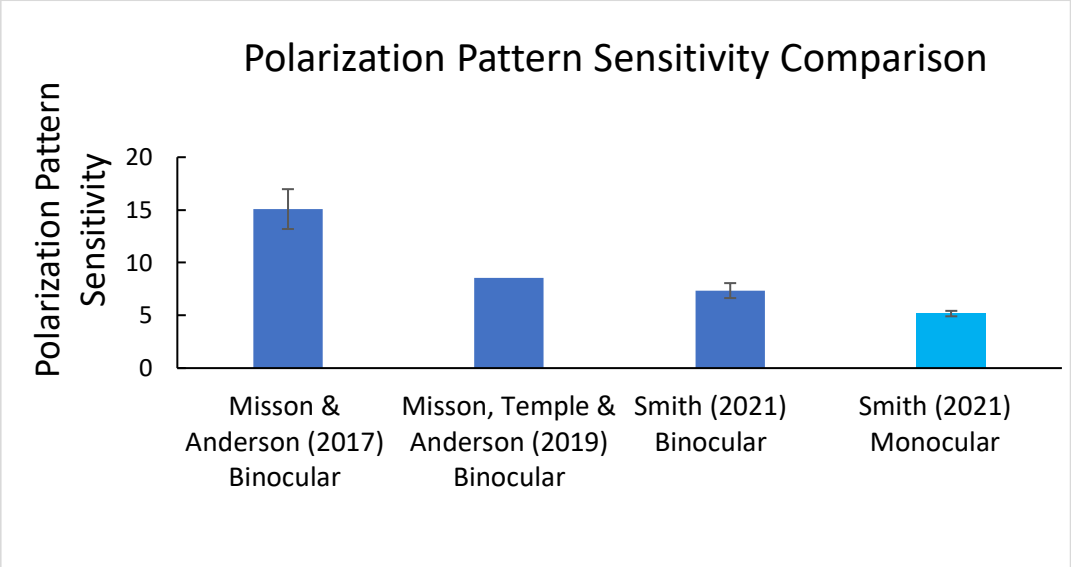

Figure 22. *Bar chart comparing mean PPP sensitivity results with previously published data. Error bars represent ± one SEM. Bars one and two depict polarization sensitivity results from Misson and Anderson (2017) and Misson et al. (2019), respectively. These studies were conducted using comparable protocols and equipment to those used in this project. Bars three (binocular) and four (monocular) show the data from this project.*

Minimum angle of polarization difference is the smallest **e-**vector orientation difference between the differently polarized bars of the grating stimulus that the participant can discriminate. Across all 84 participants, this gave an average ability to discriminate stimuli differing by just eight degrees. The minimum value recorded by a highly acute participant in this study was just three degrees. The details of this conversion from polarization contrast sensitivity to minimum angle of polarization difference are given in

Appendix 1. This is comparable to Misson and Anderson (2017), who reported that the minimum angle a participant could discriminate was 4.4 degrees.

The **e**-vector discrimination values reported here and in other human studies approach those reported for many invertebrate species with dedicated polarization sensitive visual systems (Temple et al., 2012). The smallest minimum angle of polarization difference detected by an animal to date has been recorded in the Mourning Cuttlefish, discriminating stimuli differing by just over one degree (Temple et al., 2012).

3.1.3.2. Repeatability measures

There were no significant differences between the mean polarization pattern perception sensitivities between the first and second (Mann-Whitney U = 3421, p =.733) and second and third runs (Mann-Whitney U = 3415, p =.720) for the 84 participants. Furthermore, there did not appear to be any significant fatigue or learning effect between the first and third runs (Mann-Whitney U = 3518, p =.975).

The repeatability of PPP sensitivity measures was assessed on a subgroup of 34 participants. The results are shown in figure 23, which shows monocular PPP sensitivity measured on visit 1 against the sensitivity measured on visit 2. There is a statistically significant, positive relationship, between monocular repeated PPP measurements (Spearman's rank correlation coefficient = 0.839, n = 68 eyes, $p < 0.001$). R^2= 64.6%. This is demonstrated graphically through the similarity between the trend line (blue line) and the line of no effect (orange line).

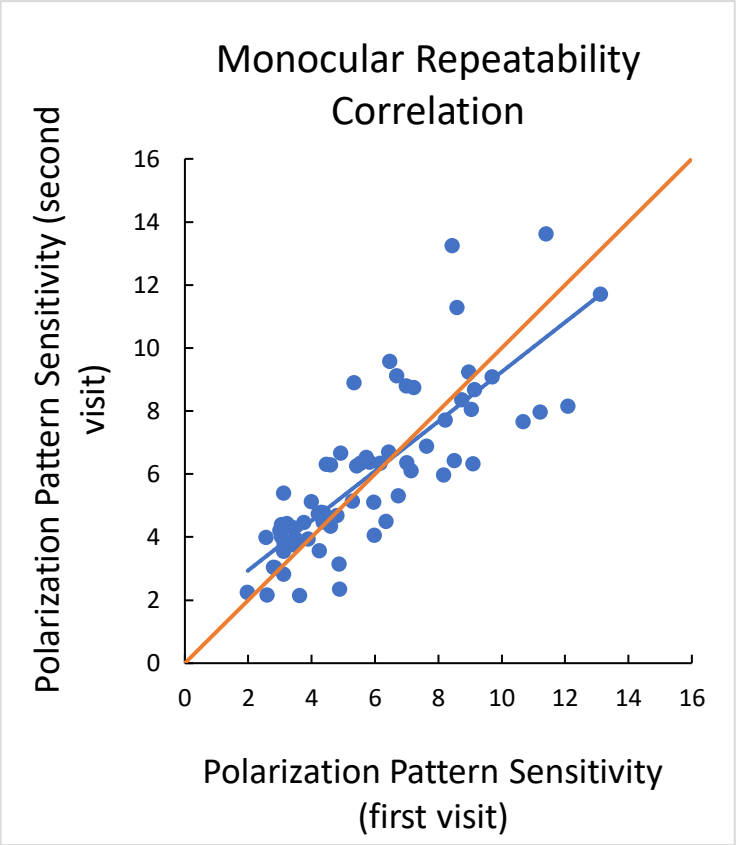

Figure 23. *Scatter graph comparing the relationship between first and second visit PPP sensitivity for each participant. The blue regression line shows a statistically significant (*p < .001*), positive relationship, between monocular repeated PPP measurements. The orange line is the line of no effect.*

Note that, although statistically significant, there is a sizable spread of data points away from the trend line in figure 23, especially at higher sensitivities. This spread indicates a level of variability in the data. The repeatability of the polarization measures was further assessed using a Bland-Altman plot, shown in figure 24. Bland-Altman plots are a useful graphical representation that allow the user to compare the agreement between two different methods, or the repeatability of a single method using a series of participants. A coefficient of repeatability (COR) can be calculated from the plot, which gives the value at which one can be 95% confident that there is a significant difference from the original reading. A lower COR indicates a more reliable clinical measurement technique.

Here, the COR was 3.19, which shows that a clinician could be 95% confident there was a significant difference between a three-run repeated PPP sensitivity reading if it lies more than ± 3.19 from the original. This value is relatively large when compared with other clinical techniques, (e.g. MPOD measured using the MPSII has a COR of 0.08); see (Howells et al., 2013).

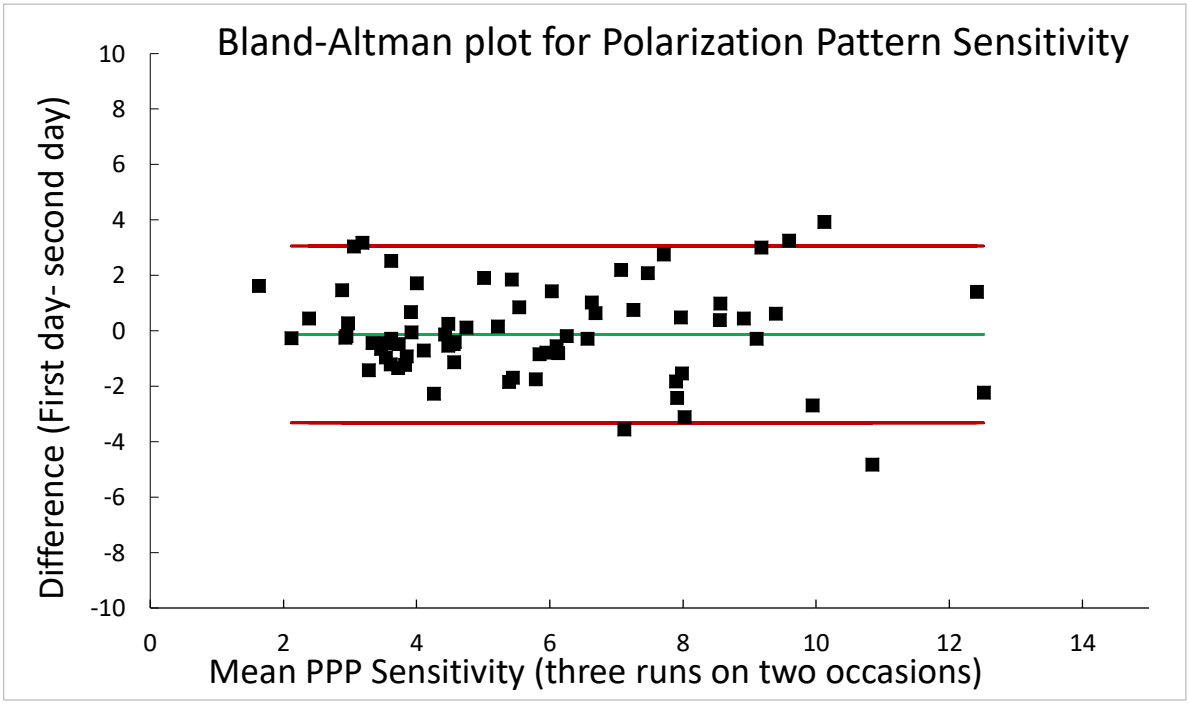

Figure 24. *Repeatability data displayed as a Bland-Altman plot, n=68 eyes from 34 participants completing the repeatability study. The data shows narrow limits of agreement and no significant bias. Bias/mean difference -0.13, Standard deviation of the differences 1.63, Coefficient of Repeatability 3.19, Lower 95% confidence limit -3.32, Upper 95% confidence limit 3.06. This Bland-Altman plot was plotted using PPP sensitivity, plotted as the mean of the first three sensitivity readings minus the mean of the second three readings.*

3.1.3.3. Summary

The effect of age and the repeatability of polarization pattern perception measures were assessed using a forced-choice psychophysical measure of contrast sensitivity to polarized light stimuli. The main aim of this experimental part was met by establishing the monocular sensitivity to polarization patterned stimuli as a function of age (19-59 years), see figure 19. The repeatability of the PPP technique was also presented and described. The test-retest values shown in figure 23 show a statistically significant correlation between repeated measures. This statistical significance reduces the likelihood that the presented data and trends found are due to chance alone and is promising for the variation in PPP to be due to differences in an underlying physical characteristic. This positive correlation in figure 23 showed promise for PPP's future development. Figure 24, however, highlighted a relatively large COR which would need improvement for this to be developed into a useful, reliable, clinical test and macular screening tool.

3.2. Experimental Part 2

The Influence of MPOD on Polarization Pattern Sensitivity

3.2.1. Introduction and Aims

Macula lutea means ‘yellow spot’, a name derived from the high concentration of yellow pigment carotenoids, lutein, zeaxanthin and mesozeaxanthin, found at the macula (Howells et al., 2011). These carotenoids are obtained through the diet, or can be obtained as supplements (Wu et al., 2015, Neuringer et al., 2004). The macular pigments have a proposed protective role in filtering out harmful blue light and acting as a free-radical scavenger (Bernstein et al., 2016, Barker et al., 2011, Hammond et al., 2001), which is understood to have a preventative role in age-related macular degeneration (McGill et al., 2016, Wu et al., 2015, Beatty et al., 2001, Bone et al., 2001, Landrum and Bone, 2001, Hammond and Caruso-Avery, 2000, Khachik et al., 1997). In addition, macular pigment is thought to improve vision by reducing light scatter (Stringham and Hammond, 2007) and minimising chromatic aberrations, within the eye (Reading and Weale, 1974).

Macular pigment optical density (MPOD) is a value for the sum of the optical densities of the carotenoids located in the macula region, and varies significantly between individuals (Howells et al., 2011). Although there is no universally accepted procedure (Putnam, 2017, Howells et al., 2011), the main psychophysical method used to measure MPOD in a clinical environment is heterochromatic flicker photometry (Putnam, 2017).

Individual variability in MPOD may not only affect an individual’s macular health but could also influence their polarization sensitivity. The widely accepted radial diattenuator model of human polarization perception states that the orientation of dichroic macular pigments situated in the Henle fibres is the basis for human polarization sensitivity (see figure 4) (Misson and Anderson, 2017, Bone, 1980, Naylor and Stanworth, 1954a). It was hypothesized that participants with more macular pigment would achieve higher PPP sensitivity readings, as their additional pigments would absorb more polarized light and generate a stronger contrast response to the polarized light stimulus (see section 1.3.2).

The aim here was to compare monocular sensitivity to polarization pattern stimuli with macular pigment optical density measures, as assessed using heterochromatic flicker photometry.

3.2.1.1 Justification for using the MPS II

Many modified heterochromatic flicker photometry instruments exist (e.g. using different stimulus sizes, wavelengths, bandwidths, locations and flicker frequencies) (Loughman et al., 2012, Howells et al., 2011, Bartlett et al., 2010a, Stringham et al., 2008, Loane et al., 2007). The flicker frequency used is vital: too low and it is difficult to obtain the point of minimal flicker; too high and there are a wide range of null flicker points (Nolan et al., 2008, Stringham et al., 2008, Loane et al., 2007). Modern instruments, including the MPS II, overcome the variability of flicker sensitivity between individuals (Snodderly and Hammond, 1999) by fitting an algorithmic function to each individual's critical flicker frequency data set. The MPS II also benefits from asking participants to respond to the flicker appearance rather than disappearance, as this criterion has been shown to be easiest for naïve participants (van der Veen et al., 2009). Estimating the peripheral location from age norms, as in the standard mode, was faster and has been shown to give acceptable values (see figure 16) (Makridaki et al., 2009).

Currently, heterochromatic flicker photometry has "gained general acceptance as the clinical standard" and is an affordable and established method (Putnam, 2017). The MPS II was chosen as it is compact, portable, and efficient. It also outperforms other heterochromatic flicker photometry devices (e.g. the Macuscope) in reliability studies. Howells et al. (2013) advocated protocol modifications to include removing suboptimal graphs and data, and repeating the result at least twice to give a COR of 0.08 (Howells et al., 2013). To alleviate any concerns, the experiments in this research project incorporated the advice on technique modification. By using only acceptable shaped graphs with minimal variability, and repeating the readings three times, it was felt that the MPOD measurement established was a reliable measure to compare with the participants' PPP results.

3.2.2. Methods

A detailed account of the participants, polarization stimuli, equipment, and experimental procedures are provided in chapter 2 (General Methods). The specific methods related to this section are reported here.

Twenty-nine participants consented to MPOD and PPP measurements. An MPS II macular pigment optical density scanner was used to measure MPOD readings. Three values were obtained for each participant. The device provides a reliability guide for each MPOD reading, and any poor-quality readings were repeated (i.e. only curves with the expected downward S, U or V shape with definite low points were accepted (see Appendix 3)). Mean macular pigment optical density values were compared with each participant's polarization contrast sensitivity value from experimental part one.

The peak MPOD value was derived, using the MPS II, by computing the log ratio of the intensity of blue light at the central and estimated parafoveal locations (Putnam, 2017). A graphical output shows the frequency required to perceive the onset of flicker at each blue-green ratio. A shift of the minimum point towards the right along the x-axis indicates that more blue light was required in the ratio, thus giving a higher MPOD value for that participant (Davey et al., 2016, Loughman et al., 2012). Examples of expected graphs shapes with an obvious low point and defined minima, and inclusion and exclusion criteria for reliability graph shapes are displayed in Appendix 3.

3.2.3. Results and Discussion

Macular pigment optical density was plotted against polarization contrast sensitivity for 29 participants in figure 25. There was a statistically significant positive correlation between MPOD and PPP in figure 25 (Spearman's rank correlation coefficient = 0.642, $n = 29$, $p < .001$, two-tailed). The standard error of the slope and Y-intercept were 2.56 and 1.18 respectively.

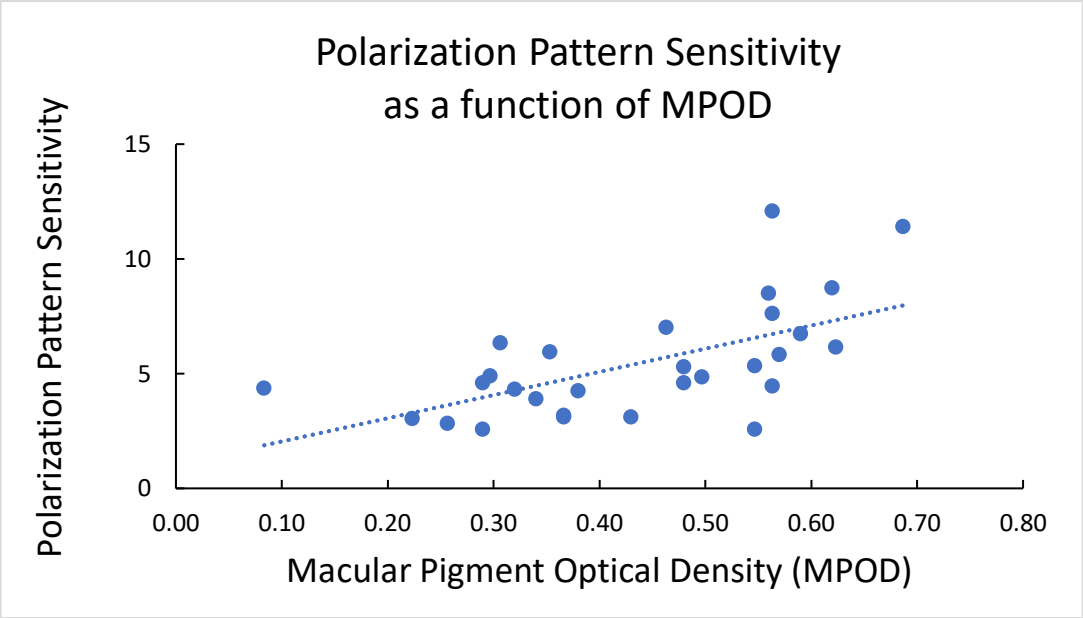

Figure 25. *The relationship between macular pigment optical density and polarization contrast sensitivity (first three readings) for all participants in the MPOD study group. The equation of the dotted blue regression line was PPP = (10.03* MPOD) + 1.07).*

The positive correlation established between PPP and MPOD, as displayed in figure 25, supports the radial diattenuator model for polarized light perception (see figure 4). It is postulated that this relationship reflects the increased volume of macular pigments in individuals with higher MPOD (see section 1.3.2). These results are promising for the ongoing development of PPP as a tool to screen for low MPOD, a known risk factor for age-related macular degeneration (Trieschmann et al., 2003, Beatty et al., 2001, Bone et al., 2001).

The scatter graph in figure 26 depicts the relationship between each participant's macular pigment optical density and their age. The mean MPOD value of the 29 participants was 0.44, with a range of 0.08 to 0.69. This correlates well with the expected norms for a population from studies using equivalent heterochromatic flicker photometry methods to the MPS II used in the research project. For example, a large study (n=5581) reported an MPOD of 0.33± 0.187 (van der Veen et al., 2009). Another found a similar MPOD of 0.35 ± 0.14 (n=40, aged 18-50 years), (Bartlett et al., 2010b). Davey et al. (2016) studied 72 participants (aged 22-68 years) and found an MPOD of 0.45 ± 0.19 and 0.44 ±0.14 for the dominant eyes of men and women respectively.

It has been shown previously that MPOD remains relatively stable with age, providing there is no pathology (Meyer Zu Westrup et al., 2016, Beirne, 2014, Demirel et al.,

2014). The results shown in figure 26 support this finding, as there was no significant slope to the trend line (dotted blue line), and no statistically significant correlation between MPOD and age (Pearson's correlation coefficient = -0.00063, n = 29, p = .997, two-tailed). Note that, a Shapiro Wilk test showed that both the MPOD and age data are normally distributed, and as such parametric statistical analyses were used to assess the relationship between them (see Figure 26).

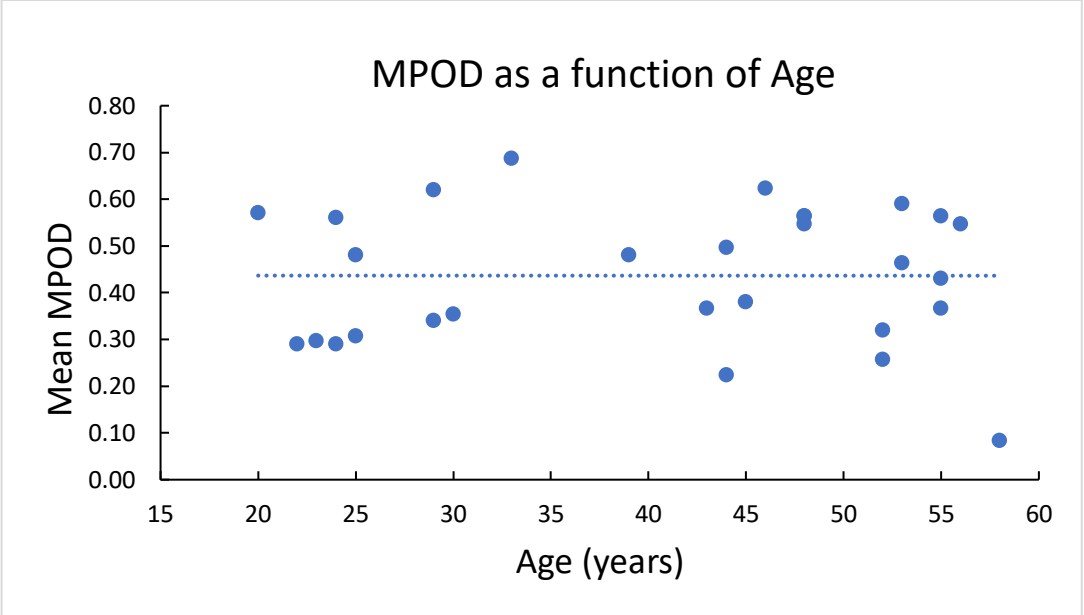

Figure 26. *Scatter graph depicting the relationship between age and macular pigment optical density. There was no significant relationship found between the two variables (p >> 0.05). The blue dotted line shows the regression line, plotted with the equation y = -7E-06x + 0.4367.*

The bar chart in figure 27 is included to demonstrate the repeatability of the MPOD readings obtained for each participant. The data supports the use of the MPS II readings in this experiment, as there was limited variation between repeated MPOD measurements. The standard deviation for MPOD measurements was ± 0.03.

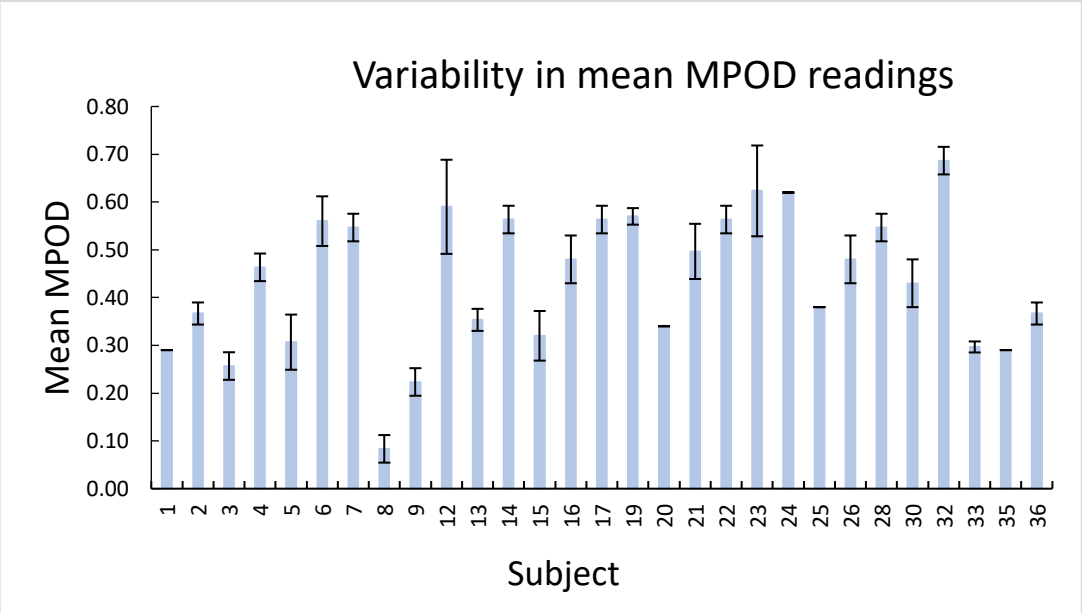

Figure 27. *Bar chart demonstrating the variability in MPOD readings for each individual participant. This is displayed as ± one standard deviation error bars, based on the three MPOD readings from the MPS II for each participant.*

3.2.3.1. Summary

The aim of this experiment was to assess if an individual's polarization sensitivity was affected by their macular pigment optical density, measured using the MPS II. The results provide evidence that those with higher MPOD were significantly more likely to have more acute polarization sensitivity (see figure 25). These results provide additional support for the radial diattenuator model of PPP (see section 1.3.2). The macular pigment origin of polarization perception makes these results promising for the future development of polarization sensitivity and PPP a tool to screen for risk factors such as low MPOD and macular disease. A larger sample size will be needed to establish more concrete trends from this data and is currently underway by other members of this Aston research group.

3.3. Experimental Part 3

The influence of refraction, foveal and corneal characteristics, and ocular dominance on PPP.

3.3.1. Introduction and Aims

Experimental parts one and two presented normative PPP values, and displayed how they change with age and MPOD, respectively. Section 1.4.1 and 1.4.2. introduced the idea that there is considerable variability between individual's ocular characteristics e.g. MPOD and corneal birefringence. Interindividual variability is especially important when it relates to the components of the eye that are birefringent and hence can act as optical retarders (primarily the cornea and macula) as these structures can alter the state of polarized light and hence influence polarization perception (Rothmayer et al., 2007). Corneal retardance has been shown to affect individual's polarization perception (see section 1.4.2). This experiment investigates refractive error, central corneal thickness, central foveal thickness, corneal retardance magnitude, corneal birefringence and ocular dominance to determine what effect they have on PPP, and whether any of the variability in the PPP data can be explained by variability in these presented characteristics.

Understanding which factors (if any) may affect PPP is vital if PPP is to be developed as a clinical test of macular function. Moreover, understanding more about the impact of corneal retardation on PPP could impact on the development of future technologies, by improving the individualised accuracy of retinal measurements (Knighton et al., 2008, Knighton and Huang, 2002).

The optical retardation of linearly polarized light rays entering the eye depends primarily on corneal birefringence and thickness (Temple et al., 2015, Knighton and Huang, 2002). These vary widely among the population (Knighton and Huang, 2002, Zhou and Weinreb, 2002), and are known to affect Haidinger's brush perception (see figure 15) (Rothmayer et al., 2007), and may affect PPP to an unknown degree. Extrapolating from data in previous Haidinger's brush perception studies, it is expected that individuals with highly retardant corneas are likely to have lower PPP sensitivity values, as they will experience a larger phase shift and ellipticity of incoming light for certain orientations (Temple et al., 2015, Rothmayer et al., 2007).

Central corneal thickness was measured and reported because it is a highly variable characteristic within a population. The corneal stroma is highly birefringent due to its collagen fibril arrangement; thus, it was possible that those with thicker corneas could have displayed more retardation to the incoming polarized light as there was a larger thickness of birefringent material to pass through. Measuring central corneal thickness was also required to calculate individual participant's corneal birefringence.

The effects of ametropia, ocular dominance and foveal thickness were also assessed, as the possible influence of these attributes on polarization pattern perception are currently unknown. Foveal thickness data was included because foveal thickness was variable between participants, and any variability between participants' eyes, especially within the birefringent macula or cornea, may influence polarization detection. It was hypothesized that those with thicker foveas, may have had a different macular structure or more macular pigment available than those with thinner foveas, which could have influenced polarization perception. Participants' eye dominance data was included in this experiment because a previous study had highlighted a possible difference in polarized light perception between dominant and non-dominant eyes. Le Floch et al. (2010) noticed that individuals in their study perceived Haidinger's brush differently in each eye and suggested that this could be used as a way of assessing eye dominance.

3.3.2. Methods

Detailed methods on the participants, stimuli, materials, and procedures are reported in the general methods (Chapter 2) and the supplementary material (Appendix 1).

In summary, an optical coherence tomographer was used to measure corneal and macular characteristics on the dominant eye of 84 participants. These values, along with their refraction, were compared with polarization contrast sensitivity measures (see figure 19). Thirty-four participants from the repeatability study group completed further GDx VCC, optical coherence tomography and polarization pattern perception measures on both eyes.

3.3.3. Results and Discussion

3.3.3.1. Refraction and PPP

Best-vision spherical refraction was highly variable between participants, as no exclusion criteria based on refraction were implemented in the protocol. This was done

to reflect a normal clinical practice environment. Importantly, all participants were fully corrected and had good optimally corrected visual acuity.

Figure 28 is a scatter graph plotting each participant's polarization contrast sensitivity against their best vision sphere refraction. This cohort included best vision sphere refractions between -7.00DS to +3.00DS (μ -0.60DS). There was no statistically significant relationship between refraction and PPP (Spearman's rank correlation coefficient = -0.113, n = 84, p = .306, two-tailed). The dotted trend line depicts the line of best fit through the scatter graph data points. Note that the individual data points are widely scattered about the near-horizontal dotted blue trend line.

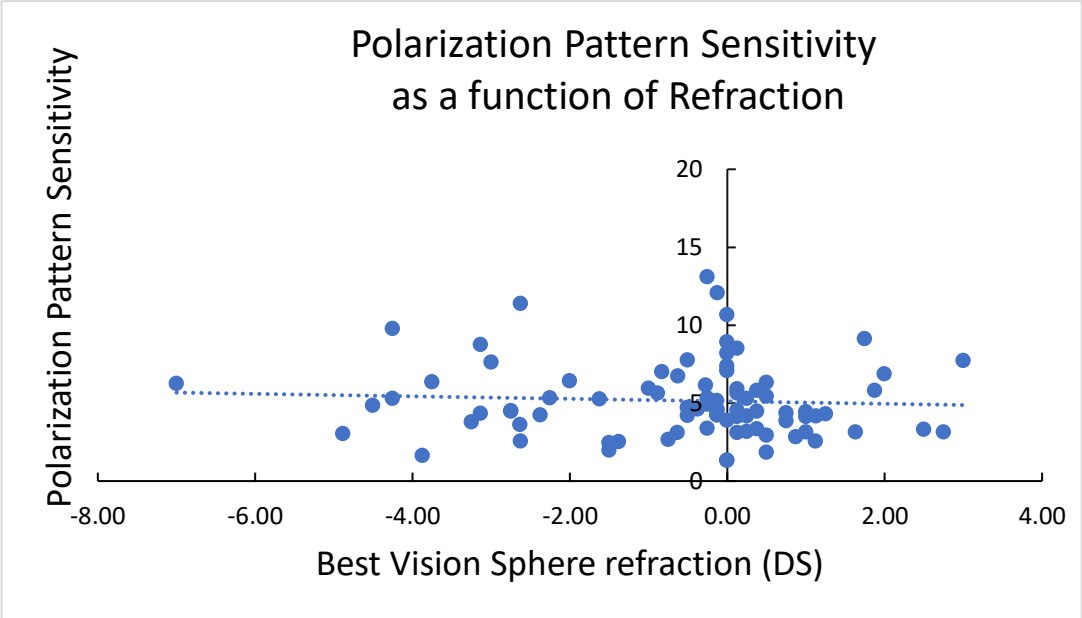

Figure 28. *Polarization pattern sensitivity for all participants' dominant eyes, plotted against their dominant eye best-sphere refraction. There was no statistically significant relationship (p > .05) between refraction and PPP. The blue dotted line is a regression line, plotted with the equation y = -0.0799x + 5.1171.*

These results provide evidence that an individual's underlying refraction does not influence their sensitivity to polarization patterns. The lack of correlation between refraction and PPP has not been reported before, adding new information to this evolving field. From these results it can be inferred that, providing participants are wearing their up-to date refraction in optically isotropic trial lenses for one meter, a clinical polarization pattern perception device would not have to incorporate a correction factor for refractive error.

3.3.3.2. Foveal thickness and PPP

The relationship between central foveal thickness and polarization contrast sensitivity is shown in figure 29, for the dominant eye of 84 participants. The range of foveal thickness was 193µm-313µm (µ 232µm, σ 23). The dotted blue trend line depicts the line of best fit through the scatter graph data points. There is a wide scatter of data points around the trend line, which shows a minimal negative slope. There was no statistically significant relationship between central foveal thickness and PPP (Spearman's rank correlation coefficient = -0.177, n = 84, p = .107, two-tailed).

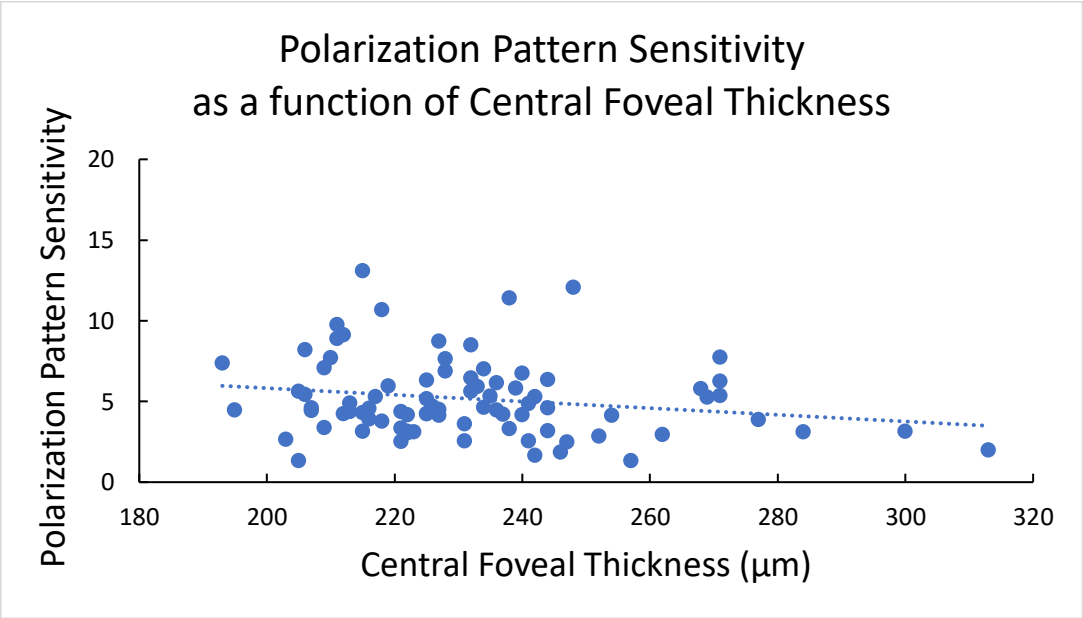

Figure 29. *Polarization pattern sensitivity for all participants' dominant eyes, plotted against their central foveal thickness. The negative slope of the trend line shows a non-significant decline in polarization sensitivity with an increase in foveal thickness (p > .05). The blue dotted line is a regression line, plotted with the equation y = -0.0206x + 9.9527.*

3.3.3.3. Corneal Characteristics and PPP

The following four graphs (figures 30-33) display the inherent variability between human corneas, one of the main retarding structures in the eye (Rothmayer et al., 2007). The aim here was to investigate the effect of differences between participant's corneal characteristics of central cornea thickness, corneal retardation, and corneal birefringence, on their polarization perception.

Central corneal thickness is plotted against polarization sensitivity in figure 30, for the dominant eyes of 84 participants. The range for central corneal thickness in this study was 460-637µm, with a mean of 531µm. This aligns well with the normative ranges

published by a large population study, 554.2 ±34.8µm (Hoffmann et al., 2013), and the Rotterdam eye study, 537.4µm, range 427-620µm (Wolfs et al., 1997), helping to show the experimental study sample is representative for the general population.

Note that there was no significant slope to the trend line, and no statistically significant relationship between the two variables (Spearman's rank correlation coefficient = 0.048, n = 84, p = 0.664, two-tailed). These results provide evidence that central corneal thickness itself does not account for any of the variability found in polarization perception.

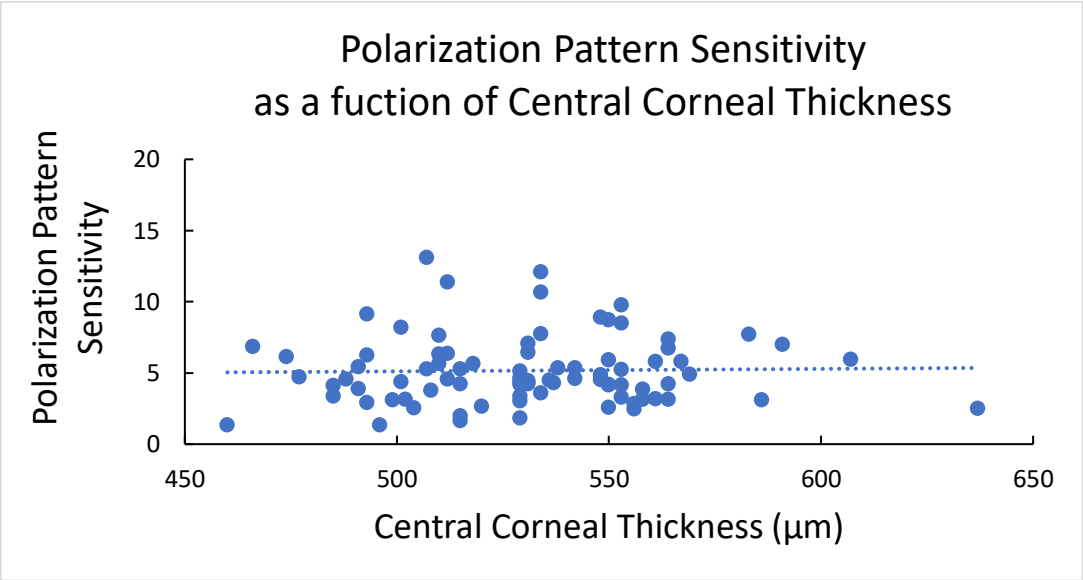

Figure 30. *Polarization pattern sensitivity for all participants' dominant eyes, plotted against their central corneal thickness. The range of CCT was 460nm-637µm (µ 531nm, σ 32). There was no statistically significant relationship (p > .05) between CCT and PPP. The blue dotted line is a regression line, plotted with the equation y = 0.0017x + 4.2446.*

Corneal retardance magnitude, measured by the GDx VCC, is plotted in figure 31, against the participant's polarization pattern sensitivity in their dominant eye. The cornea has fast and slow axes lying orthogonal to each other. Corneal retardation is the difference in phase shift between these two orthogonal components of light exiting the cornea. Corneal birefringence is a property of the cornea to have a different refractive index depending on the polarization orientation of the incoming light (Knighton and Huang, 2002). The near horizontal trend line and diffuse scattering of data in figure 31 displays graphically that there was no statistically significant relationship between corneal retardance and polarization pattern sensitivity. There was no statistically significant relationship (p > .05) between corneal retardance and PPP

(Spearman's rank correlation coefficient = 0.212, n = 68 eyes, p = .083, two-tailed). Corneal retardance varied from 4nm to 94nm (μ 46nm, σ 19).

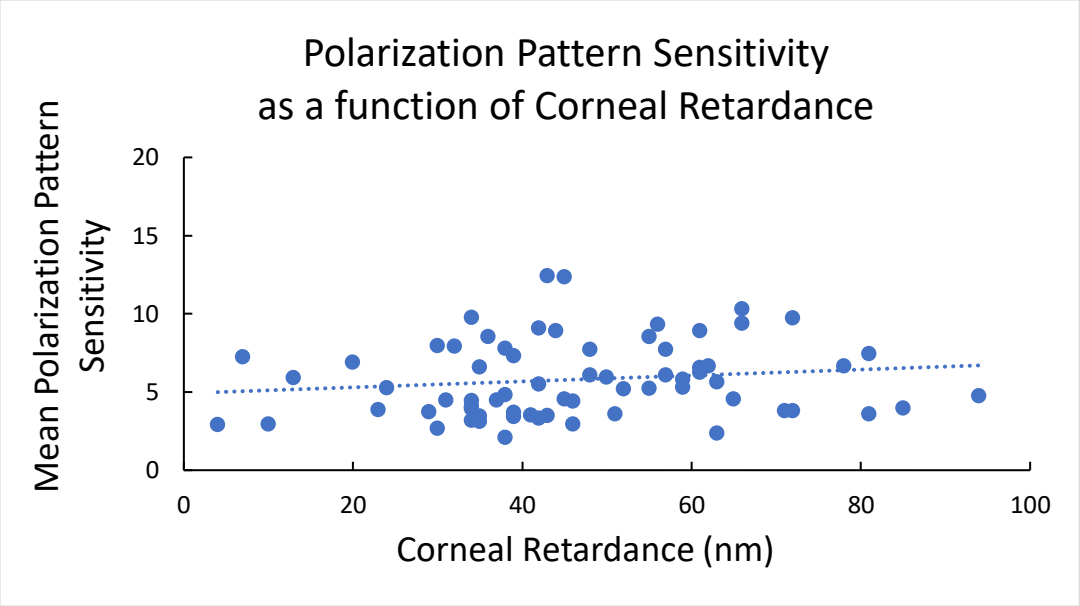

Figure 31. *The relationship between corneal retardance and PPP sensitivity readings across 6 repeat readings, plotted for those completing the repeatability study. There was no statistically significant relationship (p > .05) between corneal retardance and PPP. The blue dotted line is a regression line, plotted with the equation y = 0.019x + 4.9182.*

Corneal birefringence was calculated by dividing corneal retardance by central corneal thickness. Corneal birefringence values are plotted against individual's polarization pattern sensitivity measurements in figure 32. Similarly to the corneal retardation data, corneal birefringence did not have a statistically significant impact on polarization pattern sensitivity, when measured using this technique.

Mean corneal birefringence was 8.7 $x10^{-5}$. There was no statistically significant relationship (p > .05) between corneal birefringence and PPP using this study paradigm (Spearman's rank correlation coefficient = 0.193, n = 68, p = .115, two-tailed).

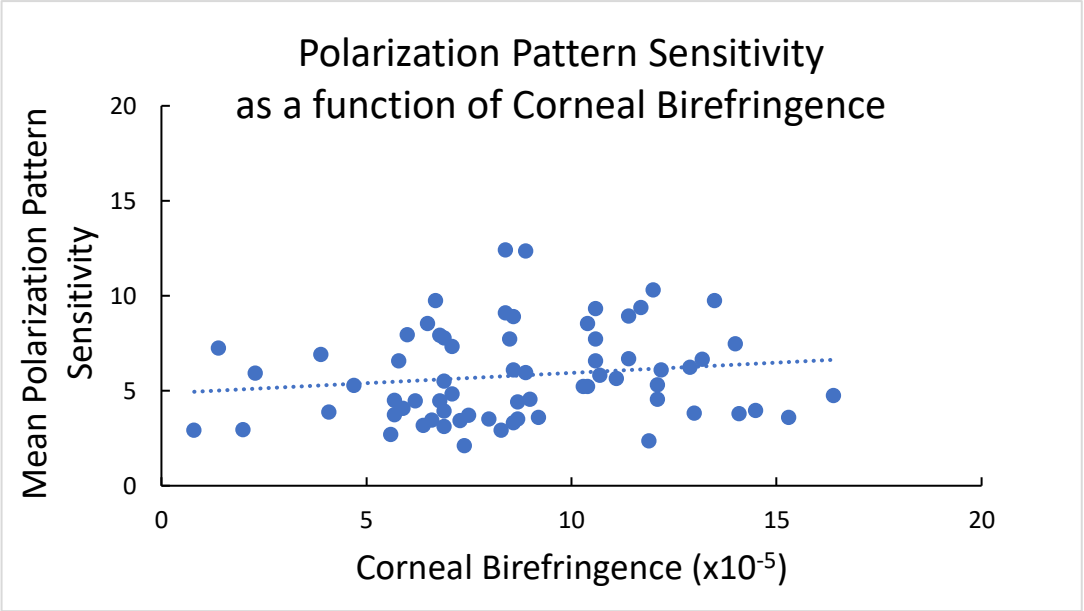

Figure 32. *The relationship between central corneal birefringence and PPP sensitivity readings across 6 repeat readings, plotted for those completing the repeatability study. There was no statistically significant relationship (p > .05) between corneal birefringence and PPP. The blue dotted line is a regression line, plotted with the equation y = 0.108x + 4.8605.*

Most people have corneal retardation values between 20nm-70nm (Knighton and Huang, 2002, Weinreb et al., 2002). The experiment participants had a mean corneal retardance of 46nm, well within the established normal range. The orientation of the slow axis of the cornea is variable between individuals, but usually lies between 10 and 30° nasally downwards (Temple et al., 2015, Knighton et al., 2008, Knighton et al., 2002, Misson, 1993, Bone, 1980, Naylor and Stanworth, 1954a). In this project's experimental population, the slow axis orientation varied from 0° to 45.9°, mean 20.4°, nasally downwards.

There are two orientations of angle of polarization relative to retardation fast/slow axes that have zero effect on polarization (parallel and perpendicular to the axes), and two orientations where the retarder has maximum effect (±45° to fast/slow axes) (see figure 15) (Rothmayer et al., 2007). As Haidinger's brush can be seen at these points, even in those with high retardation values, a technique that displays polarization stimuli at varying orientations such as by rotating Haidinger's brush, allows all participants the opportunity to view the polarization stimuli at some points (Temple et al., 2019).

This may help to explain why there was no significant relationship found between corneal retardation and polarization pattern sensitivity in this experiment (figure 31),

where the polarization-modulated grating was displayed at only four orientations (horizontal, vertical and ± 45°).

The bar chart in figure 33 displays the corneal azimuth of the participants, analysed in terms of three corneal azimuth bins: -11 to +11 (average 0 degrees); +11 to +34 (average 22.5 degrees); +34 to +56 (average 45 degrees). It was thought that polarization pattern sensitivity values may have been higher for those with a slow axis near the horizontal (0° bin) or most oblique (45° bin), than those with slow axis orientations in-between (22.5° bin), because those individuals had corneas more closely aligned with the polarization grating stimuli orientations (horizontal, vertical and ± 45°).

A participant with strong horizontal corneal retardation, should be able to perceive the polarization stimuli more easily when it is displayed horizontally and vertically where the retarder does not have any effect, compared to when it is displayed ±45° obliquely where there is a maximal retardation effect. Conversely, if a participant had strong 45° retardation, they should perceive the target more easily with the ±45° oblique gratings but struggle to perceive the horizontal and vertical gratings. Those with strong corneal retardation near 22.5° would perceive the polarization grating equally for all four orientations.

Figure 33 shows that this trend was not found in this study. However, the effect may have been overshadowed by the potentially stronger influences of differences in birefringence and MPOD. Further analysis was conducted by considering only the most highly birefringent eyes (≥12 $x10^{-5}$ corneal birefringence; n = 13 eyes), but again no significant effect of corneal azimuth orientation and polarization contrast sensitivity were found (Spearman's Rank Correlation Coefficient 0.104, p = .734). It is accepted that a larger sample may reveal an effect of corneal azimuth in highly birefringent corneas.

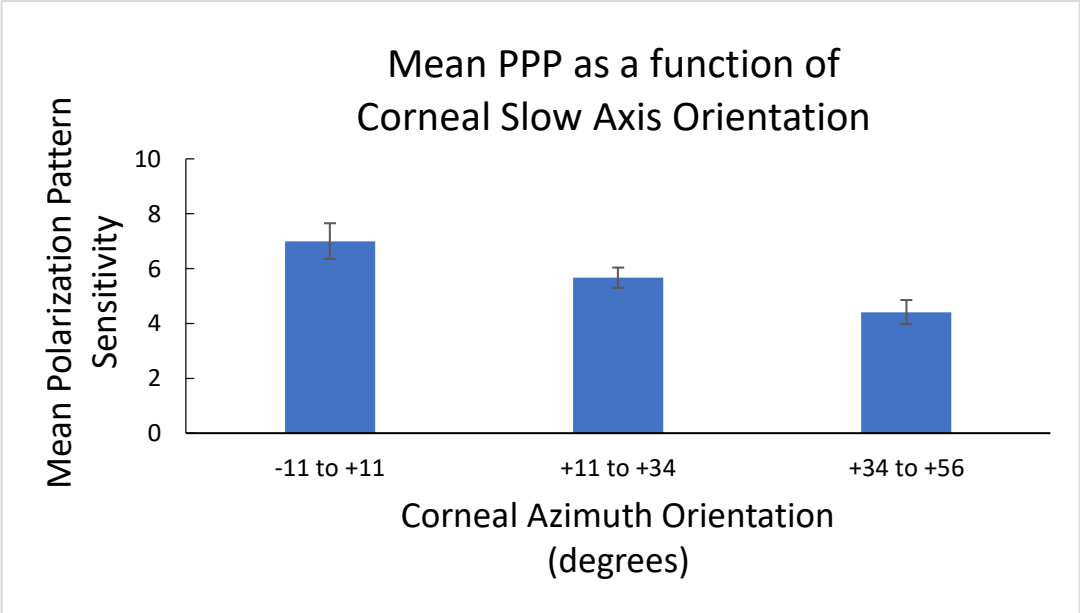

Figure 33. *Bar chart comparing corneal azimuth orientation, measured in degrees in the nasally downward direction, with polarization contrast sensitivity for 68 eyes from 34 participants. Error bars show SEM. Analysed in terms of three corneal azimuth bins: -11 to +11 (average 0); +11 to +34 (average 22.5); +34 to +56 (average 45). See explanation in text.*

3.3.3.4. Ocular Dominance and PPP

The bar chart in figure 34 displays the mean polarization contrast sensitivity measurements of the 35 participants' dominant and non-dominant eyes. This is displayed alongside the scatter graph in figure 35 which is included to give a comparison of the influence of dominance in each of the participants individually. The mean PPP sensitivity was 5.6, SEM 0.43 for dominant eyes, and 5.8, SEM 0.41 for non-dominant eyes.

In figure 34, the bar graph depicts that there was no significant difference in PPP sensitivity between the participant's dominant and non-dominant eyes. The error bars in figure 34 show considerable overlap, so the difference between the two means was not statistically significant ($p > .05$). Figure 35 shows that there was a statistically significant positive correlation between the eyes of each participant, meaning those with highly acute PPP in one eye, were also likely to have good PPP in their fellow eye (Spearman's rank correlation coefficient = 0.853, $p < 0.001$).

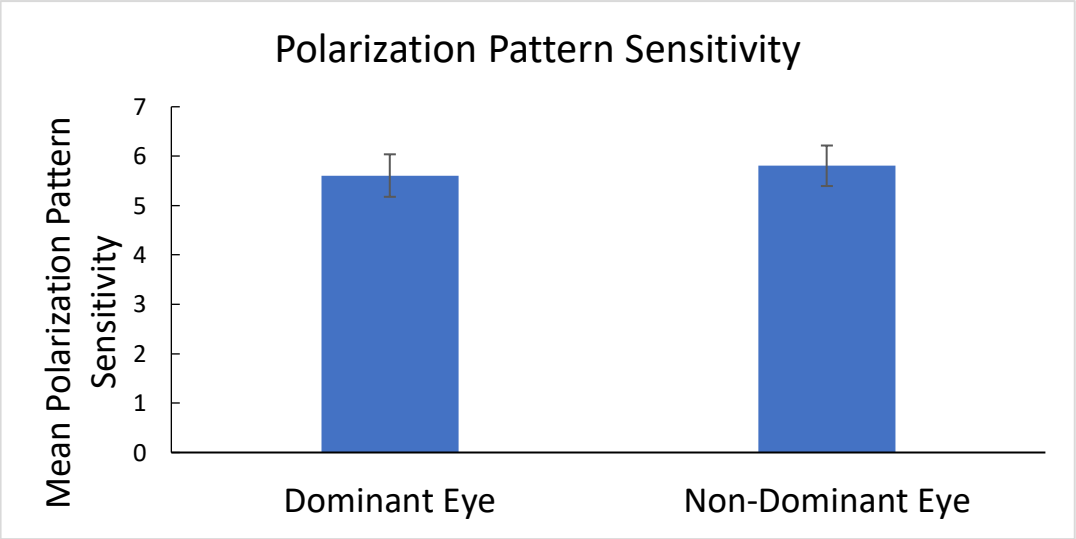

Figure 34. *Bar chart comparing PPP sensitivity readings for 35 participants in the repeatability studies dominant and non-dominant eyes. Error bars show SEM for each group.*

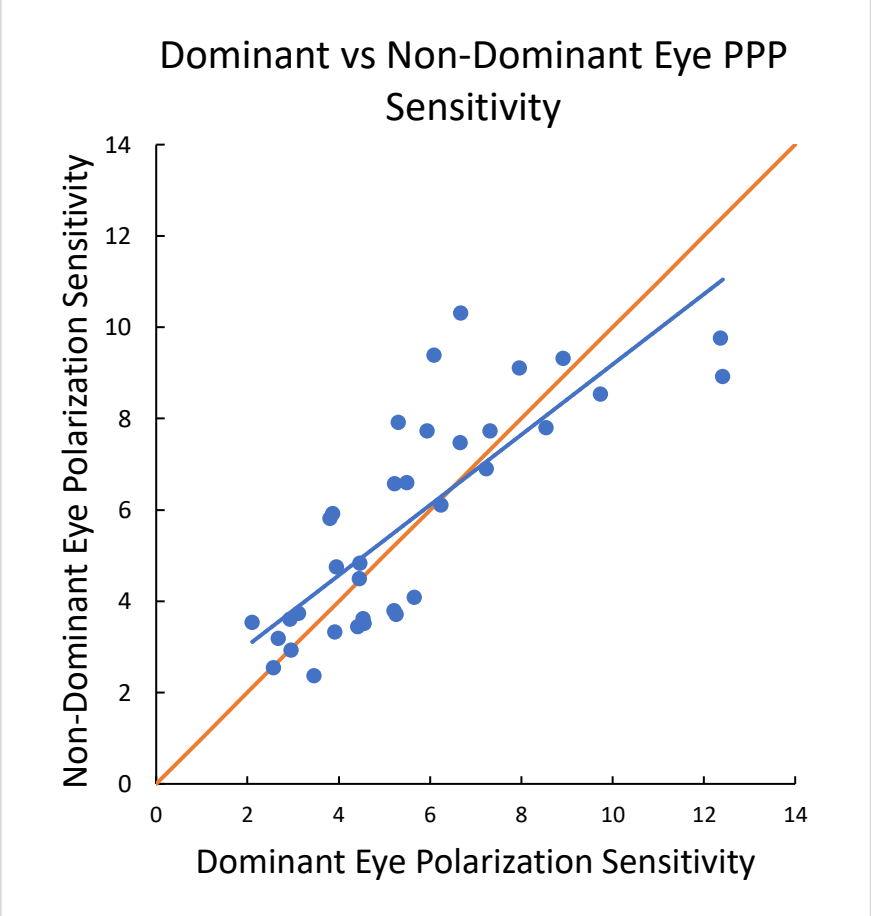

Figure 35. *Scatter graph plotting the polarization contrast sensitivity results between the dominant and non-dominant eye, for each of the 35 participants. The blue solid line shows the regression line with equation, y = 0.7697x + 1.4893, the orange solid line is the line of no effect.*

No significant difference in PPP was found between the dominant and non-dominant eye of participants (see figures 34 and 35) which provides evidence against Le Floch et al. (2010)'s statement of using polarized light perception to assess ocular dominance. This similarity between the eyes may be to do with the participants having good and equal acuity in both eyes and no binocular vision anomalies, as per the inclusion criteria. This finding also promotes accepting the inclusion of data from dominant and non-dominant eyes into the same graph, as done for the corneal retardation and birefringence graphs (figures 31 and 32), presented in this way to give a larger sample to better highlight the trends.

No significant differences in MPOD were reported by Davey et al. (2016) between dominant and non-dominant healthy eyes. As MPOD was the only factor shown within this research project to significantly affect PPP, this lack of significance shown in figure 34 provides confirmatory evidence of equal MPOD between the eyes of these individuals.

The slow axis of the cornea and retardance magnitude are usually mirror symmetric between the right and left eye (Knighton and Huang, 2002), this similarity may contribute to the similarities in polarization pattern sensitivity between the fellow eyes of participants (see figure 35).

3.3.3.5. Summary

The aim of this experiment was to investigate various ocular attributes to determine what effect, if any, they have on PPP, and whether any of the variability in the PPP data could be explained by any variability in these presented characteristics. The results of this section provide evidence that polarization pattern perception is not affected by refractive error, central corneal thickness, central foveal thickness, corneal retardance, corneal birefringence or eye dominance. With regard to these particular functional and anatomical attributes, it is concluded that polarization pattern perception is a robust method of examining macular function, unaffected by individual ocular characteristics or age. As MPOD was the only factor shown to affect PPP in these experimental parts, PPP has promise for future development into a useful macular monitoring and screening tool.

Chapter 4 – Conclusions

4.1. General Summary

Until recently, the rudimental Haidinger's brush phenomena were believed to constitute the full extent of human polarization sensitivity. However, more recent research showed that the human visual system was capable of detecting other, more detailed visual stimuli, modulated solely by light polarization (Misson et al., 2015, Temple et al., 2015). Misson and Anderson (2017) demonstrated that human polarization pattern perception was significantly more acute than previously thought, was quantifiable, confined to the macula, and matched the spectral characteristics and distribution of macular pigments. Their novel phenomenon, Polarization Pattern Perception, was explored experimentally in this research project.

Previously unknown normative PPP values across several decades of life, repeatability data and the influence of an individual's corneal and macular characteristics were presented and discussed. It is concluded that the significant positive correlation between MPOD and PPP, together with the lack of influence from variations in other ocular characteristics, make a measure of PPP potentially beneficial for macular assessment and measurement of macular pigment density.

Early diagnosis of macular dysfunction is important as it could prompt early advice and/or treatment e.g. for macular degeneration. PPP has shown promise for this role and has shown superiority over static polarization stimuli such as Haidinger's brush. This area deserved to be explored further because of the known protective functions of the macular pigments, the association of low MPOD with susceptibility to macular degeneration, and the need to find an effective, rapid, and cost-effective test.

Below, I will give a summary of the major experimental findings, their implications in health and disease, and the implications on these findings on future research.

4.2. Summary of Experimental Findings

The principal aim of this research project was to determine, as a function of age, a normative data set for sensitivity to patterned polarization stimuli (PPP), as assessed using a recently published technique employing sensitivity measures to polarization-modulated square-wave grating stimuli (Misson and Anderson, 2017, Misson et al., 2015). Additional aims included comparing and contrasting these measures against individual variations in corneal and macula characteristics, assessing the repeatability

of the PPP technique, and evaluating the concordance between macular pigment optical density and PPP measures.

4.2.1. Normative values, Age and MPOD

The monocular polarization pattern sensitivity for healthy, adult, naïve participants aged 19-59 was 5.17, obtained from a sample of 84 individuals. This equated to an average ability to discriminate stimuli differing by 8 degrees difference in angle of polarization. The minimum angle of discrimination difference recorded by a participant in this study was just 3 degrees. This provided evidence in support of the human ability to perceive polarized light to a much higher degree than previously expected and was similar to data from previously published pilot studies developing the technique (see figure 22) (Misson et al., 2019, Misson and Anderson, 2017). There was no significant change in human PPP across the age range 19-59 years (see figures 19 and 20). Test-retest measures showed a positive correlation (figure 23), but the overall repeatability of the technique would need improvement if it were to become a useful clinical measurement (figure 24).

Experimental part one showed that there was no significant decline in polarization pattern sensitivity with age across the age range 19-59 years (see figures 19 and 20). Reasons for this stability were discussed in section 3.1.3.1, primarily the general stability of the macular structure and MPOD throughout this age range in the absence of any pathology.

It is acknowledged that there may be a significant decline in polarization pattern sensitivity beyond the age range studied (i.e. 60 years and over). This may present from various non-pathological, age-related changes in the eye that give rise to changes in visual sensitivity. Decreases in most visual functions are common with age but begin at different ages and progress at different rates (Salvi et al., 2006, Rubin et al., 1997). Contrast sensitivity has been shown to remain relatively stable up to approximately 65 years, then rapidly decline, (see figure 21) (Haegerstrom-Portnoy et al., 1999). A study measuring visual acuity in 18- to 80-year-olds showed that visual acuity improves up to age 30, then declined gradually after this (Elliott et al., 1995). Physical changes occur in the eye with age, a study showed that those over 66 years showed a loss of retinal thickness, ganglion cells, synapses and capillaries, compared to those under 22 years (Cavallotti et al., 2004). A large systematic review of those 50 years and over showed that aging has the effect of ‘rearranging’ the retinal structure which could detrimentally affect visual functional abilities (Subhi et al., 2016). An exponential loss of function has been shown with increasing age for disability glare, glare recovery time, stereopsis,

colour discrimination, restriction of the peripheral visual field, and visual acuity in a study with participants aged 58 to 102 years (Haegerstrom-Portnoy et al., 1999).

In experimental part two, a significant, positive, relationship between MPOD and polarization sensitivity was reported (see figure 25). This supports the role of macular pigment in polarization sensitivity and provides confirmatory evidence in support of the radial diattenuator model of human polarization perception. Those with a higher MPOD were able to absorb polarized light more strongly in certain orientations, thus creating a greater luminance contrast stimulus, thus achieving better polarization perception.

The measurement of PPP was stable against other measures of age (figure 19), refraction (figure 28), foveal thickness (figure 29), central corneal thickness (figure 30), and eye dominance (figure 34). The fact that PPP was not influenced by these factors, described in part three, provides evidence in support of PPP being a robust method of examining the macula. This offers promise towards its future development into a useful and reliable macular screening and monitoring tool, as well as a potential role as an alternative MPOD measure.

The modified LCD screen set-up used to measure PPP was compact, portable, and low cost. In this study, the novel device was successfully incorporated into the optometrist's eye examination and suited the clinical environment. All participants were able to detect the polarized stimuli to some degree and understood the measurement process. This reinforces its feasibility for development into a future clinical role in optometry, as well as for use in research settings. PPP testing was practical to administer, gave quantitative information on the macula and the normative values were shown to follow the expected age-related minimal decline of other visual characteristics. These factors promote the ongoing study of this technique.

In summary, the three experimental sections showed that PPP was both comparable to previously published pilot data, and stable against all other measures presented, except MPOD. As PPP derives from the organisational structure of the macula, these results show promise for future study and the development of PPP for the early detection, screening, and monitoring of macular disease.

4.2.2. Corneal Characteristics

Variations in the participants' corneal retardance and birefringence did not show any significant effect on polarization pattern sensitivity (see figure 31 and 32, respectively). Corneal birefringence is known to affect polarization sensitivity to Haidinger's brush at certain orientations, but this effect is likely to have been masked in this study as

differing angles of polarization and stimulus orientations were used to obtain a threshold. As there are two orientations where corneal retardance has minimal effect on polarization sensitivity, along the fast and slow axis, and two where it has maximal effect, ±45° from the fast/slow axis, the stimuli would be visible to all participants at some points during the testing. Averaging using numerous orientations has the potential benefit of negating the impact of individual corneal differences. This is of benefit to the future development of the PPP technique as it has been shown to overcome the impact of differences in corneal birefringence, thus providing a more robust measurement of macula function (see experimental part three for details). It was slightly unexpected that a significant change with corneal birefringence was not demonstrated, as previous research suggested individuals were likely to achieve lower polarization sensitivity with higher corneal retardation. Potential reasons explaining this have been given in section 3.3.3.3.

There have been comprehensive studies on corneal retardation variability within and between individuals (Knighton and Huang, 2002, Weinreb et al., 2002). Linearly polarized light becomes partially elliptical when it is not aligned along the fast or slow axis of an optical retarder (Temple et al., 2015). An individual cornea with high retardation will generate greater ellipticity in most orientations compared to a cornea with lower retardation. A highly retardant cornea should therefore reduce the contrast of a polarization stimulus (Rothmayer et al., 2007, Misson, 1993). The effects of this variability on Haidinger's brush perception have been studied theoretically (Misson et al., 2018, Rothmayer et al., 2007) and experimentally (Temple et al., 2015), and were described in detail in the introduction and general discussion sections. These studies reinforced that differences in corneal birefringence significantly impacts the rotational dynamics and perceptions of Haidinger's brush, thus these characteristics were expected to affect polarization perception sensitivity measures in this research project.

It has long been known that there are significant differences in the perception, motion, and contrast of a perceived Haidinger's brush between individuals. There are many influential papers describing this, for example (Misson, 1993, Bone, 1980, Naylor and Stanworth, 1954b, De Vries et al., 1950). More recently, Rothmayer et al. (2007) added useful data to this (see figure 15), stating that these variations in ocular retardance were primarily due to the cornea and macula, and were likely to strongly influence individual polarization sensitivity. Temple et al. (2015) provided experimental evidence in support of a non-linear relationship between presented and perceived polarization angle, when a polarized Haidinger's brush stimulus was rotated. Misson et al. (2018) acknowledged the complex influence of the cornea and the extensive variability

between individuals (Misson et al., 2018). Their simulation adjusted the corneal retardation values and reported significant variations in the dynamic appearance of Haidinger's brush. The brush was only seen as a brush when aligned with the retardation axes at high corneal retardation values, rather than as a smoothly rotating brush as with low values. Misson et al. concluded that variations in corneal retardance, as well as macular pigment density and distribution, could be the reason behind individual differences in Haidinger's brush and polarization perception. However, they noted that corneal retardation values high enough to significantly affect the perception of Haidinger's brush only occurred in a minority of individuals.

Many studies looking into polarization perception do not include measures of the individual participant's corneal characteristics, but acknowledge that differences are likely to affect polarization perception in those with high birefringence values (Misson et al., 2020b, Misson et al., 2019, Misson and Anderson, 2017).

In this research project, 8 out of the 68 eyes measured on the GDx VCC had corneal retardation values above the normal 70nm, the maximum corneal retardation value measured in one participant was 94nm, and 31 eyes demonstrated a corneal azimuth outside the 10-30° nasally downwards range. This high number of outliers highlighted the need to investigate the effects of corneal retardation when developing a polarization-sensitive technique.

4.3. Limitations, Ongoing and Future PPP Work

As polarization pattern perception is a relatively new area of research, there are many avenues to explore.

It is acknowledged that the normative data presented here from a primarily Caucasian population from one optometric practice may not be fully representative of the whole population, as the participants were from a similar ethnic and social background. It is acknowledged that differences in results may be obtained from studies using other ethnicities, and further studies into this may be required.

Polarization pattern sensitivity has been shown to vary significantly among individuals. Differences in macular pigment density have been shown to contribute to this but other, higher cognitive functions are also likely to play a part. For example, as Haidinger's brush is a low contrast phenomenon, its perception demands a considerable degree of visual attention. Visual attention is known to play a significant role in the ability to detect

visual stimuli (Yamagishi et al., 2010) and, therefore, some of the individual variation in polarization sensitivity may be due to individual variations in visual attention.

4.3.1. Future Work- The Macular in Health and Disease

It is expected that this research will lead to future work to measure the effect of PPP in individuals with a range of macular diseases, rather than just in healthy individuals. An exploratory study using various polarized patterned stimuli in normal and abnormal eyes was recently published (Misson et al., 2020a). They found that polarization perception was significantly reduced in those with abnormal eyes, compared with normal eyes, which supports the hypothesis that PPP could be developed into a clinically useful test, at least with respect to the detection of macular disease.

This research project focussed on providing healthy normative adult data but studying those over 60 who were not included in this study should be explored later. The effect of cataracts and ocular media changes on PPP will need to be investigated as they are prevalent in the population age likely to benefit from macular disease monitoring.

Although work into the potential role of PPP in MPOD measurement and macular screening is promising, this research project has shown that the repeatability of the technique should be improved prior to widespread clinical use. As the coefficient of repeatability was relatively large (see figure 24), the next steps for research would be to improve the repeatability of the PPP technique to increase its feasibility in becoming a useful clinical measurement. This could be done by using an alternative psychophysical technique, such as movement direction, which may be an easier task than detection of gratings orientation. Work is currently underway in this area using rotating of Haidinger's brush (Temple et al., 2019).

4.3.2. Future Work- Macular Pigment

It is acknowledged that a larger sample size for MPOD data, and full macular pigment density profiles rather than central MPOD readings as measured here, would be beneficial to improve our understanding and the conclusions reached on the influence of MPOD on polarization sensitivity. Larger scale studies and further exploration of the differences in PPP with individual macular characteristics (e.g. macular pigment volume, macular fibre and foveal structure, macular pigment distribution) are required.

Polarization pattern perception must be compared to other current methods (heterochromatic flicker photometry and autofluorescence) and novel methods (Haidinger's brush rotation) used to measure MPOD. This will give an insight into the

reliability and feasibility to provide meaningful measurements in a clinical setting. The relationship between MPOD and PPP reported here (see figure 25) is promising for future development of the technique, see also the work by Temple et al. (2019) for Haidinger's brush rotation.

Macular pigment density declines to a varying degree in different types of macular disease (Muller et al., 2016), so the relationship between PPP and types of macular disease would need to be established.

The spatial distribution pattern and density of the macular pigments vary considerably among individuals (Ctori and Huntjens, 2017, Bernstein et al., 2010, Berendschot and van Norren, 2006, Sharifzadeh et al., 2006, Davies and Morland, 2004, Hammond et al., 1997). Macular pigment density can drop exponentially into the periphery or form ring like structures with higher concentrations in the perifovea (Ctori and Huntjens, 2017, Meyer Zu Westrup et al., 2016, Berendschot and van Norren, 2006, Sharifzadeh et al., 2006). A study in 2006 concluded that as well as a central peak, around 50% of people have a ring of raised pigment density 0.7° from the fovea (Berendschot and van Norren, 2006). As the macular pigment profile differs significantly between individuals, these differences in distribution pattern, as well as MPOD variability, may contribute to differences in individual polarization perception. A recent study provided computational simulations of Haidinger's brush perception with variable macular pigment density and distribution patterns (Misson et al., 2018). In the future it would be interesting to compare these profiles experimentally with quantifiable PPP or Haidinger's brush polarization measures.

This research project used adult participants with no underlying conditions and sound ability to understand and consent to procedures, so it was deemed that the less expensive, more widely available, subjective heterochromatic flicker photometry method was appropriate to use in experimental part two. More detailed MPOD techniques, such as fundus autofluorescence, are likely to be required when full spatial profiles and distribution patterns are to be compared with polarization sensitivity.

Lutein, Zeaxanthin and Mesozeaxanthin are macular pigments in the retina (Nolan et al., 2013). On average Zeaxanthin is dominant centrally and Lutein dominates in the periphery. At 0-0.25mm the lutein:zeaxanthin ratio is 1:2.4, but changes to 2:1 beyond 8mm where there are negligible macular pigments present (Bone et al., 1988). Zeaxanthin predominately orients itself perpendicularly across the lipid bilayer, whilst lutein aligns itself at around 23° (Whitehead et al., 2006, Sujak et al., 2000). As these

ratios and volumes change significantly among individuals, it would also be interesting to determine if this variation influences individual PPP perception.

4.3.3. Future Work- Cornea

Future studies into the corneal birefringence effect and its influence on an individual's polarization perception would be beneficial to ensure that this would not need to be incorporated into a final macular screening or MPOD type device. The lack of significant changes in PPP with high corneal birefringence values reported by this research project is promising for PPP, as it supports it as a robust way to investigate the macula, without being affected by differences in corneal characteristics.

It was unexpected that a significant change with corneal birefringence was not demonstrated as this went against the findings of previous research, and potential reasons for this have been discussed in experimental part three. This research highlights the benefit of using a wide variety of angles of polarization/orientations, to minimise the influence of corneal birefringence when assessing polarization sensitivity.

4.4. Alternative Polarization Perception Methods of Interest

This research project provided an overview of current research into PPP and added new insight into normative values, repeatability and how it is influenced, or not, by individual ocular characteristics. The angle of polarization was altered to provide the grating stimuli here, but a previous study utilising a similar gratings method, instead changed the degree of polarization between the bars (Temple et al., 2015). A recent study compared both methods and established that humans are approximately twice as sensitive to changes in angle, than degree of polarization (Misson et al., 2019). From this, they concluded that changing the angle may prove to be a more valuable, robust measure, as it is easier for participants to detect when distinguishing between normal and abnormal macular function.

Most studies into human polarization perception, including this research project, use subjective measures. An objective method using visual evoked potentials was developed recently which provided a unique means of assessing and monitoring macular function. The researchers found that cortical responses can be measured in response to viewing polarization-modulated patterns and showed that this could give an objective measure of PPP. This study also provided confirmatory evidence that the delaminated LCD screen used in this research project does not elicit any cortical response due to luminance artefacts, as a similar delaminated LCD screen did not

evoke cortical responses until the polarization-modulated stimuli were shown (Anderson et al., 2020).

4.4.1. Haidinger's Brush Rotation

A static Haidinger's brush is a transient phenomenon, lasting only a few seconds due to the Troxler effect. It can be difficult to perceive as it is subtle in its appearance which would be detrimental to its use as a clinical test. PPP was developed by manipulating static Haidinger's brushes into defined edges, as it was thought that grating orientation would be a familiar task for untrained individuals, however, other solutions have been explored to overcome the problems of a static Haidinger's brush.

Researchers have found that Haidinger's brush can also be rotated, with participants given the task of stating whether it is moving clockwise or anti-clockwise. This can give a quantifiable measure by varying the degree of polarization of the brush until its direction is no longer visible. This method was used by Temple, Roberts and Misson (2019) who produced a theoretical model between MPOD and polarization perception using Haidinger's brush rotation and validated this experimentally. They reported that the task was understood by all participants and found that individuals with more macular pigments were able to detect the polarization stimuli to lower thresholds (see figure 13), mirroring the results seen in this research project (see figure 25). Using Haidinger's brush rotation to measure polarization threshold gave an exponential relationship between polarization threshold and MPOD (see figure 13). Using their proposed single descent method, on 32 participants, gave a COR of 0.119, which compares well with other MPOD techniques for use in a clinical environment. They stated that the speed and ease of the technique meant it could be used for large scale macular screening. The MP-eye device has recently become commercially available (Azul Optics Ltd., Bristol) based on the results of this paper. The device decreases the degree of polarization of a rotating Haidinger's brush stimulus in ten steps, thus giving a threshold score out of 10. It has been shown to be a fast and reliable device which can be incorporated into a clinical setting (Temple et al., 2019).

Further study on a larger sample is required to determine if Haidinger's brush rotation or PPP provide the most robust model for quantifying human polarization sensitivity.

4.4.2. Maxwell's Spot

Maxwell's spot (Maxwell, 1856) is a luminance effect that appears as a darker circle, approximately 3° in diameter, centred on the fixation point (Misson et al., 2020b). It is visible when looking at a uniform field of unpolarized light alternated between a colour

that is preferentially absorbed by the macular pigments and one that is transmitted. Its appearance is dependent on viewing conditions and individual anatomy (Spencer, 1967, Miles, 1954). It is not considered a polarization phenomenon, although it has recently been shown that its appearance can be modified by changing the polarization components of the light (Misson et al., 2020b).

If the perception of any stimuli is altered by changing the polarization components of light, it can show promise for development to measure human polarization perception and ultimately assess macular health and disease in the future (Misson et al., 2020b, Muller et al., 2016, Goldschmidt, 1950, Forster, 1954, Naylor and Stanworth, 1955). As the perception of Maxwell's spot varies with polarization (Misson et al., 2020b), it could soon be developed into an alternative quantifiable polarization perception technique. It is thought to share a common detection mechanism with Haidinger's brush. It may also be of benefit in the diagnosis and monitoring of amblyopia (Flom and Weymouth, 1961) and dyslexia (Le Floch and Ropars, 2017).

4.5. Alternative MPOD methods of Interest

It was proposed that PPP may be able to give an indication of an individual's MPOD and macular health, and be used in the future to determine low, medium and high risk for age-related macular degeneration. Detecting low MPOD earlier allows practitioners to tailor diet and supplementation advice to their patients (Weigert et al., 2011), which can lower age-related macular degeneration risk (Putnam, 2017, Dennison et al., 2013). As more is understood about the role of the macular pigments, measuring MPOD, and potentially PPP, are likely to become more commonplace in clinics (Putnam, 2017).

There are a selection of *in-vivo* MPOD methods currently available for use in clinic. However, none are widely used in routine clinical practice, perhaps because they are time consuming and expensive (Robson et al., 2003). It can be inferred from the results presented in this research project (see especially figure 25) that measuring an individual's PPP may provide a rapid indication of their macular health in a high street setting, allowing appropriate advice to be given in a timely manner.

There are many alternative methods available to measure MPOD. For the interested reader Putnam (2017) provides a useful summary. Subjective methods are usually effective for most patients in clinic, e.g. heterochromatic flicker photometry (see section 1.4.4 and 1.4.5), objective methods can provide detailed MPOD distribution data, but are often more expensive and used in research settings. A widely used objective

method is fundus reflectometry e.g. the Visucam 200, which uses analysis of reflected light from the retina e.g. by spectral analysis (Creuzot-Garcher et al., 2014, Howells et al., 2011, Berendschot and van Norren, 2004). A newer objective method is fundus autofluorescence, such as in the Heidelberg Retina Angiograph, which utilises the fluorescence properties of lipofuscin pigment to establish MPOD (Putnam, 2017, Trieschmann et al., 2006, Robson et al., 2005, Delori et al., 2001). It can give a full spatial profile of macular pigments up to 5.5° (Putnam, 2017, Canovas et al., 2010, Robson et al., 2003), and is a fast and reliable non-invasive method for measuring MPOD *in vivo*. Hyperspectral image analysis requires further validation prior to widespread use (Putnam, 2017, Fawzi et al., 2011, Lee et al., 2010, Gellermann and Bernstein, 2004).

At this stage, based on the results of this research project, it is clear that polarization pattern perception is not aiming to compete with these other methods to provide a detailed MPOD quantifiable measurement, but rather, to give a general indication of MPOD/macular health rapidly in clinic.

4.6. Conclusion

Polarization Pattern Perception was shown to be an easily recognisable stimuli and was able to give quantifiable data, which could be used to assess macular function. It was shown to be a rapid, inexpensive, and compact method, understood by all the participants, and easily incorporated into routine optometric practice. This novel technique may be especially beneficial where other equipment, such as optical coherence tomography or autofluorescence, is not available. With some development it is believed that PPP could have a quantifiable role in at home monitoring of the macula for those at risk of macular degeneration, prompting them to see a health care professional in a timely manner, and ultimately save vision. A continued effort from researchers to learn more about this newly discovered sense will not only improve current knowledge but could ultimately benefit patients. As human polarization sensitivity measurement is a newly emerging field it may become more commonplace in clinic and develop many, currently unknown, uses.

The repeatability of the novel technique, as well as previously unknown normative PPP values across a range of ages were presented and discussed, with reference to each participant's corneal and macular characteristics. It is concluded that the significant positive correlation between MPOD and PPP, together with the lack of influence from variations in other ocular characteristics, make a measure of PPP potentially highly beneficial for macular assessment. The level of polarization sensitivity achieved in the

participants aligns with results from recent studies (Misson et al., 2019, Misson and Anderson, 2017), and is much more acute that previously thought. Animals are known to use this ability to aid survival, but the purpose of such a highly acute polarization sense in humans cannot yet be explained.

References

ANDERSON, S. J., EDSON-SCOTT, A. & MISSON, G. P. 2020. The electrophysiological response to polarization-modulated patterned visual stimuli. *Vision Res,* 174**,** 1-9.

ARDELJAN, D. & CHAN, C. C. 2013. Aging is not a disease: distinguishing age-related macular degeneration from aging. *Prog Retin Eye Res,* 37**,** 68-89.

AREDS2 2013. Lutein + zeaxanthin and omega-3 fatty acids for age-related macular degeneration: the Age-Related Eye Disease Study 2 (AREDS2) randomized clinical trial. *Jama,* 309**,** 2005-15.

BACH, M. 2007. The Freiburg Visual Acuity Test-variability unchanged by post-hoc re-analysis. *Graefes Arch Clin Exp Ophthalmol,* 245**,** 965-71.

BAKER, D. H., LYGO, F. A., MEESE, T. S. & GEORGESON, M. A. 2018. Binocular summation revisited: Beyond radical2. *Psychol Bull,* 144**,** 1186-1199.

BARKER, F. M., 2ND, SNODDERLY, D. M., JOHNSON, E. J., SCHALCH, W., KOEPCKE, W., GERSS, J. & NEURINGER, M. 2011. Nutritional manipulation of primate retinas, V: effects of lutein, zeaxanthin, and n-3 fatty acids on retinal sensitivity to blue-light-induced damage. *Invest Ophthalmol Vis Sci,* 52**,** 3934-42.

BARTESELLI, G., BARTSCH, D. U., VIOLA, F., MOJANA, F., PELLEGRINI, M., HARTMANN, K. I., BENATTI, E., LEICHT, S., RATIGLIA, R., STAURENGHI, G., WEINREB, R. N. & FREEMAN, W. R. 2013. Accuracy of the Heidelberg Spectralis in the alignment between near-infrared image and tomographic scan in a model eye: a multicenter study. *Am J Ophthalmol,* 156**,** 588-592.

BARTLETT, H., ACTON, J. & EPERJESI, F. 2010a. Clinical evaluation of the MacuScope macular pigment densitometer. *Br J Ophthalmol,* 94**,** 328-31.

BARTLETT, H., STAINER, L., SINGH, S., EPERJESI, F. & HOWELLS, O. 2010b. Clinical evaluation of the MPS 9000 Macular Pigment Screener. *Br J Ophthalmol,* 94**,** 753-6.

BEATTY, S., MURRAY, I. J., HENSON, D. B., CARDEN, D., KOH, H. & BOULTON, M. E. 2001. Macular pigment and risk for age-related macular degeneration in subjects from a Northern European population. *Invest Ophthalmol Vis Sci,* 42**,** 439-46.

BEIRNE, R. O. 2014. The macular pigment optical density spatial profile and increasing age. *Graefes Arch Clin Exp Ophthalmol,* 252**,** 383-8.

BERENDSCHOT, T. T. & VAN NORREN, D. 2004. Objective determination of the macular pigment optical density using fundus reflectance spectroscopy. *Arch Biochem Biophys,* 430**,** 149-55.

BERENDSCHOT, T. T. & VAN NORREN, D. 2006. Macular pigment shows ringlike structures. *Invest Ophthalmol Vis Sci,* 47**,** 709-14.

BERNSTEIN, P. S., DELORI, F. C., RICHER, S., VAN KUIJK, F. J. & WENZEL, A. J. 2010. The value of measurement of macular carotenoid pigment optical densities and distributions in age-related macular degeneration and other retinal disorders. *Vision Res,* 50**,** 716-28.

BERNSTEIN, P. S., LI, B., VACHALI, P. P., GORUSUPUDI, A., SHYAM, R., HENRIKSEN, B. S. & NOLAN, J. M. 2016. Lutein, zeaxanthin, and meso-zeaxanthin: The basic and clinical science underlying carotenoid-based nutritional interventions against ocular disease. *Prog Retin Eye Res,* 50**,** 34-66.

BONE, R. A. 1980. The role of the macular pigment in the detection of polarized light. *Vision Res,* 20**,** 213-20.

BONE, R. A. & LANDRUM, J. T. 1984. Macular pigment in Henle fiber membranes: a model for Haidinger's brushes. *Vision Res,* 24**,** 103-8.

BONE, R. A., LANDRUM, J. T. & CAINS, A. 1992. Optical density spectra of the macular pigment in vivo and in vitro. *Vision Res,* 32**,** 105-10.

BONE, R. A., LANDRUM, J. T., FERNANDEZ, L. & TARSIS, S. L. 1988. Analysis of the macular pigment by HPLC: retinal distribution and age study. *Invest Ophthalmol Vis Sci,* 29**,** 843-9.

BONE, R. A., LANDRUM, J. T., MAYNE, S. T., GOMEZ, C. M., TIBOR, S. E. & TWAROSKA, E. E. 2001. Macular pigment in donor eyes with and without AMD: a case-control study. *Invest Ophthalmol Vis Sci,* 42**,** 235-40.

BOUR, L. J. 1991. Polarized light and the eye. *Vision and Visual Dysfunction,* 1**,** 310-325.

BOUR, L. J. & LOPES CARDOZO, N. J. 1981. On the birefringence of the living human eye. *Vision Res,* 21**,** 1413-21.

CANOVAS, R., LIMA, V. C., GARCIA, P., MORINI, C., PRATA, T. S. & ROSEN, R. B. 2010. Comparison between macular pigment optical density measurements using two-wavelength autofluorescence and heterochromatic flicker photometry techniques. *Invest Ophthalmol Vis Sci,* 51**,** 3152-6.

CAVALLOTTI, C., ARTICO, M., PESCOSOLIDO, N., LEALI, F. M. & FEHER, J. 2004. Age-related changes in the human retina. *Can J Ophthalmol,* 39**,** 61-8.

CLARK, F. 1960. A Study of Troxler's Effect. *Optica Acta,* 7**,** 219-236.

CREUZOT-GARCHER, C., KOEHRER, P., PICOT, C., AHO, S. & BRON, A. M. 2014. Comparison of two methods to measure macular pigment optical density in healthy subjects. *Invest Ophthalmol Vis Sci,* 55**,** 2941-6.

CRONIN, T. W. & MARSHALL, J. 2011. Patterns and properties of polarized light in air and water. *Philos Trans R Soc Lond B Biol Sci,* 366**,** 619-26.

CRONIN, T. W., SHASHAR, N., CALDWELL, R. L., MARSHALL, J., CHEROSKE, A. G. & CHIOU, T. H. 2003. Polarization vision and its role in biological signaling. *Integr Comp Biol,* 43**,** 549-58.

CRUESS, A. F., ZLATEVA, G., XU, X., SOUBRANE, G., PAULEIKHOFF, D., LOTERY, A., MONES, J., BUGGAGE, R., SCHAEFER, C., KNIGHT, T. & GOSS, T. F. 2008. Economic burden of bilateral neovascular age-related macular degeneration: multi-country observational study. *Pharmacoeconomics,* 26**,** 57-73.

CTORI, I. & HUNTJENS, B. 2017. The Association between Foveal Morphology and Macular Pigment Spatial Distribution: An Ethnicity Study. *PLoS One,* 12**,** e0169520.

DA POZZO, S., MARCHESAN, R. & RAVALICO, G. 2009. Scanning laser polarimetry - a review. *Clin Exp Ophthalmol,* 37**,** 68-80.

DAVEY, P. G., ALVAREZ, S. D. & LEE, J. Y. 2016. Macular pigment optical density: repeatability, intereye correlation, and effect of ocular dominance. *Clin Ophthalmol,* 10**,** 1671-8.

DAVIES, N. P. & MORLAND, A. B. 2004. Macular pigments: their characteristics and putative role. *Prog Retin Eye Res,* 23**,** 533-59.

DE KINKELDER, R., VAN DER VEEN, R. L., VERBAAK, F. D., FABER, D. J., VAN LEEUWEN, T. G. & BERENDSCHOT, T. T. 2011. Macular pigment optical density measurements: evaluation of a device using heterochromatic flicker photometry. *Eye (Lond),* 25**,** 105-12.

DE VRIES, H., JIELOF, R. & SPOOR, A. 1950. Properties of the human eye with respect to linearly and circularly polarized light. *Nature,* 166**,** 958-9.

DELORI, F. C., GOGER, D. G., HAMMOND, B. R., SNODDERLY, D. M. & BURNS, S. A. 2001. Macular pigment density measured by autofluorescence spectrometry: comparison with reflectometry and heterochromatic flicker photometry. *J Opt Soc Am A Opt Image Sci Vis,* 18**,** 1212-30.

DEMIREL, S., BILICI, S., BATIOGLU, F. & OZMERT, E. 2014. The effect of age and cataract surgery on macular pigment optic density: a cross-sectional, comparative study. *Graefes Arch Clin Exp Ophthalmol,* 252**,** 213-8.

DENNISON, J. L., STACK, J., BEATTY, S. & NOLAN, J. M. 2013. Concordance of macular pigment measurements obtained using customized heterochromatic

flicker photometry, dual-wavelength autofluorescence, and single-wavelength reflectance. *Exp Eye Res,* 116**,** 190-8.
ELLIOTT, D. B., YANG, K. C. & WHITAKER, D. 1995. Visual acuity changes throughout adulthood in normal, healthy eyes: seeing beyond 6/6. *Optometry and vision science : official publication of the American Academy of Optometry,* 72**,** 186-191.
ELSHOUT, M., WEBERS, C. A., VAN DER REIS, M. I., DE JONG-HESSE, Y. & SCHOUTEN, J. S. 2017. Tracing the natural course of visual acuity and quality of life in neovascular age-related macular degeneration: a systematic review and quality of life study. *BMC Ophthalmol,* 17**,** 120.
EVANS, J. R. & LAWRENSON, J. G. 2017. Antioxidant vitamin and mineral supplements for slowing the progression of age-related macular degeneration. *Cochrane Database Syst Rev,* 7**,** Cd000254.
FAUL, F., ERDFELDER, E., BUCHNER, A. & LANG, A. G. 2009. Statistical power analyses using G*Power 3.1: tests for correlation and regression analyses. *Behav Res Methods,* 41**,** 1149-60.
FAWZI, A. A., LEE, N., ACTON, J. H., LAINE, A. F. & SMITH, R. T. 2011. Recovery of macular pigment spectrum in vivo using hyperspectral image analysis. *J Biomed Opt,* 16**,** 106008.
FLOM, M. C. & WEYMOUTH, F. W. 1961. Centricity of Maxwell's spot in strabismus and amblyopia. *Arch Ophthalmol,* 66**,** 260-8.
FORSTER, H. W., JR. 1954. The clinical use of the Haidinger's brushes phenomenon. *Am J Ophthalmol,* 38**,** 661-5.
FOSTER, J. J., TEMPLE, S. E., HOW, M. J., DALY, I. M., SHARKEY, C. R., WILBY, D. & ROBERTS, N. W. 2018. Polarisation vision: overcoming challenges of working with a property of light we barely see. *Naturwissenschaften,* 105**,** 27.
GELLERMANN, W. & BERNSTEIN, P. S. 2004. Noninvasive detection of macular pigments in the human eye. *J Biomed Opt,* 9**,** 75-85.
GOLDSCHMIDT, M. 1950. A new test for function of the macula lutea. *Arch Ophthal,* 44**,** 129-35.
HAEGERSTROM-PORTNOY, G., SCHNECK, M. E. & BRABYN, J. A. 1999. Seeing into old age: vision function beyond acuity. *Optom Vis Sci,* 76**,** 141-58.
HAGEN, S., KREBS, I., GLITTENBERG, C. & BINDER, S. 2010. Repeated measures of macular pigment optical density to test reproducibility of heterochromatic flicker photometry. *Acta Ophthalmol,* 88**,** 207-11.
HAIDINGER, W. 1844. Über das direkte erkennen des polarisierten lichts und der lage der polarisationsebene. *Ann Phys,* 139**,** 29-39.
HAMMOND, B. R., JR. & CARUSO-AVERY, M. 2000. Macular pigment optical density in a Southwestern sample. *Invest Ophthalmol Vis Sci,* 41**,** 1492-7.
HAMMOND, B. R., JR., WOOTEN, B. R. & CURRAN-CELENTANO, J. 2001. Carotenoids in the retina and lens: possible acute and chronic effects on human visual performance. *Arch Biochem Biophys,* 385**,** 41-6.
HAMMOND, B. R., JR., WOOTEN, B. R. & SMOLLON, B. 2005. Assessment of the validity of in vivo methods of measuring human macular pigment optical density. *Optom Vis Sci,* 82**,** 387-404.
HAMMOND, B. R., JR., WOOTEN, B. R. & SNODDERLY, D. M. 1997. Individual variations in the spatial profile of human macular pigment. *J Opt Soc Am A Opt Image Sci Vis,* 14**,** 1187-96.
HEMENGER, R. P. 1982. Dichroism of the macular pigment and Haidinger's brushes. *J Opt Soc Am,* 72**,** 734-7.
HOFFMANN, E. M., LAMPARTER, J., MIRSHAHI, A., ELFLEIN, H., HOEHN, R., WOLFRAM, C., LORENZ, K., ADLER, M., WILD, P. S., SCHULZ, A., MATHES, B., BLETTNER, M. & PFEIFFER, N. 2013. Distribution of central corneal thickness and its association with ocular parameters in a large central European cohort: the Gutenberg health study. *PLoS One,* 8**,** e66158.

HORVATH, G., TAKACS, P., KRETZER, B., SZILASI, S., SZAZ, D., FARKAS, A. & BARTA, A. 2017. Celestial polarization patterns sufficient for Viking navigation with the naked eye: detectability of Haidinger's brushes on the sky versus meteorological conditions. *R Soc Open Sci,* 4**,** 160688.

HOWELLS, O., EPERJESI, F. & BARTLETT, H. 2011. Measuring macular pigment optical density in vivo: a review of techniques. *Graefes Arch Clin Exp Ophthalmol,* 249**,** 315-47.

HOWELLS, O., EPERJESI, F. & BARTLETT, H. 2013. Improving the repeatability of heterochromatic flicker photometry for measurement of macular pigment optical density. *Graefes Arch Clin Exp Ophthalmol,* 251**,** 871-80.

JOHNSEN, S. 2011. Polarization. In: *The optics of life: a biologist's guide to light in nature* [online]. Princeton, N.J. : Princeton University Press, 170.

JOHNSON, M. A. & CHOY, D. 1987. On the definition of age-related norms for visual function testing. *Applied Optics,* 26**,** 1449-1454.

KAMERMANS, M. & HAWRYSHYN, C. 2011. Teleost polarization vision: how it might work and what it might be good for. *Philos Trans R Soc Lond B Biol Sci,* 366**,** 742-56.

KHACHIK, F., BERNSTEIN, P. S. & GARLAND, D. L. 1997. Identification of lutein and zeaxanthin oxidation products in human and monkey retinas. *Invest Ophthalmol Vis Sci,* 38**,** 1802-11.

KIRBY, M. L., GALEA, M., LOANE, E., STACK, J., BEATTY, S. & NOLAN, J. M. 2009. Foveal anatomic associations with the secondary peak and the slope of the macular pigment spatial profile. *Invest Ophthalmol Vis Sci,* 50**,** 1383-91.

KNIGHTON, R. W. & HUANG, X. R. 2002. Linear birefringence of the central human cornea. *Invest Ophthalmol Vis Sci,* 43**,** 82-6.

KNIGHTON, R. W., HUANG, X. R. & CAVUOTO, L. A. 2008. Corneal birefringence mapped by scanning laser polarimetry. *Opt Express,* 16**,** 13738-51.

KNIGHTON, R. W., HUANG, X. R. & GREENFIELD, D. S. 2002. Analytical model of scanning laser polarimetry for retinal nerve fiber layer assessment. *Invest Ophthalmol Vis Sci,* 43**,** 383-92.

KONDRASHEV, S. L., GNYUBKINA, V. P. & ZUEVA, L. V. 2012. Structure and spectral sensitivity of photoreceptors of two anchovy species: Engraulis japonicus and Engraulis encrasicolus. *Vision Res,* 68**,** 19-27.

LABHART, T. 2016. Can invertebrates see the e-vector of polarization as a separate modality of light? *J Exp Biol,* 219**,** 3844-3856.

LANDRUM, J. T. & BONE, R. A. 2001. Lutein, zeaxanthin, and the macular pigment. *Arch Biochem Biophys,* 385**,** 28-40.

LATASIEWICZ, M., GOURIER, H., YUSUF, I. H., LUQMANI, R., SHARMA, S. M. & DOWNES, S. M. 2017. Hydroxychloroquine retinopathy: an emerging problem. *Eye (Lond),* 31**,** 972-976.

LE FLOCH, A. & ROPARS, G. 2017. Left-right asymmetry of the Maxwell spot centroids in adults without and with dyslexia. *Proc Biol Sci,* 284**,** 1865.

LE FLOCH, A., ROPARS, G., ENOCH, J. & LAKSHMINARAYANAN, V. 2010. The polarization sense in human vision. *Vision Res,* 50**,** 2048-54.

LEE, N., WIELAARD, J., FAWZI, A. A., SAJDA, P., LAINE, A. F., MARTIN, G., HUMAYUN, M. S. & SMITH, R. T. 2010. In vivo snapshot hyperspectral image analysis of age-related macular degeneration. *Conf Proc IEEE Eng Med Biol Soc,* 2010**,** 5363-6.

LOANE, E., STACK, J., BEATTY, S. & NOLAN, J. M. 2007. Measurement of macular pigment optical density using two different heterochromatic flicker photometers. *Curr Eye Res,* 32**,** 555-64.

LOUGHMAN, J., SCANLON, G., NOLAN, J. M., O'DWYER, V. & BEATTY, S. 2012. An evaluation of a novel instrument for measuring macular pigment optical density: the MPS 9000. *Acta Ophthalmol,* 90**,** e90-7.

MAKRIDAKI, M., CARDEN, D. & MURRAY, I. J. 2009. Macular pigment measurement in clinics: controlling the effect of the ageing media. *Ophthalmic Physiol Opt,* 29**,** 338-44.

MAPP, A. P., ONO, H. & BARBEITO, R. 2003. What does the dominant eye dominate? A brief and somewhat contentious review. *Percept Psychophys,* 65**,** 310-7.

MARMOR, M. F., KELLNER, U., LAI, T. Y., MELLES, R. B. & MIELER, W. F. 2016. Recommendations on Screening for Chloroquine and Hydroxychloroquine Retinopathy (2016 Revision). *Ophthalmology,* 123**,** 1386-94.

MARSHALL, N. J., POWELL, S. B., CRONIN, T. W., CALDWELL, R. L., JOHNSEN, S., GRUEV, V., CHIOU, T. S., ROBERTS, N. W. & HOW, M. J. 2019. Polarisation signals: a new currency for communication. *J Exp Biol,* 222**,** 134213.

MAXWELL, J. 1856. On the unequal sensibility of the foramen centrale to light of different colours. *Athenaeum, 1505***,** 1093.

MCGILL, T. J., RENNER, L. M. & NEURINGER, M. 2016. Elevated Fundus Autofluorescence in Monkeys Deficient in Lutein, Zeaxanthin, and Omega-3 Fatty Acids. *Invest Ophthalmol Vis Sci,* 57**,** 1361-9.

MCGREGOR, J., TEMPLE, S. & HORVÁTH, G. 2014. Human Polarization Sensitivity. *In:* HORVÁTH, G. (ed.) *Polarized Light and Polarization Vision in Animal Sciences.* Berlin, Heidelberg: Springer**,** 303-15.

MELLES, R. B. & MARMOR, M. F. 2014. The risk of toxic retinopathy in patients on long-term hydroxychloroquine therapy. *JAMA Ophthalmol,* 132**,** 1453-60.

MEYER ZU WESTRUP, V., DIETZEL, M., ZEIMER, M., PAULEIKHOFF, D. & HENSE, H. W. 2016. Changes of macular pigment optical density in elderly eyes: a longitudinal analysis from the MARS study. *Int J Retina Vitreous,* 2**,** 14.

MILES, W. R. 1954. Comparison of functional and structural areas in human fovea. I. Method of entoptic plotting. *J Neurophysiol,* 17**,** 22-38.

MISSON, G., ANDERSON, S., ARMSTRONG, R., GILLETT, M. & REYNOLDS, D. 2020a. The Clinical Application of Polarization Pattern Perception. *Trans. Vis. Sci. Tech,* 9**,** 31.

MISSON, G. P. 1993. Form and behaviour of Haidinger's brushes. *Ophthalmic Physiol Opt,* 13**,** 392-6.

MISSON, G. P. & ANDERSON, S. J. 2017. The spectral, spatial and contrast sensitivity of human polarization pattern perception. *Sci Rep,* 7**,** 16571.

MISSON, G. P., TEMPLE, S. E. & ANDERSON, S. J. 2018. Computational simulation of Haidinger's brushes. *J Opt Soc Am A Opt Image Sci Vis,* 35**,** 946-952.

MISSON, G. P., TEMPLE, S. E. & ANDERSON, S. J. 2019. Computational simulation of human perception of spatially dependent patterns modulated by degree and angle of linear polarization. *Journal of the Optical Society of America A,* 36**,** B65-B70.

MISSON, G. P., TEMPLE, S. E. & ANDERSON, S. J. 2020b. Polarization perception in humans: on the origin of and relationship between Maxwell's spot and Haidinger's brushes. *Sci Rep,* 10**,** 108.

MISSON, G. P., TIMMERMAN, B. H. & BRYANSTON-CROSS, P. J. 2015. Human perception of visual stimuli modulated by direction of linear polarization. *Vision Res,* 115**,** 48-57.

MITCHELL, J. & BRADLEY, C. 2006. Quality of life in age-related macular degeneration: a review of the literature. *Health Qual Life Outcomes,* 4**,** 97.

MULLER, P. L., MULLER, S., GLIEM, M., KUPPER, K., HOLZ, F. G., HARMENING, W. M. & CHARBEL ISSA, P. 2016. Perception of Haidinger Brushes in Macular Disease Depends on Macular Pigment Density and Visual Acuity. *Invest Ophthalmol Vis Sci,* 57**,** 1448-56.

NAYLOR, E. J. & STANWORTH, A. 1954a. Retinal pigment and the Haidinger effect. *J Physiol,* 124**,** 543-52.

NAYLOR, E. J. & STANWORTH, A. 1954b. The measurement of the Haidinger effect. *J Physiol,* 123**,** 30-1.

NAYLOR, E. J. & STANWORTH, A. 1955. The measurement and clinical significance of the Haidinger effect. *Trans Ophthalmol Soc U K,* 75**,** 67-79.

NEURINGER, M., SANDSTROM, M. M., JOHNSON, E. J. & SNODDERLY, D. M. 2004. Nutritional manipulation of primate retinas, I: effects of lutein or zeaxanthin supplements on serum and macular pigment in xanthophyll-free rhesus monkeys. *Invest Ophthalmol Vis Sci,* 45**,** 3234-43.

NOLAN, J. M., MEAGHER, K., KASHANI, S. & BEATTY, S. 2013. What is meso-zeaxanthin, and where does it come from? *Eye (Lond),* 27**,** 899-905.

NOLAN, J. M., STRINGHAM, J. M., BEATTY, S. & SNODDERLY, D. M. 2008. Spatial profile of macular pigment and its relationship to foveal architecture. *Invest Ophthalmol Vis Sci,* 49**,** 2134-42.

NUSINOWITZ, S., WANG, Y., KIM, P., HABIB, S., BARON, R., CONLEY, Y. & GORIN, M. 2018. Retinal Structure in Pre-Clinical Age-Related Macular Degeneration. *Curr Eye Res,* 43**,** 376-382.

OKUBO, A., ROSA, R. H., JR., BUNCE, C. V., ALEXANDER, R. A., FAN, J. T., BIRD, A. C. & LUTHERT, P. J. 1999. The relationships of age changes in retinal pigment epithelium and Bruch's membrane. *Invest Ophthalmol Vis Sci,* 40**,** 443-9.

PERENIN, M. T. & VADOT, E. 1981. Macular sparing investigated by means of Haidinger brushes. *Br J Ophthalmol,* 65**,** 429-35.

PUTNAM, C. M. 2017. Clinical imaging of macular pigment optical density and spatial distribution. *Clin Exp Optom,* 100**,** 333-340.

QUARTILHO, A., SIMKISS, P., ZEKITE, A., XING, W., WORMALD, R. & BUNCE, C. 2016. Leading causes of certifiable visual loss in England and Wales during the year ending 31 March 2013. *Eye (Lond),* 30**,** 602-7.

READING, V. M. & WEALE, R. A. 1974. Macular pigment and chromatic aberration. *J Opt Soc Am,* 64**,** 231-4.

ROBERTS, N. W., PORTER, M. L. & CRONIN, T. W. 2011. The molecular basis of mechanisms underlying polarization vision. *Philos Trans R Soc Lond B Biol Sci,* 366**,** 627-37.

ROBSON, A. G., HARDING, G., VAN KUIJK, F. J., PAULEIKHOFF, D., HOLDER, G. E., BIRD, A. C., FITZKE, F. W. & MORELAND, J. D. 2005. Comparison of fundus autofluorescence and minimum-motion measurements of macular pigment distribution profiles derived from identical retinal areas. *Perception,* 34**,** 1029-34.

ROBSON, A. G., MORELAND, J. D., PAULEIKHOFF, D., MORRISSEY, T., HOLDER, G. E., FITZKE, F. W., BIRD, A. C. & VAN KUIJK, F. J. 2003. Macular pigment density and distribution: comparison of fundus autofluorescence with minimum motion photometry. *Vision Res,* 43**,** 1765-75.

ROTHMAYER, M., DULTZ, W., FRINS, E., ZHAN, Q., TIERNEY, D. & SCHMITZER, H. 2007. Nonlinearity in the rotational dynamics of Haidinger's brushes. *Appl Opt,* 46**,** 7244-51.

RUBIN, G. S., WEST, S. K., MUNOZ, B., BANDEEN-ROCHE, K., ZEGER, S., SCHEIN, O. & FRIED, L. P. 1997. A comprehensive assessment of visual impairment in a population of older Americans. The SEE Study. Salisbury Eye Evaluation Project. *Invest Ophthalmol Vis Sci,* 38**,** 557-68.

SACCONI, R., CORBELLI, E., QUERQUES, L., BANDELLO, F. & QUERQUES, G. 2017. A Review of Current and Future Management of Geographic Atrophy. *Ophthalmol Ther,* 6**,** 69-77.

SALVI, S. M., AKHTAR, S. & CURRIE, Z. 2006. Ageing changes in the eye. *Postgrad Med J,* 82**,** 581-7.

SHARIFZADEH, M., BERNSTEIN, P. S. & GELLERMANN, W. 2006. Nonmydriatic fluorescence-based quantitative imaging of human macular pigment distributions. *J Opt Soc Am A Opt Image Sci Vis,* 23**,** 2373-87.

SHERMAN, M. E. & PRIESTLEY, B. S. 1962. The Haidinger brush phenomenon: a new clinical use. *Am J Ophthalmol,* 54**,** 807-12.
SHUTE, C. C. 1974. Haidinger's brushes and predominant orientation of collagen in corneal stroma. *Nature,* 250**,** 163-4.
SHUTE, C. C. 1978. Haidinger's brushes. *Vision Res,* 18**,** 1467.
SLEIGHT, J. L. & MASHIKIAN, M. 1971. Haidinger brush diagnosis and treatment of binocular suppression scotoma in intermittent, accommodative and postoperative esotropia. *Am Orthopt J,* 21**,** 96-100.
SLOAN, L. L. & NAQUIN, H. A. 1955. A quantitative test for determining the visibility of the Haidinger brushes: clinical applications. *Am J Ophthalmol,* 40**,** 393-406.
SNODDERLY, D. & HAMMOND, B. 1999. I*n vivo psychophysical assessment of nutritional and environmental influences on human ocular tissues: lens and macular pigment*. *In:* TAYLOR, A. (ed.) *Nutritional and environmental influences on the eye.* Boca Raton, FL: CRC Press**,** 251-73.
SNODDERLY, D. M., AURAN, J. D. & DELORI, F. C. 1984a. The macular pigment. II. Spatial distribution in primate retinas. *Invest Ophthalmol Vis Sci,* 25**,** 674-85.
SNODDERLY, D. M., BROWN, P. K., DELORI, F. C. & AURAN, J. D. 1984b. The macular pigment. I. Absorbance spectra, localization, and discrimination from other yellow pigments in primate retinas. *Invest Ophthalmol Vis Sci,* 25**,** 660-73.
SPENCER, J. A. 1967. An investigation of Maxwell's Spot. *Br J Physiol Opt,* 24**,** 103-47.
STOCKMAN, A., SHARPE, L. T., MERBS, S. & NATHANS, J. 2000. Spectral sensitivities of human cone visual pigments determined in vivo and in vitro. *Methods Enzymol,* 316**,** 626-50.
STRINGHAM, J. M. & HAMMOND, B. R., JR. 2007. The glare hypothesis of macular pigment function. *Optom Vis Sci,* 84**,** 859-64.
STRINGHAM, J. M., HAMMOND, B. R., NOLAN, J. M., WOOTEN, B. R., MAMMEN, A., SMOLLON, W. & SNODDERLY, D. M. 2008. The utility of using customized heterochromatic flicker photometry (cHFP) to measure macular pigment in patients with age-related macular degeneration. *Exp Eye Res,* 87**,** 445-53.
SUBHI, Y., FORSHAW, T. & SORENSEN, T. L. 2016. Macular thickness and volume in the elderly: A systematic review. *Ageing Res Rev,* 29**,** 42-9.
SUJAK, A., OKULSKI, W. & GRUSZECKI, W. I. 2000. Organisation of xanthophyll pigments lutein and zeaxanthin in lipid membranes formed with dipalmitoylphosphatidylcholine. *Biochim Biophys Acta,* 1509**,** 255-63.
TEMPLE, S. E., MCGREGOR, J. E., MILES, C., GRAHAM, L., MILLER, J., BUCK, J., SCOTT-SAMUEL, N. E. & ROBERTS, N. W. 2015. Perceiving polarization with the naked eye: characterization of human polarization sensitivity. *Proc Biol Sci,* 282**,** 25150338.
TEMPLE, S. E., PIGNATELLI, V., COOK, T., HOW, M. J., CHIOU, T. H., ROBERTS, N. W. & MARSHALL, N. J. 2012. High-resolution polarisation vision in a cuttlefish. *Curr Biol,* 22**,** 121-2.
TEMPLE, S. E., ROBERTS, N. W. & MISSON, G. P. 2019. Haidinger's brushes elicited at varying degrees of polarization rapidly and easily assesses total macular pigmentation. *Journal of the Optical Society of America A,* 36**,** B123-B131.
TRIESCHMANN, M., HEIMES, B., HENSE, H. W. & PAULEIKHOFF, D. 2006. Macular pigment optical density measurement in autofluorescence imaging: comparison of one- and two-wavelength methods. *Graefes Arch Clin Exp Ophthalmol,* 244**,** 1565-74.
TRIESCHMANN, M., SPITAL, G., LOMMATZSCH, A., VAN KUIJK, E., FITZKE, F., BIRD, A. C. & PAULEIKHOFF, D. 2003. Macular pigment: quantitative analysis on autofluorescence images. *Graefes Arch Clin Exp Ophthalmol,* 241**,** 1006-12.
VAN DE KRAATS, J., KANIS, M. J., GENDERS, S. W. & VAN NORREN, D. 2008. Lutein and zeaxanthin measured separately in the living human retina with fundus reflectometry. *Invest Ophthalmol Vis Sci,* 49**,** 5568-73.

VAN DER VEEN, R. L., BERENDSCHOT, T. T., HENDRIKSE, F., CARDEN, D., MAKRIDAKI, M. & MURRAY, I. J. 2009. A new desktop instrument for measuring macular pigment optical density based on a novel technique for setting flicker thresholds. *Ophthalmic Physiol Opt,* 29**,** 127-37.

WEHNER, R. 2001. Polarization vision- a uniform sensory capacity? *J Exp Biol,* 204**,** 2589-96.

WEIGERT, G., KAYA, S., PEMP, B., SACU, S., LASTA, M., WERKMEISTER, R. M., DRAGOSTINOFF, N., SIMADER, C., GARHOFER, G., SCHMIDT-ERFURTH, U. & SCHMETTERER, L. 2011. Effects of lutein supplementation on macular pigment optical density and visual acuity in patients with age-related macular degeneration. *Invest Ophthalmol Vis Sci,* 52**,** 8174-8.

WEINREB, R. N., BOWD, C., GREENFIELD, D. S. & ZANGWILL, L. M. 2002. Measurement of the magnitude and axis of corneal polarization with scanning laser polarimetry. *Arch Ophthalmol,* 120**,** 901-6.

WHITEHEAD, A. J., MARES, J. A. & DANIS, R. P. 2006. Macular pigment: a review of current knowledge. *Arch Ophthalmol,* 124**,** 1038-45.

WICK, B. 1976. A home pleoptic method. *Am J Optom Physiol Opt,* 53**,** 81-4.

WOLFS, R. C., KLAVER, C. C., VINGERLING, J. R., GROBBEE, D. E., HOFMAN, A. & DE JONG, P. T. 1997. Distribution of central corneal thickness and its association with intraocular pressure: The Rotterdam Study. *Am J Ophthalmol,* 123**,** 767-72.

WU, J., CHO, E., WILLETT, W. C., SASTRY, S. M. & SCHAUMBERG, D. A. 2015. Intakes of Lutein, Zeaxanthin, and Other Carotenoids and Age-Related Macular Degeneration During 2 Decades of Prospective Follow-up. *JAMA Ophthalmol,* 133**,** 1415-24.

WUSTEMEYER, H., MOESSNER, A., JAHN, C. & WOLF, S. 2003. Macular pigment density in healthy subjects quantified with a modified confocal scanning laser ophthalmoscope. *Graefes Arch Clin Exp Ophthalmol,* 241**,** 647-51.

YAMAGISHI, N., ANDERSON, S. J. & KAWATO, M. 2010. The observant mind: self-awareness of attentional status. *Proc Biol Sci,* 277**,** 3421-6.

YUSUF, I. H., SHARMA, S., LUQMANI, R. & DOWNES, S. M. 2017. Hydroxychloroquine retinopathy. *Eye (Lond),* 31**,** 828-845.

ZHOU, Q. & WEINREB, R. N. 2002. Individualized compensation of anterior segment birefringence during scanning laser polarimetry. *Invest Ophthalmol Vis Sci,* 43**,** 2221-8.

Appendix 1- Physical Characteristics and Calibration of the Modified LCD Screen

The modification, calibration, graphs and calculations in this supplementary material for the LCD screen were kindly completed by Prof Gary Misson for this research project.

1.1. Screen Details

The screen was delaminated by removing the front polariser from the LCD screen (dLCD) and modified by adding a blue filter between the backlight assembly and the back polarizer of the LCD. This was done as previously described in the methods and supplementary materials sections of these studies (Misson and Anderson, 2017, Misson et al., 2015, Temple et al., 2015).

Original (unmodified) screen characteristics:

Brand Name: ZGYNK
Model Number: TB7009
Size:173x121x33mm, 7" screen
Response Time: 8ms
Brightness: 300cd/m^2
Interface Type: AV/BNC/VGA
Contrast Ratio: 400:1
Resolution: 1024x600
Place of Origin: Guangdong, China (Mainland)

1.2. Photometry

Performed with a Minolta Luminance Meter LS-110 (Minolta Camera Co. Ltd. Japan) for greyscale increments 0 – 255, supplementary figure 1.

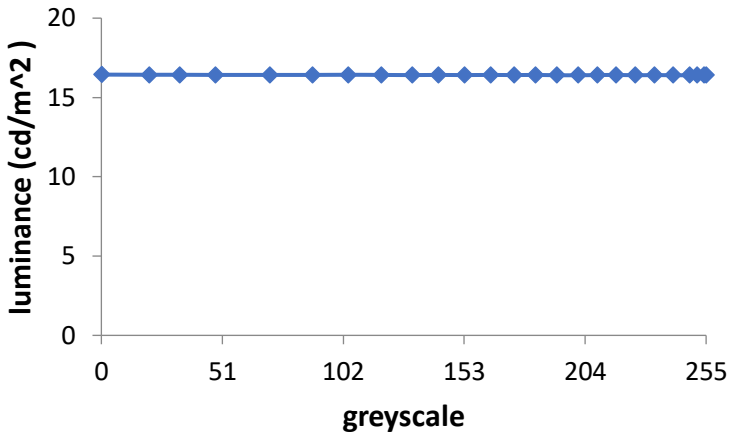

Supplementary figure 1. *Photometry data graph displaying the luminance output measured for each given greyscale.*

Supplementary figure 1 shows that the light output is constant at 16.4 cdm^{-2} for all greyscale values used in this study.

1.3. Spectrometry

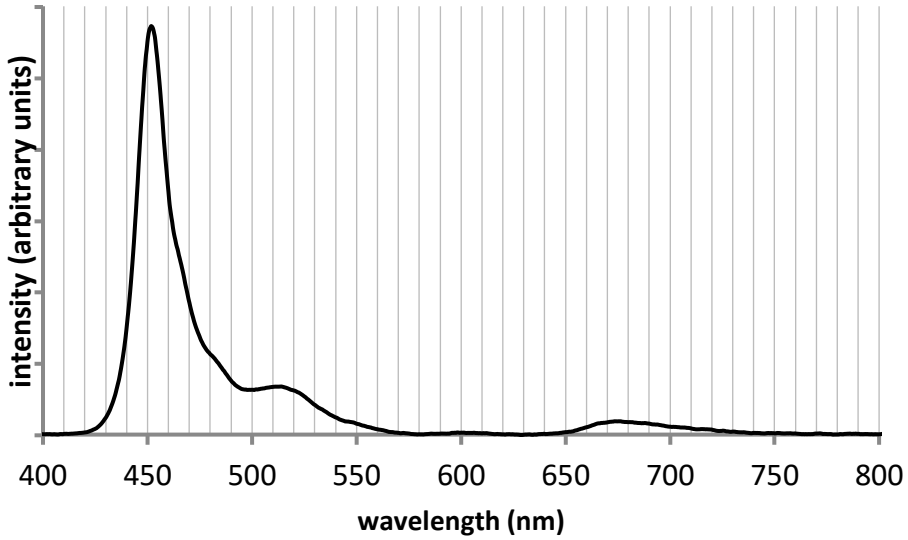

Supplementary figure 2. *Graph displaying the screen's spectral characteristics, measured for greyscale 255, but constant for all greyscale values.*

The spectral output of the dLCD with filter *in situ* was determined using an Ocean Optics spectrometer (USB2+40448), plotted in supplementary figure 2. This graph shows that the dominant peak was at 452nm with a smaller peak around 515nm. There was no significant output below 400nm or above 570nm. These spectral characteristics were constant for all greyscale values.

1.4. Polarimetry

1.4.1. Method and Definitions

The polarization output of the delaminated LCD was determined using an optical bench-mounted polarimeter comprising a Fresnel rhomb achromatic quarter-wave retarder, a Glan-Thompson polarizer and an Ocean Optics spectrometer with appropriate software. The method is described elsewhere (Foster et al., 2018, Misson and Anderson, 2017, Temple et al., 2015), and determines polarization angle (*AoP*), ellipticity (b/a), and degree of polarisation (*DoP*).

Angle of polarisation (*AoP*) is the angle anticlockwise from horizontal looking into the beam of maximum **e**-vector amplitude.

Ellipticity is the ratio of magnitudes of the minor (b) to major (a) axes of the polarisation ellipse, (e.g. b/a = 0 for linear polarisation, 1 for circular polarisation).

Degree of polarisation (*DoP*) is the extent to which the beam is polarised and given by

$$DoP = \frac{I_{pol}}{I_{total}} = \frac{\sqrt{S_1^2 + S_2^2 + S_3^2}}{S_0^2}$$

Where S_0, S_1, S_2, S_3 are the Stokes' parameters of the beam measured by polarimetry; I_{pol} is the intensity of polarized light, I_{total} in the total light (polarized + depolarized) intensity.

For this experiment, a high degree of polarization and minimal ellipticity is required to give fully linearly polarized light. The angle of polarization was dependent on greyscale and was altered between grating bars to obtain a polarization threshold.

1.4.2. Results

Results for this screen are plotted in supplementary figure 3. It shows that the degree of polarization was constantly > 0.93, which can be considered to be fully polarised for this study. Ellipticity magnitude varies nonlinearly with greyscale between grey levels 000 and 118 but between grey levels 118 – 255 was consistently < 0.05. For the greyscale values used in this study this output can be regarded as linearly polarised. The angle of polarisation followed a 4th order polynomial (R^2 = 0.9988, black line):

AoP = **4.94470E-08x^4 - 3.00372E-05x^3 + 4.51582E-03x^2 + 3.29911E-01x - 4.03806E+01**

Eq. 1

Where x is the grayscale value (0 – 255)

The results from this experiment fall within the contrast threshold ranges 7% (grey fore 168, back 180) to 50% (grey fore 119, back 217). Supplementary figure 3 shows that the ellipticity within this range is < 0.05. This ellipticity is minimal, meaning the output from the monitor could be considered as linear during the write-up.

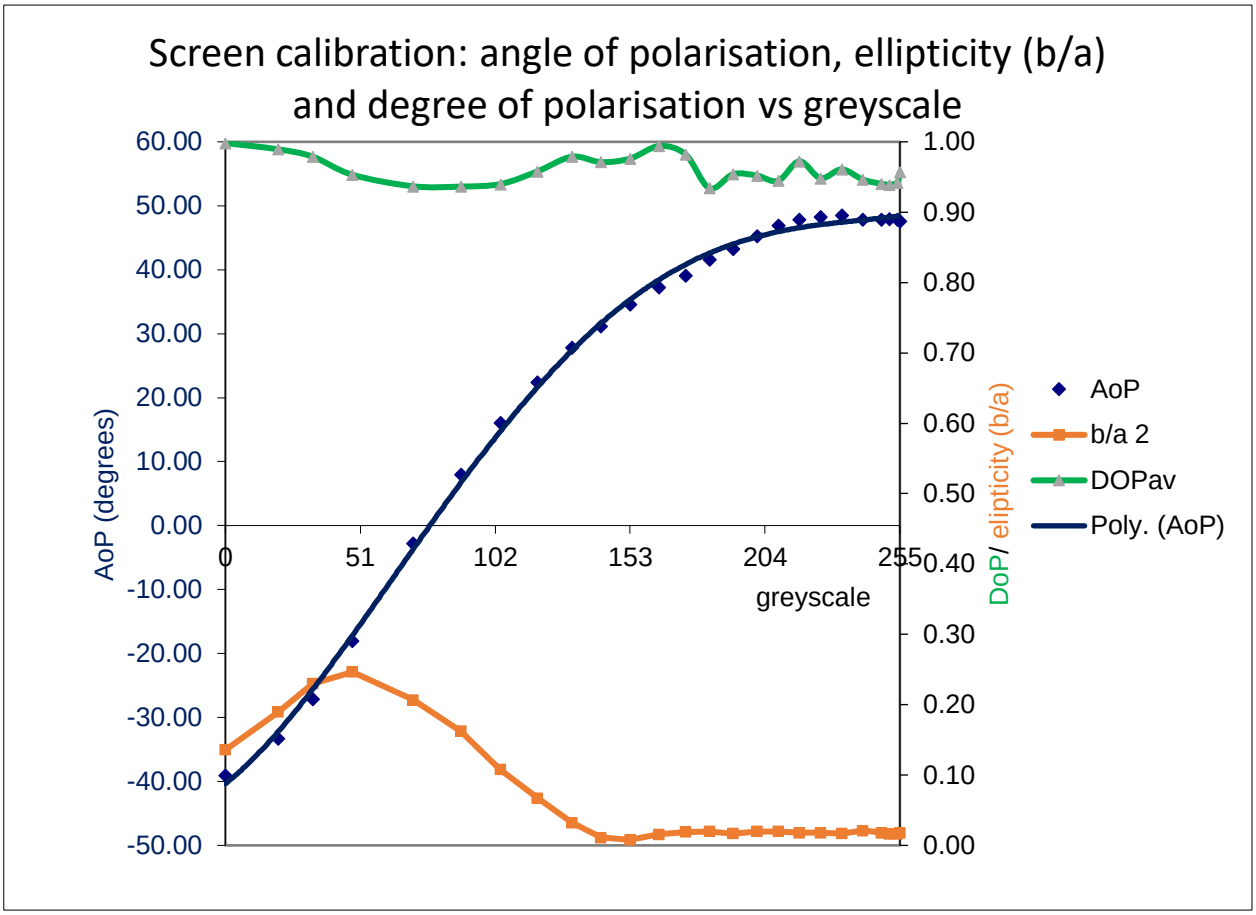

Supplementary figure 3. *Screen calibration: angle of polarisation, ellipticity (b/a) and degree of polarisation vs. greyscale. Horizontal axis is greyscale of image on the delaminated LCD screen. Left vertical axis shows AoP in degrees anticlockwise from horizontal (blue regression curve and diamonds); Right axis shows DoP (green curve, triangles) and ellipticity (brown curve, squares).*

1.5. FrACT Characteristics

1.5.1. Greyscale for given contrast output

The relationship between greyscale values of the foreground and background shading of FrACT images of a given contrast is depicted in supplementary figure 4.

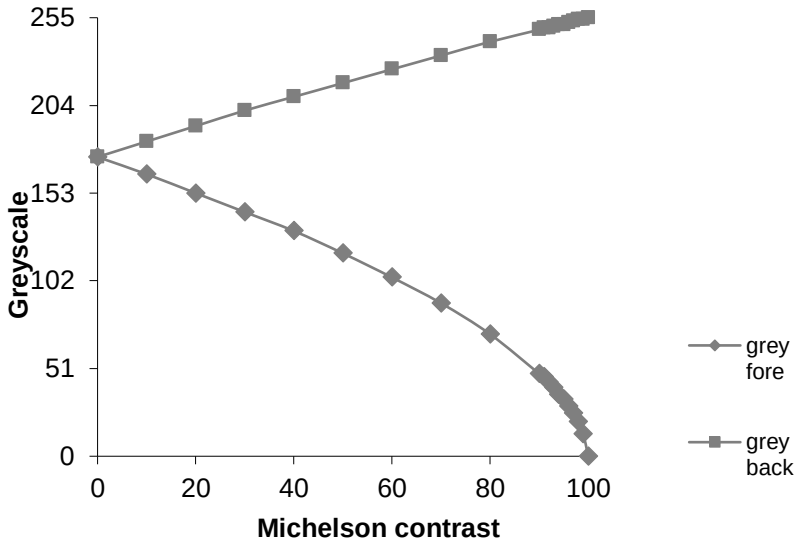

Supplementary figure 4. *Fore/background greyscale values for FrACT Michelson Contrast.*

1.5.2. Greyscale, contrast, *AoP* and difference in *AoP*

Using the results depicted in figure 4 and the regression Eq. 1, FrACT Michelson contrast can be related to output *AoP* of foreground and background and hence a fore/background difference in *AoP* (see supplementary figure 5).

- The relationship between difference in *AoP* (Δ*AoP*) and contrast fits (R^2 = 0.999) the following 4th order polynomial:

$$\Delta AoP = 1.80688E\text{-}06x^4 - 2.64749E\text{-}04x^3 + 1.52013E\text{-}02x^2 + 1.76218E\text{-}01x + 4.46572E\text{-}01$$

Eq. 2

where x is the FrACT Michelson Contrast.

This equation was used to convert contrast threshold into *AoP* difference.

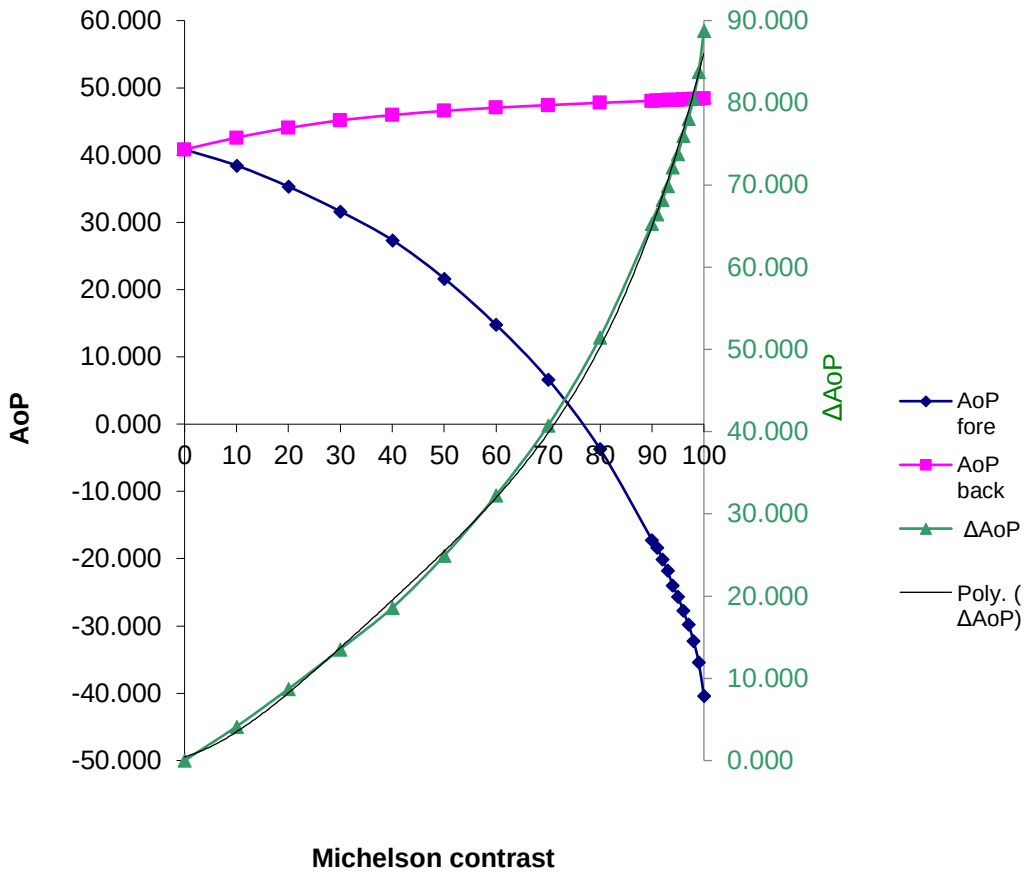

Supplementary figure 5. *Fore (blue, left vertical axis)/background (pink, left vertical axis) AoP values and difference in AoP (ΔAoP, green, right vertical axis) for FrACT Michelson Contrast (horizontal axis). Black line is the 4th order polynomial regression between contrast and greyscale.*

Appendix 2- Participant Information Sheets and Consent Forms

Two versions of the participant information sheet and consent forms were used. The first version is for the main study participants who undertook a routine eye examination, optical coherence tomography scan and PPP measurements for one eye. The second is for participants who were involved in the repeatability study as they attended the practice more than once, performed scans for both eyes, and had additional scans.

Participant Information Sheet (Group 1)

Main Study #1405

Version 3- 02/10/2018

Research workers, school, and subject area responsible

Miss Jasmine Smith, Prof Stephen Anderson, and Prof Gary Misson.

School of Life & Health Sciences, Vision Sciences, Aston University.

Project Title

Visual sensitivity to polarization pattern perception: implications for the assessment of macular function in health and disease.

Invitation

You are being invited to participate in a research study. Before you decide it is important for you to understand your role in the research and why it is being carried out. Please take the time to read the following information carefully.

What is the purpose of the study?

Many animals are sensitive to both ordinary light and polarized light. It has recently been discovered that, under special viewing conditions, humans can also see polarized light. This is potentially important as polarized light may be a useful means of assessing the health of the most important part of the retina, the macular.

This study will help determine how well healthy normal eyes can see polarized light. In the future, this technique may help us detect some eye diseases much earlier than currently possible. As part of this study, we would also like to take some specialised pictures of the back of your eyes to help with our analysis.

Why have I been chosen?

You have been asked to participate because your optometrist is currently studying for her doctorate in optometry at Aston University and found that your eyes were normal and healthy during her eye examination.

What will happen to me if I take part?

If you volunteer to take part you will be giving consent for Miss Smith, your optometrist, to: (i) take a detailed picture of the back of your eye (called an OCT scan), and (ii) measure how well you can see polarized light on a specially designed blue computer screen. All examinations will be done at Aves Optometrists following your normal eye examination, and will take approximately 20 minutes. Nothing will touch or hurt your eyes. You will also be giving consent for our small research team to analyse your results from the eye examination and additional tests.

Are there any potential risks in taking part in the study?

There are no expected risks in taking part in this study. None of the tests will hurt or touch your eyes, and breaks will be provided as needed. It is possible that an undiagnosed eye problem may be found by taking the specialist images of your eyes. If Miss Smith finds anything unexpected, such as an ocular disease, on your images she will talk this through with you and manage it appropriately in her role as your Optometrist. Your data will be treated with the utmost care and your data will be anonymous. Some data will be stored on an electronic database, but any risk of a confidentiality breach is minimized by password protection and encryption of data. It is very unlikely that unauthorised members of staff or the public could access your notes. Miss Smith will be responsible for keeping this data safe and maintaining your privacy and confidentiality at all times.

Do I have to take part?

You do not have to take part if you do not wish to. If you do agree to take part, you are free to withdraw from the study at any time. Your decision will not affect the quality of your eye examination. No sanctions or consequences will be taken should you refuse to participate or want to withdraw.

Expenses and payments

There are no expenses or payments for participation in this project. Normally, we do charge for the specialist images taken of your eyes. However, as part of this study, these pictures will be taken free of charge. You will receive no direct benefit from participation in this project.

Will my taking part in this study be kept confidential?

Yes. A code will be attached to all the data you provide to maintain confidentiality.

Your personal data (name and contact details) will only be used if the researchers need to contact you to arrange study visits or collect data by phone. Analysis of your data will be undertaken using coded data. The data we collect will be stored in a secure document store (paper records) or electronically on a secure encrypted mobile device, password protected computer server or secure cloud storage device. To ensure the quality of the research, Aston University may need to access your data to check that the data has been recorded accurately.

If this is required, your personal data will be treated as confidential by the individuals accessing your data.

What will happen to the results of the research study?

Experiment analysis and results will be kept and published anonymously. We aim to publish the results of this in academic journals. Please feel free to contact me should you like to obtain a copy of the published research. Your images and normal eye examination results will be stored on your regular electronic record in Aves long-term to help monitor your eyes. Polarized light perception scores will be archived following the end of the project.

Who is organising this study and acting as data controller for the study?

Aston University is organising this study and acting as data controller for the study. You can find out more about how we use your information in Appendix A.

Who has reviewed the study?

The research has been given a favourable opinion by Aston University's Ethics committee.

What if I have a concern about my participation in the study?

If you have any concerns about your participation in this study, please speak to the research team and they will do their best to answer your questions. Please feel free to contact Miss Jasmine Smith by email at smithje@aston.ac.uk or telephone Aves Optometrists on 01920 462751.

If the research team are unable to address your concerns or you wish to make a complaint about how the study is being conducted you should contact the Aston University Director of Governance, Mr. John Walter, j.g.walter@aston.ac.uk or telephone 0121 204 4665.

Appendix A

Aston University takes its obligations under data and privacy law seriously and complies with the General Data Protection Regulation ("GDPR") and the Data Protection Act 2018 ("DPA").

Aston University is the sponsor for this study based in the United Kingdom. We will be using information from you in order to undertake this study. Aston University will process your personal data in order to register you as a participant and to manage your participation in the study. It will process your personal data on the grounds that it is necessary for the performance of a task carried out in the public interest (GDPR Article 6(1)(e). Aston University may process special categories of data about you which includes details about your health. Aston University will process this data on the grounds that it is necessary for statistical or research purposes (GDPR Article 9(2)(j)). Aston University will keep identifiable information about you for 6 years after the study has finished.

Your rights to access, change or move your information are limited, as we need to manage your information in specific ways in order for the research to be reliable and accurate. If you withdraw from the study, we will keep the information about you that we have already obtained. To safeguard your rights, we will use the minimum personally identifiable information possible.

You can find out more about how we use your information at www.aston.ac.uk/dataprotection or by contacting our Data Protection Officer at dp_officer@aston.ac.uk.

If you wish to raise a complaint on how we have handled your personal data, you can contact our Data Protection Officer who will investigate the matter. If you are not satisfied with our response or believe we are processing your personal data in a way that is not lawful you can complain to the Information Commissioner's Office (ICO).

Participant Information Sheet (Group 2)

Repeatability Study #1405

Version 3 – 02/10/2018

Research workers, school, and subject area responsible

Miss Jasmine Smith, Prof Stephen Anderson, and Prof Gary Misson.

School of Life & Health Sciences, Vision Sciences, Aston University.

Project Title

Visual sensitivity to polarization pattern perception: implications for the assessment of macular function in health and disease.

Invitation

You are being invited to participate in a research study. Before you decide it is important for you to understand your role in the research and why it is being carried out. Please take the time to read the following information carefully.

What is the purpose of the study?

Many animals are sensitive to both ordinary light and polarized light. It has recently been discovered that, under special viewing conditions, humans can also see polarized light. This is potentially important as polarized light may be a useful means of assessing the health of the most important part of the retina, the macular.

This study will help determine how well healthy normal eyes can see polarized light. In the future, this technique may help us detect some eye diseases much earlier than currently possible. As part of this study, we would also like to take some specialised pictures of the back of your eyes to help with our analysis.

Why have I been chosen?

You have been asked to participate because your optometrist is currently studying for her doctorate in optometry at Aston University and found that your eyes were normal and healthy during her eye examination.

What will happen to me if I take part?

If you volunteer to take part you will be giving consent for Miss Smith, your optometrist, to: (i) take detailed pictures of your eyes (called an OCT scan and GDx scan), and (ii) measure how well you can see polarized light on a specially designed blue computer screen. All examinations will be done at Aves Optometrists, on two separate occasions, each lasting 30 minutes or less. These can be organised at a mutually convenient time. Nothing will touch or hurt your eyes. You will also be giving consent for our small research team to analyse your results from the eye examination and additional tests.

Are there any potential risks in taking part in the study?

There are no expected risks in taking part in this study. None of the tests will hurt or touch your eyes, and breaks will be provided as needed. It is possible that an undiagnosed eye problem may be found by taking the specialist images of your eyes. If Miss Smith finds anything unexpected, such as an ocular disease, on your images she will talk this through with you and manage it appropriately in her role as your Optometrist. Your data will be treated with the utmost care and your data will be anonymous. Some data will be stored on an electronic database, but any risk of a confidentiality breach is minimized by password protection and encryption of data. It is very unlikely that unauthorised members of staff or the public could access your notes. Miss Smith will be responsible for keeping this data safe and maintaining your privacy and confidentiality at all times.

Do I have to take part?

You do not have to take part if you do not wish to. If you do agree to take part, you are free to withdraw from the study at any time. Your decision will not affect the quality of your eye examination. No sanctions or consequences will be taken should you refuse to participate or want to withdraw.

Expenses and payments

There are no expenses or payments for participation in this project. Normally, we do charge for the specialist images taken of your eyes. However, as part of this study, these pictures will be taken free of charge. You will receive no direct benefit from participation in this project.

Will my taking part in this study be kept confidential?

Yes. A code will be attached to all the data you provide to maintain confidentiality.

Your personal data (name and contact details) will only be used if the researchers need to contact you to arrange study visits or collect data by phone. Analysis of your data will be undertaken using coded data. The data we collect will be stored in a secure document store (paper records) or electronically on a secure encrypted mobile device, password protected computer server or secure cloud storage device. To ensure the quality of the research, Aston

University may need to access your data to check that the data has been recorded accurately. If this is required, your personal data will be treated as confidential by the individuals accessing your data.

What will happen to the results of the research study?

Experiment analysis and results will be kept and published anonymously. We aim to publish the results of this in academic papers. Please feel free to contact me should you like to obtain a copy of the published research. Your images and normal eye examination results will be stored on your regular electronic record in Aves long-term to help monitor your eyes. Polarized light perception scores will be archived following the end of the project.

Who is organising this study and acting as data controller for the study?

Aston University is organising this study and acting as data controller for the study. You can find out more about how we use your information in Appendix A.

Who has reviewed the study?

The research has been given a favourable opinion by Aston University's Ethics committee.

What if I have a concern about my participation in the study?

If you have any concerns about your participation in this study, please speak to the research team and they will do their best to answer your questions. Please feel free to contact Miss Jasmine Smith by email at smithje@aston.ac.uk or telephone Aves Optometrists on 01920 462751.

If the research team are unable to address your concerns or you wish to make a complaint about how the study is being conducted you should contact the Aston University Director of Governance, Mr. John Walter, j.g.walter@aston.ac.uk or telephone 0121 204 4665.

Appendix A

Aston University takes its obligations under data and privacy law seriously and complies with the General Data Protection Regulation ("GDPR") and the Data Protection Act 2018 ("DPA").

Aston University is the sponsor for this study based in the United Kingdom. We will be using information from you in order to undertake this study. Aston University will process your personal data in order to register you as a participant and to manage your participation in the study. It will process your personal data on the grounds that it is necessary for the performance of a task carried out in the public interest (GDPR Article 6(1)(e). Aston University may process special categories of data about you which includes details about your health. Aston University will process this data on the grounds that it is necessary for statistical or research purposes (GDPR Article 9(2)(j)). Aston University will keep identifiable information about you for 6 years after the study has finished.

Your rights to access, change or move your information are limited, as we need to manage your information in specific ways in order for the research to be reliable and accurate. If you withdraw from the study, we will keep the information about you that we have already obtained. To safeguard your rights, we will use the minimum personally identifiable information possible.

You can find out more about how we use your information at www.aston.ac.uk/dataprotection or by contacting our Data Protection Officer at dp_officer@aston.ac.uk.

If you wish to raise a complaint on how we have handled your personal data, you can contact our Data Protection Officer who will investigate the matter. If you are not satisfied with our response or believe we are processing your personal data in a way that is not lawful you can complain to the Information Commissioner's Office (ICO).

Participant CONSENT FORM – Main Study #1405

Version 2 – 11/09/2018

Aston University
Life & Health Sciences

Name of Chief Researcher: Miss Jasmine Smith

Title: Visual sensitivity to polarization pattern perception: implications for the assessment of macular function in health and disease.

		Initial Box
1	I confirm that I have read and understand the information sheet for the above study. I have had the opportunity to consider the information, ask questions and have had these answered satisfactorily.	
2	I understand that my participation is voluntary and that I am free to withdraw at any time without giving any reason or legal rights being affected.	
3	I agree to my personal data and data relating to me collected during the study being processed as described in the Participant Information Sheet.	

_____ _____ _____

Name of participant Date Signature

_____ _____ _____

Name of person receiving consent Date Signature

Participant CONSENT FORM 2- Repeatability Study #1405

Version 2- 11/09/18

Name of Chief Researcher: Miss Jasmine Smith

Title: Visual sensitivity to polarization pattern perception: implications for the assessment of macular function in health and disease.

		Initial Box
1	I confirm that I have read and understand the information sheet for the above study. I have had the opportunity to consider the information, ask questions and have had these answered satisfactorily.	
2	I understand that my participation is voluntary and that I am free to withdraw at any time without giving any reason or legal rights being affected.	
3	I agree to my personal data and data relating to me collected during the study being processed as described in the Participant Information Sheet.	

_____	_____	_____
Name of participant	Date	Signature
_____	_____	_____
Name of person receiving consent	Date	Signature

Appendix 3- MPS II reliability curves

This figure demonstrates the likely graphical outputs produced by the MPSII. These reliability curves are presented here to demonstrate the protocol used to determine acceptable and unacceptable MPOD measures, used to ensure reliable MPOD values were obtained.

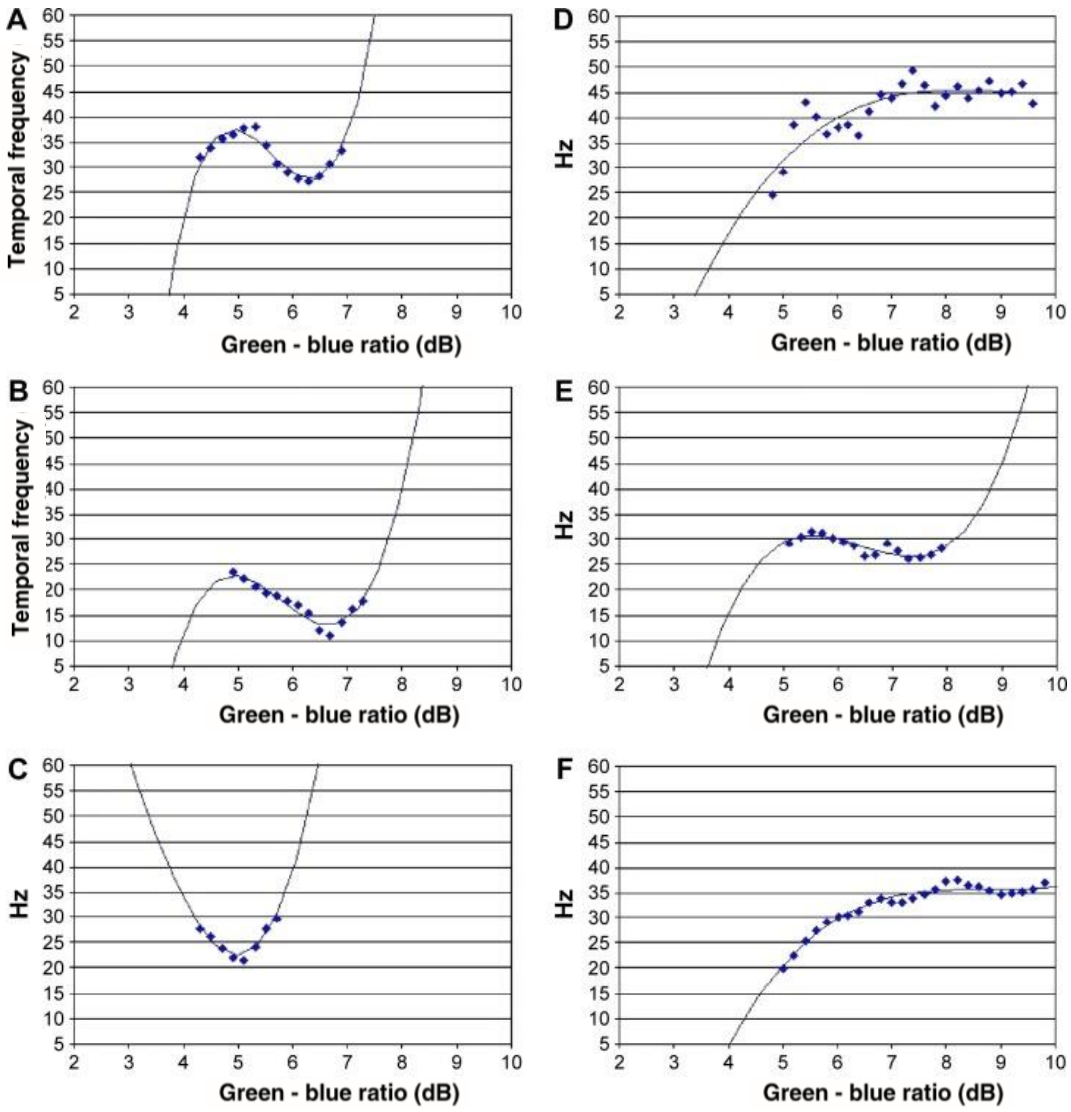

Supplementary figure 6. *Image depicting different shapes of output graph that could be obtained from the MPOD device (taken from Davey et al., 2016). Graphs A-C show acceptable examples of S, V and U-shaped graphs respectively, with a downwards slope, definite low point, three points in an upwards direction from the lowest point, and good reliability. Graphs D-F show excessive variability, no definite low point, and no downwards trend which were considered unacceptable outputs for generating a reliable MPOD reading.*